

Stony Brook University



OFFICIAL COPY

The official electronic file of this thesis or dissertation is maintained by the University Libraries on behalf of The Graduate School at Stony Brook University.

© All Rights Reserved by Author.

**Where and When to Cut: Regulation of ERCC1-
XPF Activity in Nucleotide Excision Repair**

A Dissertation Presented

by

Barbara Orelli

To

The Graduate School

In Partial Fulfillment of the

Requirements

for the Degree of

Doctor of Philosophy

in

Molecular and Cellular Pharmacology

Stony Brook University

August 2010

Stony Brook University

The Graduate School

Barbara Orelli

We, the dissertation committee for the above candidate for the Doctor of Philosophy degree, hereby recommend acceptance of this dissertation.

Orlando D. Schärer, Ph.D. – Dissertation Advisor

Associate Professor, Department of Pharmacological Sciences

Daniel F. Bogenhagen, M.D. – Chairperson of Defense

Professor, Department of Pharmacological Sciences

Carlos de los Santos, Ph.D.

Associate Professor, Department of Pharmacological Sciences

Nancy M. Hollingsworth, Ph.D.

Professor, Department of Biochemistry and Cell Biology, Stony Brook University

This dissertation is accepted by the Graduate School

Lawrence Martin
Dean of the Graduate School

Abstract of the Dissertation

**Where and When to Cut: Regulation of ERCC1-XPF
Activity in Nucleotide Excision Repair**

by

Barbara Orelli

Doctor in Philosophy

in

Molecular and Cellular Pharmacology

Stony Brook University

2010

The nucleotide excision repair (NER) pathway deals with a wide variety of lesions caused by UV-light, environmental mutagens and chemotherapeutic agents such as cisplatin. Deficiencies in NER are associated with the hereditary disorder xeroderma pigmentosum, which is characterized by a more than 1000-fold increased incidence in skin cancer. NER involves more than 30 proteins that recognize the lesion, excise a DNA fragment containing the damage and restore the integrity of the double stranded DNA. The structure-specific endonuclease ERCC1-XPF plays a key role in NER and its activity is also required for other repair pathways, in particular interstrand crosslink (ICL) repair and homologous recombination. In NER, XPA recruits ERCC1-XPF to NER complexes where it performs one of the two incisions necessary to excise the damaged DNA.

Based on the structure of an XPA peptide bound to ERCC1, we identified ERCC1 and XPA residues that are involved in this interaction. Mutations of these residues led to reduced NER activity *in vitro* and *in vivo*. In addition, clonogenic survival assays showed that cells expressing one of those mutants, ERCC1-N110A/Y145A, were specifically sensitive to UV-light but not to ICL-forming agents. Conversely, mutations in a region of XPF specifically impaired the ability of the nuclease in the repair of ICLs. In conclusion, we generated the first mutants in ERCC1-XPF specifically deficient in NER or ICL repair by selectively targeting protein binding sites. This work demonstrates that the activity of ERCC1-XPF in various repair pathways is regulated by protein-protein interactions involving specific regions of the ERCC1 and XPF proteins.

To the “Orelli Bande”

TABLE OF CONTENTS

TABLE OF FIGURES	vii
LIST OF ABBREVIATIONS	ix
ACKNOWLEDGMENTS	x
CHAPTER 1:	1
GENERAL INTRODUCTION	
INTRODUCTION	2
NUCLEOTIDE EXCISION REPAIR	3
THE MULTI-FACETED ACTIVITY OF ERCC1-XPF	9
PREVIEW	17
CHAPTER 2:	18
STRUCTURAL BASIS FOR THE RECRUITMENT OF ERCC1-XPF TO NUCLEOTIDE EXCISION REPAIR COMPLEXES BY XPA	
ABSTRACT	19
INTRODUCTION	20
RESULTS	21
DISCUSSION	31
MATERIALS AND METHODS	33
SUPPLEMENTARY DATA	43
CHAPTER 3:	46
THE XPA-BINDING DOMAIN OF ERCC1 IS REQUIRED FOR NUCLEOTIDE EXCISION REPAIR BUT NOT OTHER DNA REPAIR PATHWAYS	
ABSTRACT	47
INTRODUCTION	48
RESULTS	49
DISCUSSION	58
MATERIALS AND METHODS	61
CHAPTER 4:	66
REPAIR EFFICIENCY OF ERCC1 AND XPA MUTANTS ON DIFFERENT NER LESIONS	
INTRODUCTION	67
RESULTS	68
DISCUSSION	73
MATERIAL AND METHODS	77

CHAPTER 5:	81
THE N-TERMINAL SF2 DOMAIN OF XPF TARGETS ERCC1-XPF TO SITES OF INTERSTRAND CROSSLINK REPAIR	
INTRODUCTION	82
RESULTS	84
DISCUSSION	89
MATERIALS AND METHODS	91
REFERENCES	94

TABLE OF FIGURES

CHAPTER 1:

FIGURE 1. IMAGE OF AN XP-PATIENT AFTER SUN EXPOSURE	4
FIGURE 2. MODEL OF THE NUCLEOTIDE EXCISION REPAIR PATHWAY	6
FIGURE 3. SCHEMATIC REPRESENTATION OF XPA	8
TABLE 1. HUMAN STRUCTURE-SPECIFIC ENDONUCLEASES	12
FIGURE 3. SCHEMATIC REPRESENTATION OF THE HETERODIMER ERCC1-XPF	13

CHAPTER 2:

FIGURE 1. XPA DOMAIN ORGANIZATION AND STRUCTURE OF THE ERCC1-BINDING PEPTIDE	22
FIGURE 2. STRUCTURE OF THE XPA-ERCC1 COMPLEX	24
FIGURE 3. XPA₆₇₋₈₀ BINDS IN A SHALLOW GROOVE OF ERCC1	25
FIGURE 4. THE XPA₆₇₋₈₀ PEPTIDE IS AN EFFECTIVE INHIBITOR OF NER ACTIVITY	28
FIGURE 5. MUTATION OF THE ERCC1-BINDING EPI TOPE OF XPA ABOLISHES NER BUT NOT DNA-BINDING ACTIVITY	30
TABLE 1.	43
SUPPLEMENTARY FIGURE 1.	44
SUPPLEMENTARY FIGURE 2.	45
SUPPLEMENTARY FIGURE 3.	45

CHAPTER 3:

FIGURE 1. SEQUENCE ALIGNMENT OF THE CENTRAL DOMAIN OF ERCC1	50
FIGURE 2. STRUCTURE OF AN XPA PEPTIDE BOUND TO THE CENTRAL DOMAIN OF ERCC1	51
FIGURE 3. PURIFICATION OF WILD-TYPE AND MUTANT ERCC1 PROTEINS	52
FIGURE 4. MUTATIONS IN THE XPA-BINDING DOMAIN OF ERCC1 AFFECT NER ACTIVITY BUT NOT NUCLEASE	54
FIGURE 5. MUTATIONS IN THE XPA-BINDING DOMAIN OF ERCC1 AFFECT ITS RECRUITMENT TO SITES OF UV DAMAGE	55
FIGURE 6. UV DAMAGE PERSISTS IN UV20 CELLS EXPRESSING ERCC1-N110A/Y145A BUT NOT WILD-TYPE ERCC1	56
FIGURE 7. MUTATIONS IN THE XPA-BINDING DOMAIN OF ERCC1 INHIBIT NER BUT NOT ICL OR DSB REPAIR	57

CHAPTER 4:

FIGURE 1. EXPRESSION LEVELS OF XPA IN TRANSDUCE XP-A CELLS	69
FIGURE 2. MUTATIONS IN THE ERCC1-BINDING DOMAIN OF XPA DO NOT IMPAIR THE RECRUITMENT OF ERCC1 TO SITES OF DAMAGE SITES BUT AFFECT THE REPAIR OF UV LESIONS	70
FIGURE 3. IN VITRO NER ACTIVITY OF ERCC1 AND XPA MUTANTS ON CISPLATIN AND AAF LESIONS	72
FIGURE 4. A SECOND PUTATIVE XPA-BINDING REGION IN ERCC1	74

CHAPTER 5:

FIGURE 1. SCHEMATIC REPRESENTATION OF THE ERCC1-XPF PROTEIN	85
FIGURE 2. LOCALIZATION OF ERCC1-XPF MUTANTS TO SITES OF UV DAMAGE	87
FIGURE 3. MUTATIONS IN THE N-TERMINAL HALF OF XPF INHIBIT ICL REPAIR BUT NOT NER	88
FIGURE 4. SPECULATIVE MODEL DESCRIBING THE REGULATION OF ERCC1-XPF NUCLEASE ACTIVITY IN DIFFERENT DNA REPAIR PATHWAYS	90

LIST OF ABBREVIATIONS

ERCC:	excision repair cross-complementing
XP:	xeroderma pigmentosum
NER:	nucleotide excision repair
UDS:	unscheduled DNA synthesis
CS:	Cockayne syndrome
TTD:	trichothiodystrophy
TC-NER:	transcription coupled nucleotide excision repair
GG-NER:	global genome nucleotide excision repair
TFIIH:	transcription factor II H
RPA:	replication protein A
RFC:	replication factor C
PCNA:	proliferating cell nuclear antigen
XRCC1:	X-ray repair cross-complementing group 1
UV-DDB:	ultra violet-damaged DNA binding protein
CPD:	cyclobutane pyrimidine dimer
CAF-1:	chromatin assembly factor 1
FEN-1:	flap endonuclease 1 and five prime exonuclease 1
HJ:	Holliday junction
SLX:	synthetic lethal of unknown function
ICL:	interstrand crosslink
DSB:	double strand break
XFE:	XPF-ERCC1 syndrome
HSQC:	heteronuclear single quantum coherence
6-4PP:	6-4 photoproduct
MMC:	mitomycin C
cDDP:	cis-diaminedichloroplatinum
AAF:	acetyl aminofluorene

Acknowledgments

The work presented in this dissertation could have not been done without the help, the support and the belief in my capabilities of many persons.

First of all, I would like to thank my advisor, Orlando Schärer, for the opportunity he gave me six years ago to join his research group and to work on this exciting project. I really appreciated the fact that his door was always open; anytime I needed an answer or an advice he was there, anytime I wanted to share my results, the good and the bad ones, he was always available. He always encouraged me during all the down phases that so often occur during a PhD. Thank you, Orlando, for teaching me how to become a good scientist.

I would like to thank Lidija Staresincic, a former student in our group and a good friend of mine. We shared the same office/lab when the Schärer group was still in Zurich, Switzerland, and I have only great memories of that time. Throughout all the past years she was like a mentor for me, she taught me all the techniques and tricks I needed to know in order to be successful in my work and she knew (almost) everything I asked her about science. She is really a great scientist, but an excellent runner too. We ran our first marathon together...an unforgettable life experience. Thank you, Lidija!

In addition, I would like to thank all the past members of the group, in particular Muriel, who help me to start my project, Jawad and Miss Ilana. I would like to thank Vinh, Jérôme, Banke, Jung-Eun, AJ, Yan, Burak, Shivam, Andy and all the rotation students, who spent some time in our lab, for the nice moments we had within our four walls.

This project could have not been started and completed without the collaboration of Dr. Ellenberger's and Dr. Niedernhofer's groups. I appreciate all their efforts and discussions they shared with Orlando and me.

I would like to thank my committee members, Dr. Dan Bogenhagen, Dr. Carlos de los Santos and Dr. Nancy Hollingsworth, for their constructive comments and support during the development of my research project as well as the department of Pharmacology for providing a great academic experience.

I think that to “survive” a PhD one needs someone very close to you, on which you can always count no matter what, a person that listens to all your problems and daily complaints, that believes in you and that is able to convince you that you can make it. I am very lucky, because during the years of my PhD I had an angel next to me, Angelo. Being himself a graduate student too probably helped him to better understand what I was going through. I would like to thank him for his immense patience, for his constant support, for cooking every night and for trying to make me laugh at least once a day. I am so glad that our paths crossed. Grazie, Angi!

In addition, I would like to thank all my friends that despite being spread throughout the world I always felt them very close to me (should I thank facebook for that? No, these are true friendships!), in particular: Chiá, Jegi, Ila, Vero, Lo, Hof and Stecio. A sincere acknowledgment to the friends I made while I was here on Long Island, in particular: Yukako, Robi, Pablo, Dumaine, Akua, Damon and Monicca.

There are two more, very special, friends that mean a lot to me: Vic and Jose. I met them the first year I arrived in the U.S. and from then we became closer and closer. I shared so many great moments with them while traveling, partying, bbq-ing, running and just simply hanging out together.

A special thanks to my running team LasTeamA: Juan (the coach), Angelo, Jose, Lidija, Rolf and Vic (cheerleader). Thanks to them I discovered my passion for running.

Finally, I would like to thank my mother, Deim, Blos, Fabi and Cat. They were my biggest cheering team despite the big distance. I thank them for their support, for their encouragement, for all the hours we talked via Skype and for letting me feel their love for me from across the ocean. I love you all!

There is one more person I would like to thank, the most important person: my father. If I were able to conceive a PhD, it is especially because of him. He always believed in me (he was my biggest fan) and he always motivated me to take every new opportunity without fear because it would have been an enrichment for my life. Grazie, mio adorato papá!

Chapter 1:

General introduction

Introduction

The preservation of the DNA is of vital importance to ensure proper development and accurate transfer of the genetic information from generation to generation. Cells are constantly exposed to both endogenous and exogenous agents that damage the DNA by modifying bases, inducing distortions in the double helix and generating strand breaks. If unrepaired, these lesions can introduce mutations that alter the genetic information and eventually lead to cancer; they can also block crucial DNA processes such as DNA replication and transcription, triggering cell death. It has been estimated that 10^4 - 10^6 DNA-damaging events occur every day in a single human cell [5]. To deal with this huge amount of damage and the wide variety of lesions, organisms have evolved very efficient DNA repair systems. There are five main DNA repair pathways (direct repair, base excision repair, nucleotide excision repair, mismatch repair and homologous recombination), each of which deals with specific types of lesions. In most of these repair mechanisms lesions are removed through the excision of a damaged DNA fragment, which can range from a couple of nucleotides to patches of 30 and more nucleotides in length. The enzymes most often responsible for these excisions are a group of nucleases called structure-specific endonucleases. These proteins recognize and cleave specific DNA structures that arise during repair processes. Since formation of strand breaks can be deleterious for the cell, it is essential that the activity of these enzymes is properly regulated in order to avoid excessive accumulation of these cytotoxic lesions.

The work presented in this thesis focuses on the regulation of the activity of the endonuclease ERCC1-XPF. ERCC1-XPF participates in different DNA repair pathways that consist of multi-stage processes. It is therefore very important that ERCC1-XPF “knows” where and when to cut. To better understand this aspect, I will discuss how the activity of ERCC1-XPF is regulated in a multi-stage process using nucleotide excision repair as an example.

Nucleotide excision repair

Nucleotide excision repair (NER) is a highly versatile DNA repair pathway that eliminates a myriad of helix-distorting lesions mainly induced by environmental mutagens, such as UV-light, components of tobacco, smoke and industrial exhaust, and chemotherapeutic agents. The importance of this repair system is underscored by the occurrence of genetic diseases associated with deficiencies in NER.

The genetic implications of NER

Deficiencies in NER are associated with the hereditary genetic disorder xeroderma pigmentosum (XP). Despite its rare occurrence (1 in every 250'000 live births [6]), XP has been the object of intensive studies due to its remarkable phenotype characterized by extreme sun sensitivity and a 1000-fold higher probability to develop skin cancer (**Figure 1**) [7].

The first description of a XP patient occurred in 1870, when the dermatologist Moriz Kaposi depicted the unusual dryness and pigmentation of the patient's skin. A couple of years later the first cases of XP patients associated with neurological diseases were reported and in 1888 40 XP patients were counted worldwide [8]. It was only in 1968 that XP was associated with a defect in excision repair based on Cleaver's work that showed the inability of XP skin cells to perform unscheduled DNA synthesis (UDS) after UV irradiation [9]. Previous work showed that bacteria released short DNA patches containing thymidine dimers after UV irradiation [10, 11] and that a "non-conservative replication" of DNA occurred in both bacterial and human cells following exposure to UV light [12, 13]. This *de novo* DNA synthesis step was referred to as unscheduled DNA synthesis and was used to measure the levels of NER activity in living cells. The different severity of symptoms and different levels of UDS among XP patients pointed to a heterogeneous molecular defect for this disease. Indeed, cell fusion studies led to the identification of various

complementation groups [14], namely XP-A, -B, -C, -D, -E, -F and -G, in which the corresponding gene encoding for a specific NER protein is mutated. There is an additional “variant” class of XP patients called XP-V, in which cells are proficient in excising damaged DNA oligonucleotides, but they are deficient in synthesizing the DNA after UV irradiation [15]. The mutated protein in those cells is the DNA translesion polymerase η , which is very efficient in replicating UV-induced pyrimidine dimers [16, 17].

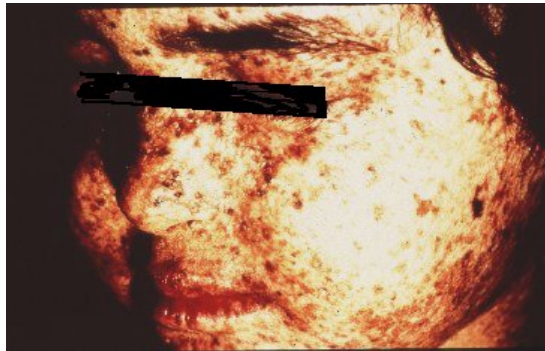


Figure 1. **Image of an XP-patient after sun exposure.** The skin of XP patients is characterized by severe blistering, sunburns and dryness. The areas around the eyes, the mouth and the neck are highly photosensitive. XP patients have a 1000-fold higher probability to develop skin cancer compared to the general population.

Two other genetic disorders characterized by UV-sensitivity have also been associated with deficiencies in genes involved in NER: Cockayne syndrome (CS) and trichothiodystrophy (TTD). Despite sharing some symptoms typical for XP, both CS and TTD patients exhibit a very different phenotype.

CS is characterized by dwarfism and mental retardation, but, unlike XP patients, CS patients are not prone to develop skin cancer unlike XP patients [7]. The genetic defects arise from mutations in the *CSA* and *CSB* genes, products of which are specifically involved in transcription-coupled NER (TC-NER) [18]. Most XP patients are also defective in TC-NER but they do not present the severe CS symptoms, indicating that the defect in TC-NER can not be the only cause of CS.

Indeed, it was suggested that CS cells have a more global impairment in transcription [19].

TTD displays a lot of CS characteristics, but has additional features such as sulfur-deficient, brittle hair and scaly skin. TTD is caused by mutations in three subunits of the transcription factor TFIIH, TTD-A, XPB and XPD. Defects in subunits of TFIIH can lead to all the aforementioned genetic disorders. This fact is explained by the dual function of TFIIH in both repair and transcription; therefore TTD is also referred to as the transcription/repair syndrome [20].

The nucleotide excision repair pathway

The mechanism to remove lesions by NER (for a detailed description of lesions processed by NER see [21]) involves the concerted action of more than 30 proteins, which are recruited in a specific and sequential order to coordinate each step of the reaction. NER consists of three main steps: recognition and verification of the lesion, excision of the damage containing DNA fragment and finally restoration of the DNA through repair synthesis and ligation (**Figure 2**) [21, 22]. NER can be divided into two partially overlapping sub-pathways depending on how the lesion is recognized and where it is located on the genome. The global-genome repair (GG-NER) pathway removes lesions genome-wide. XPC-RAD23B acts as a DNA damage sensor and triggers the assembly of the subsequent factors [23] [24] [25]. On the other hand, if the lesion is found on the transcribed strand of an expressed gene, a stalled RNA polymerase activates the transcription-coupled repair (TC-NER) [18, 26]. After the initiation step the two sub-pathways converge in a common pathway engaging the same factors to further process the lesion. The transcription and repair factor TFIIH with its helicase subunits XPB and XPD separates the DNA strands and verifies the presence of the lesion. The opening of the DNA allows the recruitment of other NER factors such as XPA, RPA and the endonuclease XPG [25, 27]. The last factor to join the pre-incision complex is ERCC1-XPF, which incises the

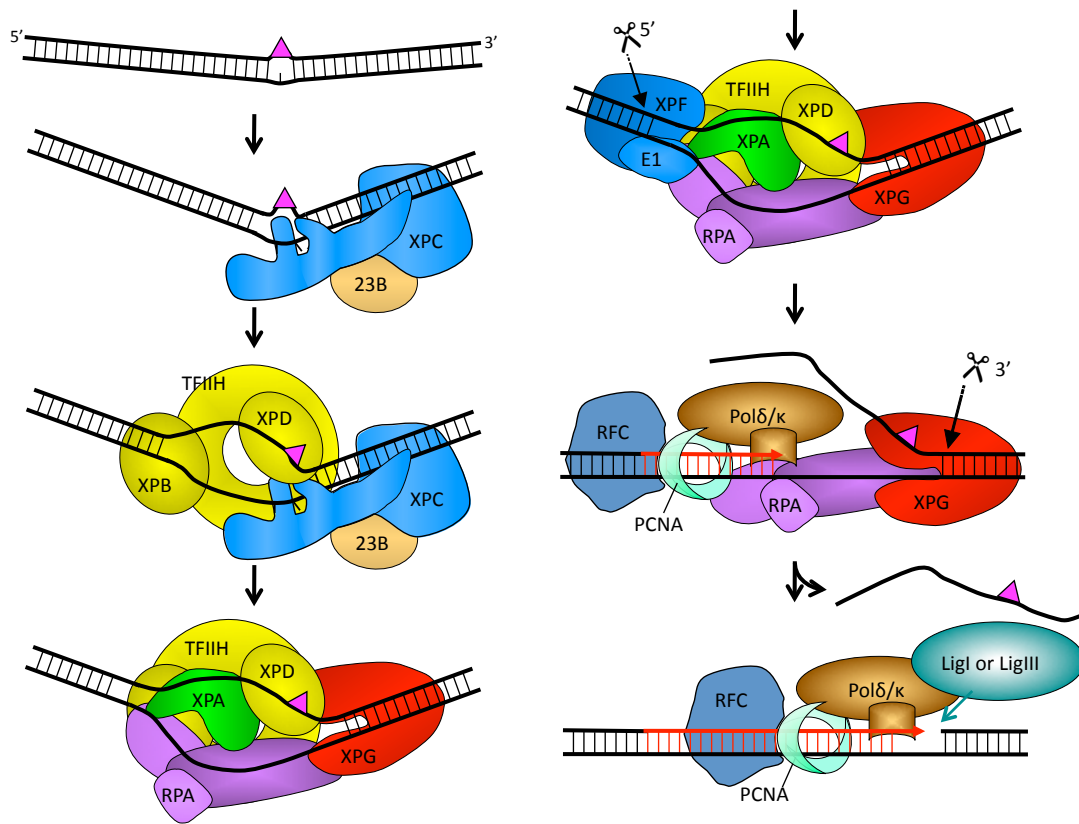


Figure 2. **Model of the nucleotide excision repair pathway.** The damaged DNA is recognized by the complex XPC-RAD23B, which subsequently recruits TFIIH. Its XPB and XPD helicase subunits unwind the DNA around the lesion in order for XPA, RPA and the endonuclease XPG to be recruited and be positioned on the open NER intermediate. The last factor to join the pre-incision complex is the endonuclease ERCC1-XPF. After dual incision of the DNA around the lesion the replication machinery composed of Pol δ/κ , PCNA and the replication factor C (RFC) synthesizes the new DNA strand, which is finally ligated by either ligase I or ligase III.

damaged strand 5' to the lesion [28], whereas XPG cleaves the DNA on the opposite site of the lesion [29]. After the dual incision around the lesion, the damaged DNA fragment is released and the resulting gap is filled by DNA polymerases δ/ϵ and κ with the help of the replication factor C (RFC), the proliferating cell nuclear antigen (PCNA) and the replication protein A (RPA). Finally, DNA ligase I or DNA ligase III/XRCC1 seals the nick and the DNA integrity is restored [30-32].

In living cells the whole NER process is even more complex due to the organization of the DNA into chromatin structures. The tight wrapping of the double helix has to be relaxed in order to detect lesions and subsequently initiate the repair process. Similarly, after removal of the lesion and DNA synthesis, the unwrapped DNA needs to be reorganized in the chromatin structures [33, 34]. The roles of some factors have been implicated with NER processes at a chromatin level. The UV-damaged DNA binding protein (UV-DDB), composed of DDB1 and DDB2, has been implicated in playing a role as a lesion detector *in vivo*. Mutations in DDB2 result in the very mild XP-E phenotype and a GG-NER deficiency in repairing CPDs [35] [36, 37]. Further studies have demonstrated that DDB2 is required to recruit XPC to DNA sites containing CPDs *in vivo* [38, 39]. The chromatin assembly factor 1 (CAF-1) is another protein that has been implicated to be a linking factor between NER sites and the remodeling of chromatin. CAF-1 functions as a histone chaperone and it was shown to be required for proper nucleosome rearrangement after NER events and to colocalize with UV-lesions in living cells in a NER-dependent manner [40-42].

XPA: a keystone in NER

The XPA protein is a key factor in the NER reaction. Its importance is underscored by the fact that XP-A patients are completely devoid of NER activity and display one of the most severe forms of XP. The 273 amino acid XPA protein interacts with different proteins involved in the NER reaction (**Figure 3**): RPA [43], XPC [44], TFIIH [2, 45] and ERCC1 [46]. The DNA-binding domain in XPA is composed of two subdomains: the N-terminal one contains a zinc-finger motif [47] essential for DNA binding and NER activity [48], the C-terminal part contains a basic cleft large enough to accommodate double-stranded DNA [49].

The role of XPA in NER was always very elusive. Because XPA binds preferentially to damaged DNA [48, 50, 51], and its affinity is enhanced by the presence of RPA [52-54], it was suggested that XPA played a role in the recognition step of NER lesions. Later, DNA damage recognition competition assays demonstrated that XPC was the earliest lesion detector factor [23]. *In vivo* studies have shown that the co-localization of XPA with UV lesions is dependent on XPC, confirming that XPC arrives to the lesion before XPA [24]. It was then proposed that XPA would perform damage verification [55] by probing DNA bending and unwinding [56]. XPA was later shown to specifically bind unusual DNA structures, such as 3-way and 4-way junctions, which could possibly arise during the NER reaction [57]. These results together with the fact that XPA interacts with other NER factors propose a more architectural function of XPA, by means of assembling and stabilizing the pre-incision complex once the presence of the lesion has been verified.

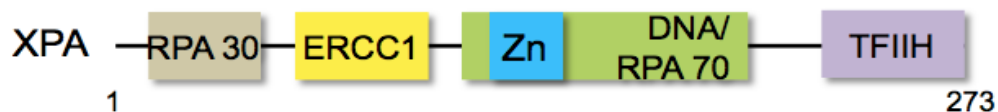


Figure 3. **Schematic representation of XPA.** The XPA regions involved in interactions with NER factors and DNA are shown. The DNA-binding domain (green) contains a zinc-finger motif (blue).

The multi-faceted activity of ERCC1-XPF

Structure-specific endonucleases

The generation of DNA single strand breaks is necessary for the proper execution of different cellular processes. As mentioned above single strand breaks are generated during DNA repair in order to remove damaged DNA fragments. Nuclease activity is also necessary during DNA replication in processing Okazaki fragments and during DNA recombination to resolve intermediate structures such as D-loops and Holliday junctions. In these processes the cleavage is not triggered by specific DNA sequences, but rather by specific DNA structures. A group of enzymes has evolved to recognize and cut different DNA intermediates, namely the structure-specific nucleases (**Table 1**). When and where an endonuclease cuts is part of an orchestrated regulation that very often involves the specific interaction between the nuclease and other proteins. The classification of endonucleases is based on their structural domains as well as on their substrate specificity. Eukaryotes have two main classes of structure-specific nucleases: the FEN-1/XPG family and the XPF/MUS81 family.

FEN-1 (originally known as DNase IV) has both an endonuclease activity in DNA repair events and an exonucleolytic activity during DNA replication (reviewed in [58, 59]); in fact its acronym stands for both flap endonuclease and five prime exonuclease. Other representatives of the FEN-1 family are XPG and its yeast homolog Rad2, T4 RNase H in bacteriophages and prokaryotic DNA polymerases I. The proteins share homology within the conserved structural/functional domains called N-, I- and C-regions. The preferred substrates of these endonucleases are branched DNA molecules with a protruding 5' single stranded flap. Exonucleolytically, FEN-1 acts preferentially on nicked double stranded DNA and less efficiently on gapped DNA. Recently, a new member has been added to the FEN-1 family: the human Holliday junctions (HJ) resolvase GEN1 [60]. HJ resolvases are structure-specific endonucleases that introduce nicks in four-way DNA junctions, intermediates that occur during

meiotic recombination and recombinational repair of double strand breaks. Despite the fact that GEN1 has a similar cleavage mechanism as non-eukaryotic HJ resolvases, which are well characterized, it does not share any sequence or structural homology with them; in fact GEN1 contains the N- and I-regions like XPG and was classified as a Rad2/XPG family member, a subcategory of the FEN-1 family [60, 61].

The XPF/MUS81 family is represented by endonucleases that preferentially cleave 3' flap structures (reviewed in [62]). In eukaryotes, each endonuclease forms a heterodimer composed of a catalytic and a non-catalytic subunit, whereas the archeal orthologs form complexes containing two catalytically active subunits. The minimal structural elements required for DNA binding and DNA incisions are the excision repair cross complementation group 4 (ERCC4) nuclease domain and a dual repeat of the helix-hairpin-helix (HhH)₂ motif. Some archeal proteins contain also a functional Superfamily 2 (SF2) helicase domain. ERCC1-XPF and MUS81/EME1 are the most relevant and well-characterized representatives. They both function in DNA repair and recombination events, but they display a slightly different substrate preference. ERCC1-XPF cleaves splayed arms and stem loops more efficiently than 3' flaps. MUS81/EME1 on the other hand prefers to incise 3'-flap, replication forks and, less efficiently, splayed arms and nicked 4-way junctions. Recently two new members have been assigned to this family, namely FANCM and FAAP24, two proteins involved in the Fanconi anemia pathway. FANCM shares a high homology with the helicase and the ERCC4 domains of the Hef protein, an archeal XPF homolog [63]. The heterodimer FANCM-FAAP24 preferentially binds 3'-flap and splayed arm structures, but it seems to lack a nuclease activity, possibly because of a substitution of one amino acid in the ERCC4 core sequence. FAAP24 was suggested to target the heterodimer FANCM/FAAP24 to specific DNA intermediates occurring during DNA repair events [64].

A lot of interest has been addressed recently to a new human protein, SLX1-SLX4. This protein acts as a HJ resolvase [65-67], but it possesses also a flap endonuclease activity and to participate in recombinational events [65, 68].

SLX1 belongs to the family of proteins that harbor the UvrC-intron-endonuclease (Uri) domain and the eukaryotic members of the family contain a C-terminal PHD-type zinc finger. Proteins belonging to the SLX4 family contain several conserved functional domains: the C-terminus harbors the SAP and CCD domains, whereas the N-terminal region contains the ubiquitin-binding UBZ domain and the BTB/POZ protein-protein interaction domain [65, 68]. Like the proteins of the XPF/MUS81 family, SLX1-SLX4 forms a heterodimer, in which SLX1 is the catalytic subunit and SLX4 acts as a regulatory unit. Interestingly, SLX4 has been shown to interact with other structure-specific endonucleases, including ERCC1-XPF and MUS81/EME1, suggesting a regulatory role for SLX4 to scaffold different enzymes to specific target sites [66].

ERCC1-XPF

To identify genes involved in NER a set of UV sensitive rodent cell lines were established and divided in different complementation groups. Human genes that were able to counteract the repair defects in those cells were designated excision repair cross-complementing (*ERCC*) [69]. ERCC1 was the first human repair gene to be cloned [70]. Unlike the other ERCC genes ERCC1 failed to complement any XP complementation group and the first human ERCC1 patient was just discovered recently [71] (see below). The human XPF gene, originally designated as ERCC4, was independently isolated by functional correction of UV sensitive rodent cells [72] and by sequence homology to the yeast Rad1 gene [28].

ERCC1- and XPF-deficient cells were not able to complement each other indicating that the two proteins might form a complex, similarly to their yeast counterparts Rad10 and Rad1, respectively [73]. It was soon demonstrated that ERCC1 and XPF form a stable complex *in vivo* [28, 73] and *in vitro* [74].


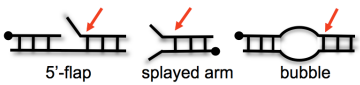
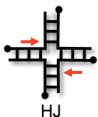
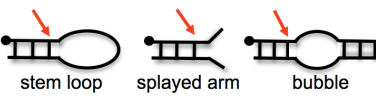
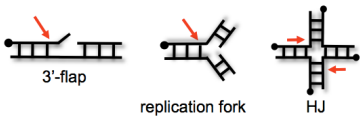
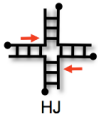
Nuclease	Family	Activity	Substrate specificity	Nuclease carrier
FEN-1	FEN-1/XPG	3' exo- and endonuclease		PCNA during replication
XPG	FEN-1/XPG	3' endonuclease		TFIIH in NER
GEN1	FEN-1/XPG	HJ resolvase		?
ERCC1-XPF	XPF/MUS81	5' endonuclease		XPA in NER SLX4 in ICL repair
MUS81-EME1	XPF/MUS81	5' endonuclease		SLX4 in ICL repair
SLX1-SLX4	UvrC-intron endonuclease	HJ resolvase		?

Table 1. **Human structure-specific endonucleases.** Endonucleases belonging to the same protein family share conserved structural elements (described in the text) that account for the cleavage polarity and the substrate specificity of the enzymes. The activity of nucleases is often regulated by specific interactions with proteins that target the endonuclease to specific DNA processes (in the table referred to as nuclease carrier). Red arrows show the approximate site of cleavage in each DNA substrate. Black circles indicate 5' termini. Abbreviations: nt: nucleotide; HJ: Holliday junction; ICL: interstrand crosslink.

The dimerisation occurs through two helix-hairpin-helix motifs, a characteristic structural consensus in DNA binding proteins, found at the C-termini of both proteins (**Figure 3**) [75, 76] and it is necessary for the stability and the functionality of the complex [28]. The N-terminus of XPF shares the same structure as the helicase domain of the archeal superfamily 2 (SF2) helicases, but it lacks the residues necessary for ATP hydrolysis [77]. The active site of the heterodimer resides in the nuclease domain of XPF, which contains the highly conserved V/IERKX₃D sequence [78, 79]. The cluster of acidic residues allows the coordination with metal ions necessary to catalyze the incision in the DNA strand [79]. The absence of archeal orthologs despite the evolutionary conservation in eukaryotes has suggested that ERCC1 might have evolved from the same XPF gene through gene duplication in lower eukaryotes [76]. Indeed the crystal structure of the ERCC1 central domain revealed a high structural homology with the overall fold of the nuclease domain found in archeal orthologs of the XPF family. In ERCC1 the groove that harbors the catalytic residues in XPF is rich in aromatic and basic amino acids implicating a role in DNA or protein binding [80]. The different functional domains in ERCC1-XPF contribute to the substrate recognition, the correct positioning of the enzyme on the DNA and the accurate execution of the incision [80-82].

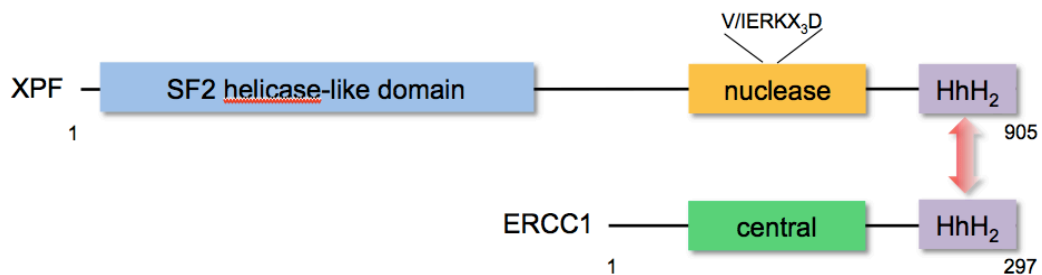


Figure 3. **Schematic representation of the heterodimer ERCC1-XPF.** The structural and functional domains of the heterodimer are shown. In XPF: the N-terminal SF2 helicase-like domain (light blue), the nuclease domain (yellow) with its highly conserved sequence necessary for catalytic activity and the C-terminal tandem repeat HhH domain (light purple) through which the dimerisation with ERCC1 occurs. IN ERCC1: the central domain (green) and the HhH₂ domain (light purple).

ERCC1-XPF preferentially cuts DNA molecules containing a junction between double stranded and single stranded DNA (ds/ss) with a 3' protruding single stranded arm such as stem-loops, splayed arms and flap substrates [28, 83]. This substrate specificity and the polarity of the incision led to the implication that ERCC1-XPF is responsible for the 5' incision during the NER reaction [28, 84].

The role of ERCC1-XPF outside NER

The fact that both ERCC1 and XPF had additional roles outside NER was already clear during the first experiments of cross-complementation with UV-sensitive rodent cell lines. ERCC1- and ERCC4 (XPF)-deficient cells showed an exquisite sensitivity to crosslinking-forming agents that was not seen in other UV sensitive strains [70, 72, 85]. Furthermore, ERCC1^{-/-} mice have a much more severe phenotype compared to other NER-deficient mice suggesting additional NER-independent roles of ERCC1-XPF [86, 87]. The mechanism of the repair of interstrand crosslinks (ICLs) is not yet fully understood. ICL repair is believed to occur through the generation of double strand breaks (DSBs), engaging proteins involved in homologous recombination as well as in nucleotide excision repair and the Fanconi anemia pathway [88]. ICLs are mainly repaired in a replication-dependent way, since this particular lesion is a strong roadblock to the replication machinery. Alternatively, the lesions can be recognized by other factors and repaired in a replication-independent way. Both pathways can be divided into four main steps: 1) recognition of the crosslink; 2) unhooking of the ICL; 3) bypass of the lesion by a translesion synthesis polymerase and 4) removal of the adduct from the DNA. Very little is known about how these steps are coordinated and which factors are involved. Nonetheless it is well-established that the activity of the endonuclease ERCC1-XPF is required for the repair of ICLs [89, 90] and recent evidence suggests SLX4 as the protein that targets ERCC1-XPF to ICL repair sites [66].

The nuclease activity of ERCC1-XPF is also necessary in different recombinational events. It has been shown that ERCC1-XPF is required to

remove non-homologous 3' tails during chromosomal rearrangements between direct repeats [91], as well as to resolve heteroduplex intermediates for targeted gene replacement [92]. Furthermore, ERCC1-XPF is also involved in telomere maintenance [93-95].

ERCC1-XPF deficiency and aging

The maintenance of the genomic integrity accounts for longevity and cell viability, implying a connection between DNA repair and aging. Indeed, most of the progeroid syndromes in humans, such as Cockayne syndrome and trichothiodystrophy, are caused by defects in genes that code for proteins involved in DNA repair processes evoking the correlation between genomic maintenance and longevity [96]. CS and TTD, which are linked to defects in transcription [97], display signs of accelerated aging, whereas XP-A patients and XPA^{-/-} mice, who have a total loss of NER, are highly cancer-prone, but do not develop premature aging symptoms [98] indicating that the loss of only NER does not account for accelerated aging. Similarly, XP-F patients, that still retain residual NER activity, present only a mild XP phenotype. In 2006, a new progeroid disorder, called XFE syndrome, was described [99]. The so far only XFE patient harbored a severe mutation in a functional domain of the XPF protein resulting in severe reduction of ERCC1-XPF protein levels. XFE cells showed residual NER activity, typical for XP and CS disorders, but the patient developed severe neurological, musculoskeletal and hematopoietic symptoms, uncharacteristic for XP or CS, classifying this clinical outcome as a new syndrome [99]. The importance of ERCC1-XPF during development was further validated by the characterization of the first and so far only ERCC1 patient. The individual had surprisingly only a mild NER impairment but developed severe pre- and postnatal development abnormalities, characteristic of the cerebro-oculo-facial-skeletal (COFS) syndrome, leading to early death [71]. Both the XFE and the ERCC1 deficient phenotype correlated very well with the phenotype of a ERCC1^{-/-} mouse model [86]. ERCC1-deficient mice showed a severe weight

reduction, delayed development, advanced neurological diseases and early death, all signs of premature aging. Cells of both XFE and ERCC1 patients and ERCC1^{-/-} mice are highly sensitive to interstrand crosslink-forming agents suggesting that this defect may be responsible for the accelerated aging phenotype [99]. In fact there is increasing evidence that imperfect genomic maintenance, caused not only by environmental agents but by cell-intrinsic sources as well, represents a critical contributor to aging [100].

ERCC1 and cancer chemotherapy

Some of the most widely used therapies to treat cancer rely on agents that damage DNA, such as platinum-based compounds and ionizing radiation. The ability of cancer cells to repair DNA lesions results in chemotherapeutic resistance. A lot of interest has been therefore directed to target proteins involved in DNA repair pathways to improve the efficacy of the therapy [101, 102]. NER was first associated with clinical resistance to cisplatin when clinical studies reported a correlation of high expression levels of some NER proteins, in particular ERCC1, with the patient response to a platinum-based therapies. Over-expression of ERCC1 correlated with poor response of treatment, therefore it was suggested that mRNA levels of ERCC1 could be a good indicator of NER activity and hence predict the clinical outcome (reviewed in [103, 104]. ERCC1 and the repair pathways, in which ERCC1-XPF is involved, might therefore been considered as potential drug targets to improve treatment efficacy.

Regulation of ERCC1-XPF in NER

The proficient repair of NER lesions requires an orchestrated regulation of the process. The main driving force of NER is the sequential recruitment of NER factors through specific protein-DNA and protein-protein interactions. The assembly of the NER complex around a lesion needs to occur in a well-defined sequential order to guarantee the recognition of the lesion, the unwinding of the DNA around the lesion, the verification of the lesion and the correct positioning of

each protein in the ensemble and finally the coordinated take-over of the replication machinery after damage excision [25].

A critical step in NER is the recruitment of ERCC1-XPF to the site of damage. The activity of ERCC1-XPF is mainly regulated at the protein level. First, the formation of the heterodimer is essential for both the stability and the activity of the complex; second, the cellular localization of the protein ensures the proper functioning of ERCC1-XPF. In this regard, recent studies have shown that the mislocalization of nuclear ERCC1-XPF is in part responsible for the low repair activities detected in XP-F and XFE patients [105]. Finally, recruitment of ERCC1-XPF to NER complexes is mediated by the specific interaction between ERCC1 and XPA, an essential step for the efficient removal of the lesion. Cells in which this association is abolished displayed high UV sensitivity [106], underscoring the importance of the XPA-ERCC1 interaction.

Preview

The aim of this thesis is to understand how the activity of ERCC1-XPF is regulated in different DNA repair pathways, in particular in NER. Starting from the structure of the central domain of ERCC1 in complex with an XPA peptide (described in Chapter 2) we identified NER-specific elements in ERCC1-XPF that led to the generation of the first NER-deficient ERCC1-XPF mutant (Chapter 3). We also investigated the effect of mutations in ERCC1 and XPA on processing different NER lesions (Chapter 4). In addition, we have identified another region in ERCC1-XPF that is necessary for the activity of ERCC1-XPF in ICL repair (Chapter 5). Implications and future directions of the results are discussed in each chapter.

Chapter 2:

Structural basis for the recruitment of ERCC1-XPF to nucleotide excision repair complexes by XPA

Adapted from the manuscript by Oleg V Tsodikov, Dmitri Ivanov, Barbara Orelli, Lidija Staresincic, Ilana Shoshani, Robert Oberman, Orlando D Schärer, Gerhard Wagner and Tom Ellenberger, published in "The EMBO Journal" in 2007, volume 26, pages 4768-4776.

Abstract

The nucleotide excision repair (NER) pathway corrects DNA damage caused by sunlight, environmental mutagens and certain antitumor agents. This multistep DNA repair reaction operates by the sequential assembly of protein factors at sites of DNA damage. The efficient recognition of DNA damage and its repair are orchestrated by specific protein–protein and protein–DNA interactions within NER complexes. We have investigated an essential protein–protein interaction of the NER pathway, the binding of the XPA protein to the ERCC1 subunit of the repair endonuclease ERCC1-XPF. The structure of ERCC1 in complex with an XPA peptide shows that only a small region of XPA interacts with ERCC1 to form a stable complex exhibiting submicromolar binding affinity. However, this XPA peptide is a potent inhibitor of NER activity in a cell-free assay, blocking the excision of a cisplatin adduct from DNA. The structure of the peptide inhibitor bound to its target site reveals a binding interface that is amenable to the development of small molecule peptido-mimetics that could be used to modulate NER repair activities *in vivo*.

Introduction

For the NER pathway, DNA cleavage by ERCC1-XPF requires physical interaction with XPA, a scaffold protein that interacts with DNA and several repair proteins, including RPA, TFIIH and the ERCC1 subunit of ERCC1-XPF [46, 106-108]. Although XPA was originally described as a DNA damage-specific sensor or verification protein, recent work suggests that XPA instead recognizes the DNA structural intermediates arising during processing by NER [51, 57]. XPA recruits ERCC1-XPF to NER complexes [24], positioning the XPF nuclease domain at the 5' side of the damage site [79]. ERCC1-XPF has other roles in DNA metabolism outside of NER, notably in interstrand crosslink repair and homologous recombination [85, 92]. The importance of these additional, NER-independent functions of ERCC1-XPF is underscored by the pronounced sensitivity to crosslinking agents caused by mutations of ERCC1 or XPF in mice and humans [86, 99, 109]. However, the exact biochemical role(s) of ERCC1-XPF in crosslink repair remain to be discovered.

Li *et al* (1994, 1995) identified residues 59–114 in XPA as the site of interaction with ERCC1, and showed that deletion of three conserved glycines (Gly72, Gly73, Gly74) abrogates the XPA-ERCC1 interaction as well as the ability of the XPA protein to confer UV resistance to XP-A cells. Furthermore, the expression of a truncated protein comprising residues 59–114 of XPA renders cells sensitive to UV light and cisplatin [110], suggesting that this region is sufficient to disrupt the interaction of the native XPA protein with ERCC1-XPF. Conversely, it can be inferred from several previous studies that residues 92–119 of ERCC1 are necessary for the interaction with XPA [46, 76, 111].

Following these seminal studies, understanding of the biochemical and structural basis for XPA's interaction with ERCC1 has not advanced, although more is known about the individual proteins. XPA contains a well-defined central domain (residues 98–219; **Figure 1A**), although the remainder of the protein including the ERCC1 interaction domain appears to be poorly structured [49, 112-114]. Residues 92–119 of ERCC1 fall within the central domain of ERCC1

[80] that is structurally homologous to the nuclease domain of the archaeal XPF-like proteins *Aeropyrum pernix* Mus81/XPF [81] and *Pyrococcus furiosus* Hef [115]. A V-shaped groove on the surface of ERCC1 corresponds to the nuclease active site of XPF [79, 81, 115], except that ERCC1's groove lacks the catalytic residues of a nuclease active site and is instead populated with basic and aromatic residues [76]. We previously showed that the central domain of ERCC1 binds to single-stranded DNA *in vitro* [80], and proposed the V-shaped groove as the DNA-binding site.

These observations prompted us to investigate the structural and functional basis for the interaction of XPA and ERCC1, and its role in recruiting the XPF-ERCC1 endonuclease to sites of NER. Here, we describe the structure of a short peptide motif from XPA in complex with the central domain of ERCC1. We show that this XPA peptide specifically inhibits the NER reaction *in vitro*, creating an opportunity for structure-based design of NER inhibitors targeting this protein–protein interaction. Point mutations in the corresponding region in XPA abolish NER activity *in vitro*, underscoring the importance of the XPA-ERCC1 interactions for NER. In addition to providing insights into how protein–protein interactions mediate progression through the NER pathways, our studies will provide a blueprint to develop small molecules that intercept the interaction between XPA and ERCC1. Such molecules should be valuable for studying the biochemical functions of ERCC1-XPF in NER and other repair pathways including DNA interstrand crosslink repair and homologous recombination by selectively inhibiting NER.

Results

Induced fit of the XPA peptide upon interaction with ERCC1

Previous reports have suggested that the ERCC1-interacting region of XPA (**Figure 1A**) is unfolded in solution, based on NMR studies and its sensitivity to proteolytic cleavage [112, 114]. To investigate the structure of the XPA ligand, we collected HSQC NMR spectra of an ¹⁵N-labeled XPA₅₉₋₉₃ peptide alone and in

complex with unlabeled central domain of ERCC1 (the ERCC1₉₂₋₂₁₄ protein; **Figure 1B**). In the absence of ERCC1, the resonance signals for XPA cluster in a narrow range of chemical shifts (**Figure 1B**, inset) that is characteristic of an unstructured polypeptide with poor spectral dispersion. In the complex with ERCC1, a subset of XPA backbone amides become well dispersed and the peaks are broader. These changes are indicative of a well-structured region within the bound XPA peptide. Only a few resonance peaks are markedly perturbed when XPA₅₉₋₉₃ is bound to ERCC1, and among these, three glycine residues (assigned as Gly72, Gly73 and Gly74) are strongly perturbed in the complex. In order to overcome the peak broadening observed in NMR spectra of the XPA₅₉₋₉₃ peptide at concentrations above 0.1 mM, we sought to identify shorter XPA peptide ligands for ERCC1. A minimal, 14-residue XPA₆₇₋₈₀ peptide (described below) was identified by examining a series of overlapping XPA fragments from the region previously shown to interact with ERCC1 [46].

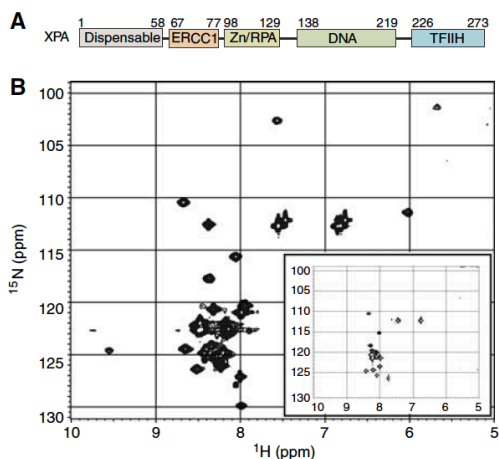


Figure 1. XPA domain organization and structure of the ERCC1-binding peptide. A) The ERCC1-binding region of XPA (residues 67-77) is located between the central domain (Zn²⁺-binding and DNA-binding subdomains; residues 98-219) and an N-terminal region (residues 1-58) that is dispensable for functional complementation of NER in whole-cell extracts from XP-A mutant cells [1] and a TFIIH-binding region [2]. B) ¹⁵N HSQC spectrum of ¹⁵N-labeled XPA₅₉₋₉₃ in complex with unlabeled ERCC1, and in the unbound state (inset). The spectrum of the unbound XPA₅₉₋₉₃ (inset) is characteristic of an unfolded peptide. The appearance of new well-dispersed NMR peaks in the XPA spectrum upon addition of ERCC1₉₂₋₂₁₄ (shown in the larger spectrum) indicates that a portion of the XPA peptide adopts a defined conformation in complex with ERCC1. Data generated by Oleg V. Tsodikov and Dmitri Ivanov.

The structure of XPA in complex with ERCC1

A synthetic XPA₆₇₋₈₀ peptide with amino-acid sequence KIIDTGGGFILEEE forms a stable complex with ERCC1₉₆₋₂₁₄ that can be purified by gel filtration chromatography. Like full-length XPA protein, the XPA₅₉₋₉₃ and the XPA₆₇₋₈₀ peptides behave similarly and efficiently co-purify with ERCC1, suggesting that XPA₆₇₋₈₀ contains all significant binding determinants. We confirmed that XPA and ERCC1 form a stoichiometric 1:1 complex by estimating the amount of each subunit in the purified complex using an Edman degradation reaction, and by analytical centrifugation of the complex. Equilibrium sedimentation data for the complex (Suppl. Figure 1C) were best fit to the expected masses for a 1:1 complex of XPA₅₉₋₉₃ and ERCC1₉₂₋₂₁₄ ($M_w = (19.4 \pm 1.2)$ kDa) and unbound ERCC1₉₂₋₂₁₄ ($M_w = (15.0 \pm 1.0)$ kDa). We confirmed that ERCC1₉₆₋₂₁₄ binds stoichiometrically to the XPA₆₇₋₈₀ peptide with a K_D of 0.78 μ M (Suppl. Figure 2). A structure of the XPA₆₇₋₈₀–ERCC1₉₆₋₂₁₄ complex (**Figure 2A**) was determined by a combination of NMR-derived distance restraints and X-ray diffraction data extending to 4 Å resolution (Table 1 in the Supplementary data and Materials and methods) as described below.

Identification of the ERCC1-binding site in complex with XPA

The binding site for XPA on the surface of ERCC1 (**Figure 2B**) was identified using two-dimensional HSQC experiments. The spectrum of unliganded ¹⁵N-labeled ERCC1₉₂₋₂₁₄ (blue, **Figure 3**) showed significant differences from that of the complex with unlabeled XPA₆₇₋₈₀ (red, **Figure 3**). However, complexes of ERCC1₉₆₋₂₁₄ with either XPA₆₇₋₈₀ or XPA₅₉₋₉₃ were identical, suggesting that the shorter XPA peptide makes all of the significant binding contacts. The ¹⁵N HSQC spectrum of the ERCC1–XPA complex is consistent with a slow-exchange regime, implying a dissociation equilibrium constant below 1 μ M for the complex. The XPA-binding site on the ERCC1 central domain was identified using the backbone assignments for ERCC1₉₆₋₂₁₄ alone and in complex with XPA (see Materials and methods). A comparison of

the ^{15}N HSQC spectra for ERCC1 in the presence and absence of XPA reveals that, with only one exception, the most prominent changes in chemical shifts involve a cluster of residues within a V-shaped groove of the ERCC1 central domain (**Figures 2B and 3**).

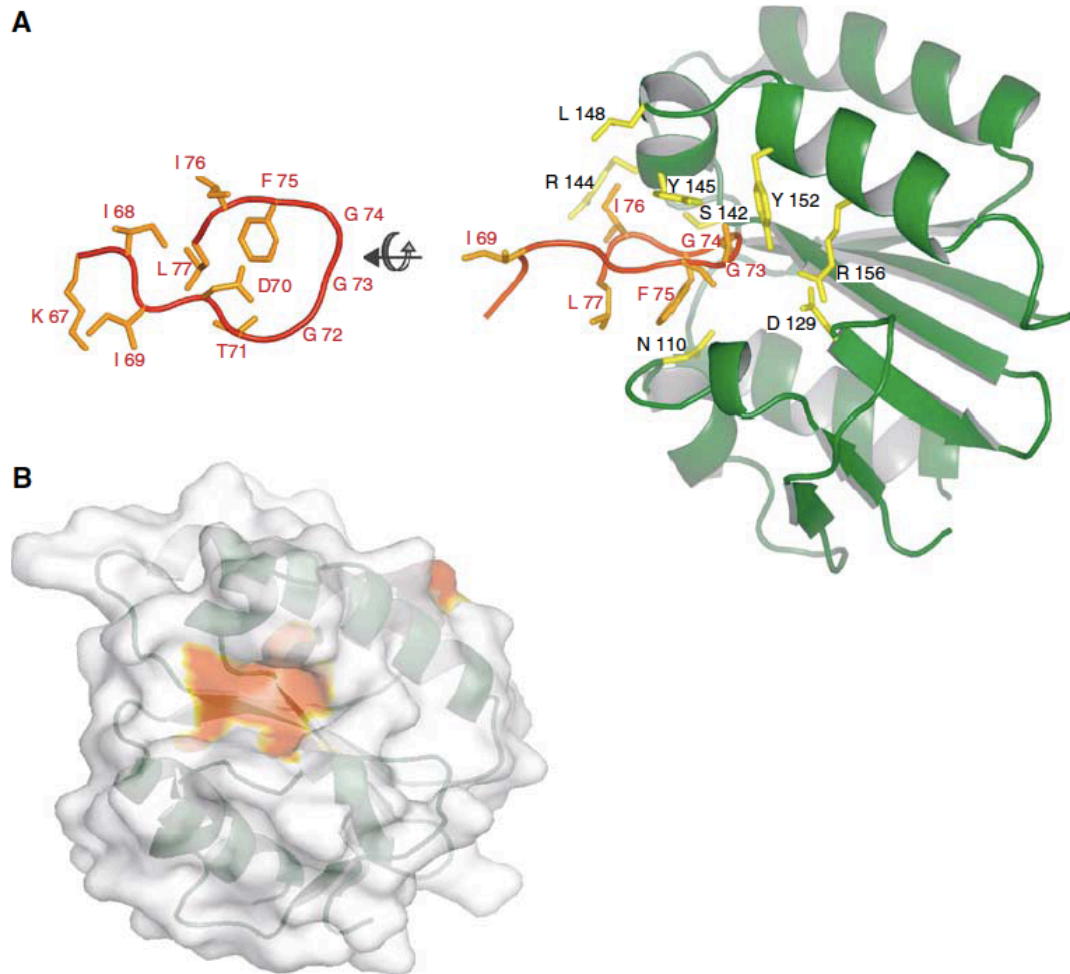


Figure 2. Structure of the XPA-ERCC1 complex. A) The XPA₆₇₋₈₀ peptide (orange) is bound to a V-shaped groove of the central domain of ERCC1₉₆₋₂₁₄ (green). An orthogonal view of the bound XPA peptide (left side) is shown in comparison to the peptide in complex with ERCC1 (right-hand site). B) The XPA-binding site on the surface of ERCC1 (colored red) was identified by resonance perturbations larger than 0.2 ppm that are indicative of direct interactions with XPA. Crystal structure was solved by Oleg V. Tsodikov.

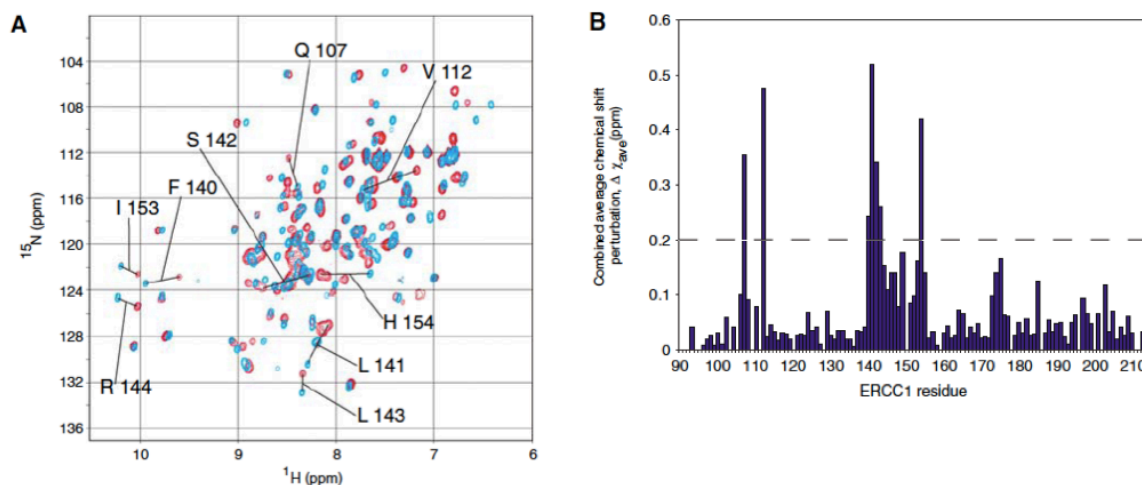


Figure 3. **XPA₆₇₋₈₀ binds in a shallow groove of ERCC1.** A) A comparison of the two-dimensional HSQC spectra for ¹⁵N-labeled ERCC1₉₂₋₂₁₄ in the presence and absence of an unlabeled XPA₆₇₋₈₀ peptide. The ¹⁵N HSQC spectra reveal significant chemical shift changes for some ERCC1 residues in the absence (blue) or presence (red) of unlabeled XPA₆₇₋₈₀. B) Combined average chemical shift perturbations are calculated as $\Delta_{X_{ave}} = (((\Delta_{X_{1H}})^2 + (\Delta_{X_{15N}/5})^2)/2)^{1/2}$ for each backbone amide of ERCC1 and shown as a histogram. NMR experiments were performed by Dmitri Ivanov.

The bound XPA peptide fits snugly into the V-shaped groove of ERCC1 (**Figure 2**) that we previously speculated could be a binding site for single-stranded DNA [80]. Three consecutive glycines (Gly72, Gly 73, Gly74) of the XPA peptide insert into the groove, making a U-turn with close steric complementary to the binding site. These are the same three conserved glycines previously reported to be essential for the interaction of XPA with ERCC1 and required for the functional complementation of XP-A cells [46, 106]. A total of 1039 Å² of accessible surface area from XPA peptide is buried in the complex with ERCC1, accounting for 61% of the solvent accessible surface area of XPA residues 67–77, which are in close proximity to the binding site. The XPA ligand derives many interactions from the core sequence motif (shown in boldface; KIID**TGGG**FILEEE) of the XPA₆₇₋₈₀ peptide. The side chains of Phe75, Leu77 and Thr71 of XPA are clustered together at the mouth of the V-shaped groove (**Figure 2A**) where Phe75 stacks against Asn110 of ERCC1, and the Ile76 side chain packs against the aliphatic portion of ERCC1 side chains Arg144 and

Leu148. The binding groove in ERCC1 is capped by XPA Leu77.

The glycine-rich loop of XPA₆₇₋₈₀ extends far into the groove of ERCC1 where main chain atoms of these XPA residues stack against the side chains of Tyr145 and Tyr152 from ERCC1 (**Figure 2A**). The main chain amides of these glycines could participate in hydrogen-bonding interactions with the ERCC1-binding site, although these interactions cannot be directly observed from our NMR experiments nor can they be reliably confirmed by low-resolution (4 Å) X-ray diffraction data (Table 1 in the Supplementary data). Based on the proximity of atoms modeled in the complex, we infer that the carbonyl oxygen of Gly74 may bond with the main chain amide of Ser142 from ERCC1. The orientations of the Tyr145 and Tyr152 side chains from ERCC1 would permit their hydroxyl groups to make hydrogen-bonding interactions with the backbone carbonyls of Thr71 and Gly73, respectively. The side chain of XPA Asp70 could participate in electrostatic interactions with the side chain His149 of ERCC1. It is notable that a solvent-exposed salt bridge between the side chains of Asp129 and Arg156 of ERCC1 (PDB code 2A1I; [80]) becomes almost completely buried when XPA is bound.

Phe75 of XPA is completely buried within the ERCC1-binding site (**Figure 2A**). We tested whether an alanine substitution at this position interferes with binding to ¹⁵N-labeled ERCC1 by measuring chemical shifts in the ¹⁵N HSQC spectra in the presence of the mutant peptide designated XPA₆₇₋₈₀-F75A. Addition of the mutant peptide failed to perturb the chemical shifts of ERCC1 seen upon addition of wild-type XPA₆₇₋₈₀ (data not shown), indicating that the mutant peptide does not bind to ERCC1. The TGGGFI-binding motif of the XPA ligand and the corresponding residues of the ERCC1-binding site are strictly conserved in higher eukaryotes. In lower eukaryotes, the corresponding sequences of both proteins have diverged from this consensus, perhaps indicating the co-evolution of these two proteins and their functions.

The XPA peptide inhibits NER in mammalian cell extracts

The direct interaction of XPA₆₇₋₈₀ peptide with the ERCC1-binding pocket raised the possibility that this peptide might specifically interfere with the recruitment of the ERCC1-XPF nuclease into the NER reaction pathway. We investigated the effect of XPA₆₇₋₈₀ and the mutant XPA₆₇₋₈₀-F75A peptide on the dual incision of a DNA lesion during NER in cell-free extracts. A plasmid containing a single site-specific 1,3-cisplatin intrastrand crosslink was incubated with HeLa cell-free extract in the presence of increasing concentrations of XPA peptide [4]. In the absence of XPA peptide, the characteristic NER excision products of 28–33 nucleotides containing the lesion were evident (**Figure 4A**, lane 1). Increasing concentrations of XPA₆₇₋₈₀ interfered with excision of the oligonucleotide, and complete inhibition was achieved at a concentration of XPA peptide in the low micromolar range (**Figure 4A**, lanes 2–6). In contrast, the addition of XPA₆₇₋₈₀-F75A did not affect NER activity at concentrations up to 92 μ M, the maximum concentration tested (**Figure 4A**, lanes 7–11).

The XPA peptide might inhibit NER activity *in vitro* by directly interfering with the endonuclease activity of ERCC1-XPF, instead of blocking its interaction with XPA. To account for the former possibility, we tested the effects of XPA peptides on the DNA incision reaction catalyzed by purified ERCC1-XPF using stem-loop DNA substrate [83]. ERCC1-XPF efficiently cleaves on the 5' side of the loop and the XPA peptide has no effect on this activity (**Figure 4B**) even at a concentration (92 μ M) that completely abolishes NER activity (**Figure 4A**). We conclude that the inhibitory effect of XPA₆₇₋₈₀ on the NER reaction results from disrupting the interaction of ERCC1 with XPA, an essential protein–protein interaction for the dual incision of DNA by the NER pathway.

Mutations in the ERCC1-binding epitope of XPA abolish NER

The specificity of inhibition of NER by XPA₆₇₋₈₀ suggested that mutations of single residues such as F75 might diminish the NER activity of the XPA protein. We generated mutant XPA proteins containing an F75A mutation and Δ G73

single and $\Delta G73/\Delta G74$ double deletion, and compared their activities to that of the wild-type XPA protein. The ability of the XPA proteins to mediate NER activity was tested by incubating a plasmid containing a 1,3-cisplatin intrastrand crosslink with a cell-free extract generated from XPA-deficient cells supplemented with purified wild-type or mutant XPA protein [4]. Addition of wild-type XPA protein to this mixture resulted in robust NER activity, as evidenced by formation of the characteristic excision products of 24–32 nts in length (**Figure 5A**, lanes 1–2). By contrast, no NER activity was observed following addition of the F75A or $G73\Delta/G74\Delta$ mutants, while the $G73\Delta$ single deletion mutant displayed marginal NER activity.

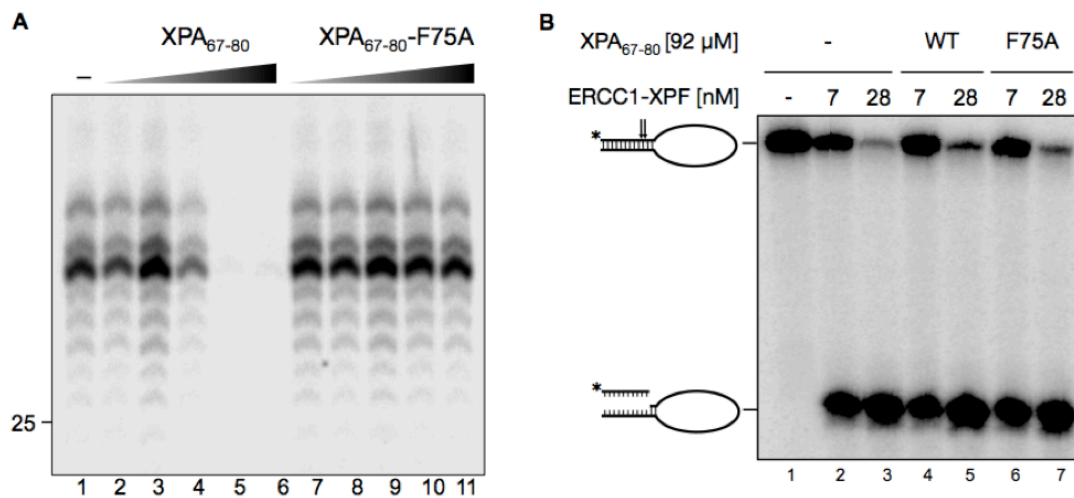


Figure 4. The XPA₆₇₋₈₀ peptide is an effective inhibitor of NER activity. A) XPA₆₇₋₈₀ inhibits the *in vitro* NER reaction, whereas the mutant XPA₆₇₋₈₀-F75A peptide has no effect. HeLa cell extracts were incubated with a plasmid containing a 1,3-intrastrand cisplatin adduct in the presence of increasing concentrations of either XPA₆₇₋₈₀ or XPA₆₇₋₈₀-F75A (lane 1, no XPA; lanes 2 and 7, 46 nM XPA peptide; lanes 3 and 8, 460 nM; lanes 4 and 9, 4.6 μ M; lanes 5 and 10, 46 μ M; lanes 6 and 11, 92 μ M). Products were visualized by a fill-in reaction following annealing to an oligonucleotide complementary to the excision product with a 4-nt overhang [4]. The marker DNA ladder is labeled LMW DNA ladder. B) XPA₆₇₋₈₀ and XPA₆₇₋₈₀-F75A do not affect the intrinsic nuclease activity of ERCC1-XPF. The stem12-loop22 substrate (6.6 nM) was incubated with different concentrations of ERCC1-XPF (lanes 2, 4 and 6: 6.7 nM ERCC1-XPF; lanes 3, 5 and 7: 26.8 nM) and 0.4 mM MnCl₂ in the presence of no peptide (lanes 1–3), 92 μ M XPA₆₇₋₈₀ (lanes 4 and 5), and 92 μ M XPA₆₇₋₈₀-F75A (lanes 6 and 7). The DNA substrate and the cleavage products are indicated.

To test if these XPA mutations only affected binding to ERCC1, we also compared the DNA-binding activities of wild-type and mutant XPA proteins. We investigated the binding of wild-type and mutant XPA to a DNA three-way junction, representing a high-affinity target for XPA in band-shift assays [56]. The wild-type, F75A, G73 Δ and G73 Δ /G74 Δ XPA proteins all bound with similar affinity to a three-way junction (**Figure 5B**), indicating that the mutant proteins are fully proficient in DNA binding and unlikely to be misfolded or otherwise inactive. These results show that single point mutations in XPA can result in a defect in NER activity by weakening the interaction between ERCC1 and XPA. Due to the highly cooperative nature of NER (Moggs et al, 1996), other NER functions and interactions may be disrupted as a result of blocking the recruitment of ERCC1-XPF.

XPA competes with single-stranded DNA for binding to ERCC1

Because XPA binds in the groove on ERCC1 (**Figure 2**) that was previously implicated in DNA-binding activity [80], we directly tested whether or not XPA competes with single-stranded DNA for binding to ERCC1. DNA-binding activity was measured by monitoring fluorescence anisotropy, using single-stranded 40-mer oligonucleotide labeled on the 5' end with 6-carboxyfluorescein. The XPA₆₇₋₈₀ peptide does not detectably bind to DNA (not shown), although it does compete with DNA for binding to ERCC1 (Suppl. Figure 3). This result confirms that the DNA-binding site on ERCC1's central domain overlaps with the XPA-binding site. The EC₅₀ for binding of XPA₆₇₋₈₀ is in the micromolar range, but quenching of the fluorescent probe by high concentrations of XPA precluded an accurate measurement of the binding constant. We previously reported an equilibrium-binding constant of 1.5 μ M for DNA binding to the central domain of ERCC1 [80]. By fitting the XPA competition titration data to a competitive binding model (Equation 9 in the Supplementary data), we obtain the estimated binding constant of $K_d = (540 \pm 280)$ nM for the XPA-ERCC1 complex. This result agrees well with the affinity determined directly for this interaction (Suppl. Figure 2).

Thus, XPA binds to the central domain of ERCC1 with approximately three-fold higher affinity than single-stranded DNA.

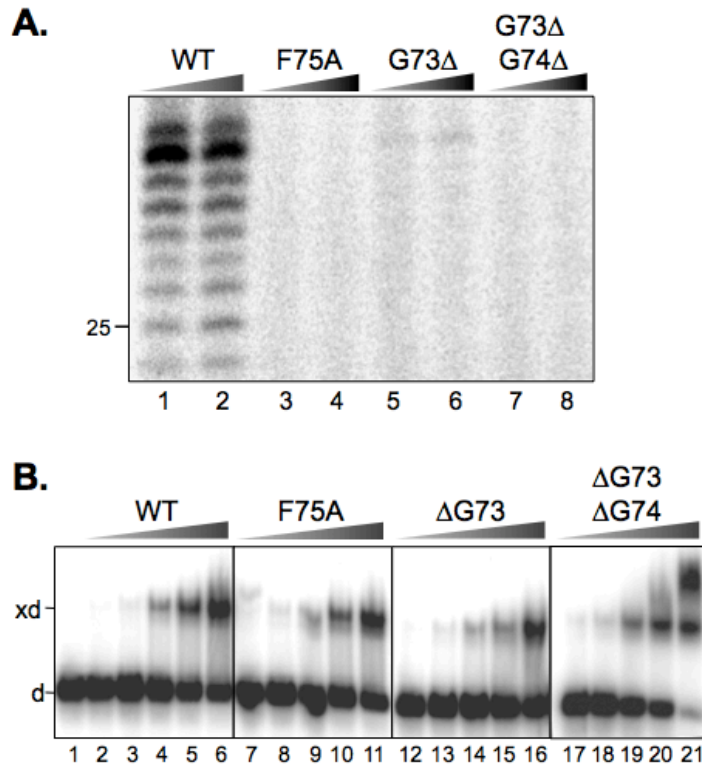


Figure 5. Mutation of the ERCC1-binding epitope of XPA abolishes NER but not DNA-binding activity. A) XP-A (XP2OS) cell extracts were incubated with a plasmid containing a 1,3-intrastrand cisplatin adduct in the presence of wild-type XPA (XPA-WT) or mutant XPA proteins (XPA-F75A, XPA-G73 Δ or XPA-G73 Δ /G74 Δ). The reaction products were visualized by a fill-in reaction after annealing the excision product to a complementary oligonucleotide with a 4-nt overhang [4]. Different XPA concentrations of 20 nM (lanes 1, 3, 5 and 7) and 80 nM (lanes 2, 4, 6 and 8) were tested. The position of a 25 mer of the LMW DNA ladder is indicated. B) A 5'-labeled DNA three-way junction (1 nM) was incubated with wild-type and mutant XPA proteins for 30min at room temperature, then the XPA-bound (xd) and free DNA (d) oligonucleotides were separated on an 8% native polyacrylamide gel. The reaction products generated with different concentrations of XPA are shown: 0 (lane 1), 4 nM (lanes 2, 7, 13, 17), 10 nM (lanes 3, 8, 13, 18), 25 nM (lanes 4, 9, 14, 19), 60 nM (lanes 5, 10, 15, 20) and 150 nM (lanes 6, 11, 16, 21). Bandshift assays performed by Ilana Shoshani.

Discussion

The removal of bulky and helix-distorting DNA lesions by the NER pathway requires the coordinated assembly of a large multi-protein complex [24, 116] that exposes the damaged DNA strand and excises an oligonucleotide containing the lesion [21]. We have investigated one of the essential protein-protein interactions in this pathway. The specific interaction of XPA with ERCC1 is responsible for recruitment of the ERCC1-XPF nuclease to the DNA repair complex [46]. Our structural studies have defined the XPA ligand as a TGGGFI sequence motif that inserts into a pocket of the central domain of ERCC1 (**Figure 2**). It was previously shown that deletion of the GGG triplet within this motif abolishes the interaction of XPA with ERCC1 [106]. These glycines insert deep into the ERCC1-binding site and are likely to make hydrogen-bonding interactions using main chain atoms (**Figure 2**). The binding site of ERCC1 is mainly a nonpolar surface that is punctuated by several large aromatic side chains (Phe145, Phe152) and a buried salt bridge between Arg156 and Asp129. We show that single point mutations in XPA (F75A or G73 Δ) effectively abolish NER activity *in vitro*, underscoring the high specificity of the binding interaction between ERCC1 and XPA.

The XPA peptide ligand is unstructured in solution (**Figure 1B**). It is therefore remarkable that a short peptide segment binds to ERCC1 with submicromolar affinity, given the associated entropic penalty for binding. This peptide-protein interaction is sufficient to block NER activity in cell-free extracts (**Figure 4A**), raising the possibility that peptido-mimetic ligands could be developed to specifically block NER activity *in vivo*. Although the competing XPA peptide prevents the double incision of lesioned DNA during NER, the peptide does not interfere with the cleavage of a model DNA substrate by purified ERCC1-XPF (**Figure 4B**). These results show that the XPA peptide does not block the nuclease activity of XPF-ERCC1 and is instead likely to interfere with the recruitment of the nuclease into the NER protein complex. Mutations in the ERCC1-binding domain of XPA similarly abolish NER activity without affecting

the intrinsic DNA-binding activity of XPA. Intriguingly, the central domain of ERCC1 binds to single-stranded DNA *in vitro* [80] and this DNA-binding activity is blocked by XPA (Supplementary Figure 3). Although these competing activities at first appear contradictory, our cleavage assays employed full-length ERCC1 protein in complex with XPF, whereas the *in vitro* binding studies used the central domain only of ERCC1. Since ERCC1-XPF has multiple DNA-binding sites [80-82, 117, 118], it is likely that some of the other DNA-binding surfaces of the XPF-ERCC1 heterodimer can compensate for the interference by the XPA peptide. With respect to the overall NER reaction, it is conceivable that DNA and the XPA protein alternatively bind to the same site on ERCC1 during different steps of the repair process. In this regard, a molecular handoff of ERCC1 from XPA to one strand of the unwound DNA substrate could be envisioned as one of multiple, individually weak interactions that drive the progression through the NER pathway in a concerted fashion [21, 119].

Homologs of the XPA and ERCC1 proteins are found only in eukaryotic organisms, despite the presence of homodimeric XPF-like endonucleases in the Archaea [115]. The ERCC1 residues constituting the XPA-binding site are poorly conserved in *Saccharomyces cerevisiae* (Rad10 protein) and *S. pombe* (Swi10 protein), and the XPA homologs (*S. saccharomyces* Rad14; *S. pombe* Rhp14) are highly divergent from mammalian XPA. Indeed, a different interaction site has recently been reported for Rad14 and Rad10/Rad1, the respective yeast homologs of XPA and ERCC1–XPF [120]. These observations suggest that XPA and ERCC1 may have co-evolved to interact specifically with each other in higher eukaryotes, perhaps in response to the added complexity and distinct functional organization of the human NER pathway. Correspondingly, a BLAST search does not identify the TGGGFI motif of the XPA ligand in any other mammalian protein.

In conclusion, we have established that only a short peptide segment of XPA is sufficient to form a stable and specific 1:1 complex with ERCC1. The interactions of three consecutive glycines (Gly72, Gly73, Gly74) and several flanking residues of XPA complement a V-shaped, hydrophobic groove in the

central domain of ERCC1. This protein-protein interaction is essential for NER activity, and the XPA peptide is an effective inhibitor of NER activity in a cell-free reaction. This work paves the way for development of specific NER inhibitors targeting the surface of ERCC1 involved in XPA binding. ERCC1 has served as a molecular marker for clinical resistance to cisplatin-based chemotherapy [104], raising the possibility of using ERCC1 antagonists as sensitizing agents for tumors resistant to this and other DNA-damaging agents in the treatment of cancer.

Materials and methods

Peptide and DNA

The XPA₆₇₋₈₀ peptide corresponding to residues 67–80 of the XPA protein and the mutant peptide XPA₆₇₋₈₀-F75A were synthesized by solid phase methods, then HPLC-purified by the Molecular Biology Core Facility at Tufts University (Boston, MA). A 40-mer DNA oligomer 5'-CCGGTGGCCAGCGCTCGGCGT₂₀-3' with a 5' 6FAM label (Integrated DNA Technologies) was gel-purified by conventional techniques.

Protein expression and purification

The central domain of ERCC1 (constructs ERCC1₉₂₋₂₁₄ or ERCC1₉₆₋₂₁₄) with an N-terminal His₆ tag was expressed and purified as previously described [80]. Fragments of the XPA protein (XPA₁₋₂₇₃, XPA₅₉₋₂₇₃, XPA₅₉₋₂₁₉, XPA₅₉₋₉₃) were cloned into pET19bpps, in which an N-terminal (His)₁₀ tag is separated from the XPA sequences by a Precision protease cleavage site (gift of Dr. Tapan Biswas), between *Nde*I and *Xho*I sites. Full-length XPA protein was expressed in bacteria from pET15b-XPA. All proteins were expressed in BL21(DE3) *E. coli* (Stratagene). The cells were grown to OD₆₀₀ = 0.5 at 37 °C, then cooled down to 22 °C and induced with 0.5 mM of IPTG at 22 °C for 15 hours. XPA proteins were purified by Ni²⁺ chromatography using a HiTrap Ni²⁺-chelating column (Amersham-Pharmacia) following manufacturer's instructions. These proteins

were dialysed overnight and the His-tag was concomitantly cleaved in a buffer containing 30mM Tris pH 8.0, 400 mM NaCl, 2 mM β -mercaptoethanol and Prescission protease in approximately a 1:100 molar ratio to XPA. The XPA and ERCC1 proteins were further purified individually on S100 HiPrep (Amersham-Pharmacia) column. In order to obtain homogeneous XPA-ERCC1 complexes, purified XPA and ERCC1 were combined in excess of ERCC1 (for XPA₁₋₂₇₃, XPA₅₉₋₂₇₃, XPA₅₉₋₂₁₉) or of XPA (for XPA₅₉₋₉₃ and XPA₆₇₋₈₀) and the same gel filtration purification step was repeated. The peak corresponding to XPA-ERCC1 was well separated from the excess ERCC1 or XPA for all XPA constructs. This separation or the shapes of the peaks was not affected in the salt concentration range of 50-400 mM NaCl. For the XPA₅₉₋₂₁₉ fragment containing the Zn²⁺-binding domain of XPA (Suppl. Figures 1A and 1B), an elemental analysis performed on the corresponding XPA-ERCC1 complex indicated that 98% of XPA₅₉₋₂₁₉ contains a Zn²⁺ atom and we conclude that the structured part of XPA remained properly folded in association with ERCC1.

Labeled proteins for NMR studies were produced in M9 minimal media containing ¹⁵N-labeled NH₄Cl and ¹³C-labeled glucose as the sole sources of nitrogen and carbon, respectively. A perdeuterated, ¹⁵N-labeled ERCC1 sample was prepared in media containing 100% D₂O with 100% deuterated glucose and ¹⁵N-labeled NH₄Cl.

Analytical ultracentrifugation

Sedimentation equilibrium experiments with ERCC1₉₂₋₂₁₄ and the complex ERCC1₉₂₋₂₁₄-XPA₅₉₋₉₃ were performed using Beckman XLA Analytical Centrifuge. In both cases, proteins were at concentrations of 0.3–0.5 mg/ml in NMR Buffer (20 mM Tris buffer pH 7.2, 50 mM NaCl, 2 mM β -mercaptoethanol and 0.1 mM EDTA).

Analysis of equilibrium sedimentation experiments

Absorbance measured in the experiment,

$$A_{280}(r) = A_{280}(a) \exp\left(\frac{\omega^2 M(1 - \rho\nu)(r^2 - a^2)}{2RT}\right) \quad (1)$$

was analyzed using equation (1) in which A_{280} is the absorbance at 280 nm, r and a are an arbitrary and a reference radial distances, $\omega = 2\pi f$ (where $f = 40,000 \text{ min}^{-1}$) is the angular velocity of the rotor, $\rho = 1 \text{ g/mL}$ is the density of water, M is the molecular weight of the sedimented species, R is the Boltzmann constant and $T = 277 \text{ K}$ is the absolute temperature.

The nonlinear regression fitting of the data to Eq. 1 to determine M was performed using SigmaPlot 9.0 (SSP). Data were fit (solid and dashed lines) using a single-component, non-interacting model and assuming partial specific volumes $\nu = 0.75 \text{ mL/g}$ for both samples. The fit (shown in Suppl. Figure 1C) yields molecular weights of $(15.0 \pm 1.0) \text{ kDa}$ and $(19.4 \pm 1.2) \text{ kDa}$ for free ERCC1₉₂₋₂₁₄ and ERCC1₉₂₋₂₁₄-XPA₅₉₋₉₃ complex respectively.

Crystallization of XPA–ERCC1 complex, data collection and analysis

The complex of ERCC1₉₆₋₂₁₄-XPA₆₇₋₈₀ was concentrated to 9 mg/ml using Amicon (Millipore) concentrator with a 5 kDa molecular weight cut-off in 30 mM Tris pH 8.0, 200 mM NaCl, 2 mM β -mercaptoethanol and 0.1 mM EDTA. Crystals were grown by vapor diffusion in hanging drops containing 1 μL of the protein solution and 1 μL of the reservoir solution (100 mM Tris pH 8.5, 2 M ammonium dihydrogen phosphate, 10% glycerol) at 21.5 °C. Single cubic crystals of XPA-ERCC1 complex grew in 1-2 weeks, reaching a size of 0.15-0.20 mm in each dimension. The crystals diffracted to 4.0 Å resolution using a rotating anode X-ray source at Harvard-Armstrong X-ray facility. $I/\sigma(I)$ decreases sharply (R_{merge} increases sharply) with increasing resolution at 4 Å. As a result, higher resolution shells contain no data useful for structure refinement.

A complete and redundant X-ray data set was collected and processed

using HKL2000 (Otwinowski and Minor, 1997). The crystals belong to space group $I4_132$ with one ERCC1–XPA complex in the asymmetric unit. The structure was determined by molecular replacement (MR) methods using the program PHASER (McCoy et al, 2005) and the crystallographic model of the ERCC1 central domain (Tsodikov et al, 2005; PDB code 2A1I) in which the residues C-terminal to residue 214 were deleted. A difference ($F_o - F_c$) electron density map calculated with phases from the MR solution revealed the bound XPA peptide. The XPA peptide was built into the difference density using distance restraint information from NMR experiments and the structure of the complex was then refined as described below, with strong geometric restraints imposed on the ERCC1 subunit due to the low-resolution diffraction data and the absence of intramolecular distance information for ERCC1. All experimental XPA–ERCC1 distance restraints were accommodated without violations using the structure of unbound ERCC1, suggesting that ERCC1 does not undergo significant conformational changes upon binding to XPA.

NMR experiments and determination of the structure of XPA–ERCC1 complex

All NMR data were acquired in the NMR Buffer described above. The protein concentrations were 0.25 mM for free ERCC1₉₆₋₂₁₄ or ERCC1₉₂₋₂₁₄ (which behaved similarly in all experiments), 0.25 mM for ERCC1₉₂₋₂₁₄ in complex with a synthetic XPA₆₇₋₈₀ peptide and 0.1 mM for ERCC1₉₂₋₂₁₄ complex with XPA₅₉₋₉₃ fragment. Higher protein concentrations resulted in line broadening and lower quality NMR spectra. Backbone assignments of the free ERCC1₉₂₋₂₁₄ and ERCC1–XPA₆₇₋₈₀ complex were performed using a standard set of triple-resonance experiments: HNCA/HN(CO)CA, HN(CA)CB/ HN(COCA)CB and HNCO/HN(CA)CO.

Structural information for the ERCC1–XPA complex was obtained with a differentially labeled sample in which ERCC1 was ¹⁵N-labeled and perdeuterated and the synthetic XPA fragment was unlabeled (D,N-ERCC1/U-XPA) [121, 122]. The assignment of the XPA peptide in this sample was performed using homonuclear 2D NOESY and 2D TOCSY experiments acquired in both H₂O and

D₂O buffers. The total of 92 intramolecular distance constraints for the XPA peptide were derived from the 2D NOESY experiment acquired in H₂O with 100 ms mixing time. Intermolecular distance restraints were derived from a ¹⁵N-dispersed NOE-HSQC experiment acquired on the D,¹⁵N-ERCC1/ U-XPA sample using 200 ms mixing time. A total of 23 intermolecular distance restraints between the amide protons of ERCC1 and the protons of XPA were derived from this experiment. The structure of the ERCC1–XPA complex was calculated using simulated annealing procedure in XPLOR-NIH [123]. The total energy term used in the calculation incorporated all of the NMR-derived distance restraints as well as the 4 Å X-ray data. Ten lowest energy structures out of 100 calculated were deposited in the PDB with accession code 2JNW. The solvent accessible surface areas were calculated for the lowest energy structure using Surface Racer 4.0 [124] with the solvent probe radius of 1.4 Å.

Competitive binding equilibrium titrations

Fluorescence anisotropy measurements were performed as previously reported [80]. The equilibrium titrations were performed in a binding buffer containing 20 mM Tris, pH 8.0, 20 mM NaCl, 2 mM β-mercaptoethanol. The concentrations of single-stranded 5' 6-FAM-labeled DNA (5'-CCG GTG GCC AGC GCT CGG CG(T)₂₀) and ERCC1₉₆₋₂₁₄ were 50 nM and 2.33 μM, respectively, the concentration of the XPA peptide was varied from 0 to 30 μM, as shown in Suppl. Figure 3. Increasing XPA peptide concentration above 30 μM caused an increase in fluorescence anisotropy and quenching of fluorescence due to nonspecific interactions with the peptide, observed in the presence or absence of ERCC1 (data not shown).

The simplest binding model used in the data analysis consisted of two competitive equilibria, binding of XPA peptide and of the single-stranded 6FAM-labeled 40-mer DNA to the central domain of ERCC1. This model is consistent with the fact that at sufficiently high XPA concentration, the fluorescence anisotropy signal approaches that of unbound DNA. Therefore the two binding equilibria could be written as:



where E, D, X represent the ERCC1, DNA and XPA species, respectively. ED and EX represent ERCC1-DNA and ERCC1-XPA complexes, and K_{DNA} and K_{XPA} are the observed equilibrium association constants, defined in terms of the equilibrium concentrations of the species from Eqs. (2a) and (2b) as:

$$K_{DNA} = \frac{[ED]}{[E][D]} \quad \text{and} \quad (3a)$$

$$K_{XPA} = \frac{[EX]}{[E][X]}. \quad (3b)$$

The total concentrations of reaction species according to conservation of material are represented as:

$$[X]_{tot} = [X] + [EX] = [X] + K_{XPA}[E][X], \quad (4a)$$

$$[E]_{tot} = [E] + [EX] + [ED] \approx [E] + K_{XPA}[E][X]. \quad (4b)$$

$$[D]_{tot} = [D] + K_{DNA}[E][D] \quad (4c)$$

The approximation made in Eq. (4b) is due to the large excess of ERCC1 over DNA at the experimental conditions. It should be noted that in our analysis we assume that each single-stranded 40-mer DNA oligonucleotide contains only one binding site for ERCC1. Because the central domain of ERCC1 occludes 10-15 nucleotides upon binding DNA [80], with a reasonable approximation, a maximum of 2-3 ERCC1 molecules could simultaneously bind to one DNA molecule without significant co-operativity. In this analysis, we use the value of

$(K_{DNA})^{-1} = 1.5 \mu\text{M}$, obtained from the direct titration of ERCC1 at constant concentration (50 nM) of the same DNA oligomer, using the same single site approximation [80]. Therefore the value of the equilibrium binding constant for XPA-ERCC1 complex formation, K_{XPA} , should be unaffected by the stoichiometry of ERCC1-DNA binding.

The system of Eqs. 4a, 4b and 4c yields expressions for [E], [X] and [D], which are then used to determine the fraction of bound DNA species, f , as follows :

$$[X] = \frac{K_{XPA}([X]_{tot} - [E]_{tot}) - 1 + \sqrt{(K_{XPA}([X]_{tot} - [E]_{tot}) - 1)^2 + 4K_{XPA}[X]_{tot}}}{2K_{XPA}}, \quad (5)$$

$$[E] = \frac{[E]_{tot}}{(1 + K_{XPA}[X])}, \quad (6)$$

$$[D] = \frac{[D]_{tot}}{(1 + K_{DNA}[E])}, \quad (7)$$

And, finally

$$f = \frac{K_{DNA}[E][D]}{[D]_{tot}} \quad (8)$$

The observed fluorescence anisotropy, r , is then given by

$$r = r_0 + (r_{\max} - r_0) f, \quad (9)$$

where r_0 and r_{\max} are fluorescent anisotropy values of unbound and fully bound DNA, respectively. We used SigmaPlot 9.0 (company) to perform non-linear regression analysis of our data using Eq 9 in order to obtain the best-fit value for K_{XPA} .

Construction and expression of mutant XPA proteins

Site-directed mutagenesis using the QuikChange kit (Stratagene) introduced point mutations in the expression vector pET15b-XPA was performed. pET15b-XPA served as template and oligonucleotide primers used to generate the mutations contained the desired mutation, and a marker restriction site for selection. The following primers were used (restriction sites are underlined and indicated, modified nucleotides are shown in italics):

XPA-F75A: GACACAGGAGGAGGCCATTCTAGAAAGAGGAAGAAG (XbaI)

XPA-ΔG74: GACACAGGAGGATTCATTCTAGAAAGAGGAAGAAG (XbaI)

XPA-ΔG73/74:GATAATTGACACAGGATTCATTCTAGAAAGAGGAAGAAG (XbaI)

Positive clones were fully sequenced to rule out the introduction of additional mutations. Mutant XPA proteins were expressed in *Escherichia coli* BL21 (DE3) pLyS cells and purified by chromatography on nickel-NTA, gel filtration and heparin columns.

Nuclease assay

ERCC1-XPF was purified and nuclease assays using a stem-loop substrate were carried out as described previously [79]. A substrate consisting of a 12 base pair stem with a 22 nucleotide loop (5'-GCCAGCGCTCGGT22CCGAGCGCTGGC) was 5' end labeled using a T4 polynucleotide kinase and [γ -³²P]-ATP. The DNA substrate (100 fmol; at a final concentration of 6.7 nM) was suspended in nuclease buffer (25 mM TrisHCl pH 8.0, 40 mM NaCl, 10% glycerol, 0.5 mM β -mercaptoethanol, 0.1 mg/ml BSA) containing 0.4 mM MnCl₂ then incubated with ERCC1-XPF (100 or 400 fmol, corresponding to 6.7 nM or 26.8 nM) in the presence of 92 μ M XPA₆₇₋₈₀ or XPA₆₇₋₈₀-F75A. The final reaction volume was 15 μ l. These DNA cleavage reactions were incubated at 30 °C for 15 min then stopped by adding 10 μ l of loading dye (90% formamide/10 mM EDTA) and heating at 95 °C for 5 min. Samples were analyzed by 15% denaturing PAGE (0.5x TBE) and the reaction products were visualized using a PhosphorImager (Typhoon 9400; Amersham Biosciences).

DNA-binding assays

The three-way junction DNA substrate described previously (substrate 7 in Table 1 of [125]) was 5'-³²P-end labeled and incubated at 1 nM concentration with various amounts of XPA in EMSA buffer (25 mM HepesKOH pH 8.0, 30 mM KCl, 10% glycerol, 1 mM DTT, 1 mM EDTA, 0.1 mg/ml BSA) at a reaction volume of 15 μ l. After equilibration at room temperature for 30 min, the samples were loaded on a 5% (37.5:1) native polyacrylamide gel containing 0.5x TBE and electrophoresed at 90 V for 2 h. Gels were dried and the radioactive bands visualized by autoradiography.

In vitro NER assay

This assay was performed using an established protocol [4]. HeLa cell extracts and plasmid containing 1,3-intrastrand cisplatin adduct were prepared as described previously [4]. HeLa cell extract (2 μ l) or XP-A (XP2OS) cell extract (3 μ l), 2 μ l of 5x repair buffer (200 mM Hepes-KOH, 25 mM MgCl₂, 110 mM phosphocreatine (di-Tris salt, Sigma), 10 mM ATP, 2.5 mM DTT and 1.8 mg/ml BSA, adjusted to pH 7.8), 0.2 μ l 2.5 mg/ml creatine phosphokinase (rabbit muscle CPK, Sigma) and either purified XPA peptide, XPA protein (WT, F75A, G73 Δ or G73 Δ /G74 Δ) or NaCl (final NaCl concentration was 70 mM) in a total volume of 10 μ l were pre-incubated at 30°C for 10 min. One μ L of a covalently-closed circular DNA plasmid (50 ng) containing the 1,3-intrastrand cisplatin crosslink was added before incubating the mixture at 30 °C for 45 min. After placing the samples on ice, 0.5 μ l of 1 μ M 35-mer oligonucleotide (5'-GGGGGAAGAGTGCACAGAAGAAGACCTGGTTCGACCP-3') was added and the mixtures heated at 95 °C for 5 min. The samples were allowed to cool down at room temperature for 15 min to allow the DNA to anneal. One μ L of a Sequenase/[α -³²P]-dCTP mix (0.5 units of Sequenase and 2.5 μ Ci of [α -³²P]-dCTP per reaction) was added before incubating at 37 °C for 3 min, 1.2 μ l of dNTP mix (100 μ M of each dATP, dTTP, dGTP; 50 μ M dCTP) was added and the mixture incubated for another 12 min. The reactions were stopped by adding 8 μ l of loading dye (90% formamide/10 mM EDTA) and heating at 95 °C for 5

min. The samples were run on a 20% sequencing gel (0.5x TBE) at 45 W for 2.5 hrs. A low molecular weight DNA marker (New England Biolabs) was used as a reference after end-labeling the DNA with [α - 32 P]-dCTP and Klenow fragment polymerase. The reactions products were visualized using a PhosphorImager (Typhoon 9400, Amersham Biosciences). Slight variation in band intensities (e.g. higher intensities in Figure 4A, lane 3 in the main text) is due to experimental variability in the amount of material loaded in different lanes of the gel.

Supplementary Data (data generated by Oleg V. Tsodikov)

Table 1. Data collection and NMR and X-ray structure determination statistics.

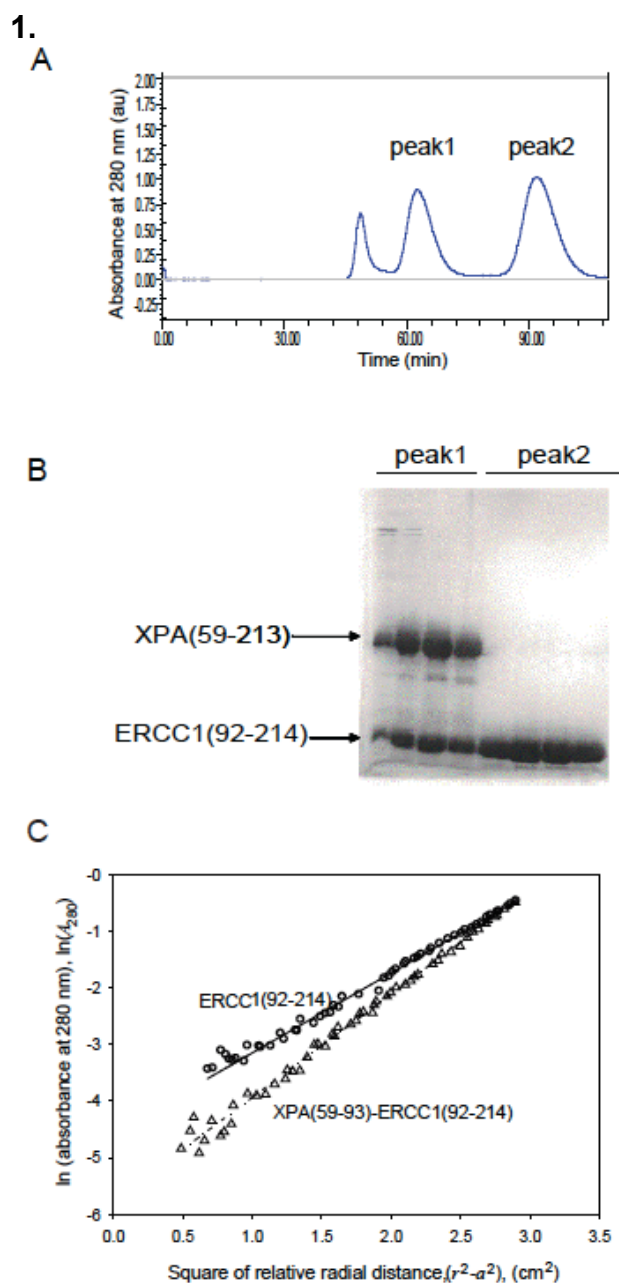
X-ray diffraction and refinement without using NMR data

Space group	I4 ₁ 32
Unit cell parameters	a = b = c = 128.6 Å
Number of XPA-ERCC1 complexes per a.u.	1
Resolution	40 – 4.1 Å (4.3-4.1 Å) ^a
I/σ	16.8 (6.0)
Redundancy	10.5 (10.5)
R _{merge}	0.15 (0.41)
Number of unique reflections	1538
R/R _{free} without XPA, prior to refinement using NMR data	0.33/0.38

NMR and refinement using X-ray data

Total NOE Distance Restraints	109
Intermolecular (ERCC1—XPA)	18
Intramolecular (XPA)	91
Intraresidue	61
Interresidue	30
Hydrogen Bond Restraints	1
Dihedral Angle Restraints	0
<RMSD> from mean structure (XPA 70-77) backbone/heavy atom (Å)	0.19/0.44
Ramachandran Plot (% residues)	
Most Favorable Region	77.6
Additionally Allowed Region	18.7
Generously Allowed Region	3.7
Disallowed Region	0

^a Data in parentheses indicate the highest resolution shell

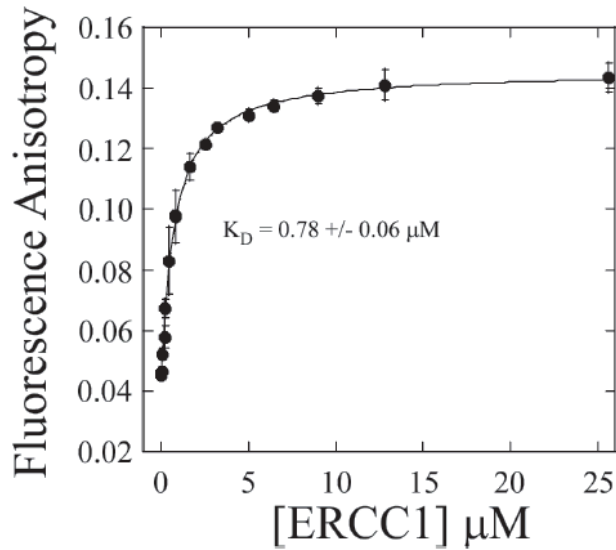


Suppl. Figure 1. **XPA₅₉₋₂₁₃ forms a stable 1:1 complex with the central domain of ERCC1.**

A) The complex of XPA₅₉₋₂₁₃ with ERCC1₉₂₋₂₁₄ was separated by gel filtration chromatography (S-100 column; Pharmacia) from an excess of ERCC1₉₂₋₂₁₄. The XPA-ERCC1 complex (peak 1) elutes before the unbound ERCC1 (peak 2). B) SDS-PAGE analysis of fractions corresponding to peaks 1 and 2 from the gel filtration experiment demonstrates the presence in peak 1 of XPA and ERCC1 at an approximately equimolar ratio of the two proteins.

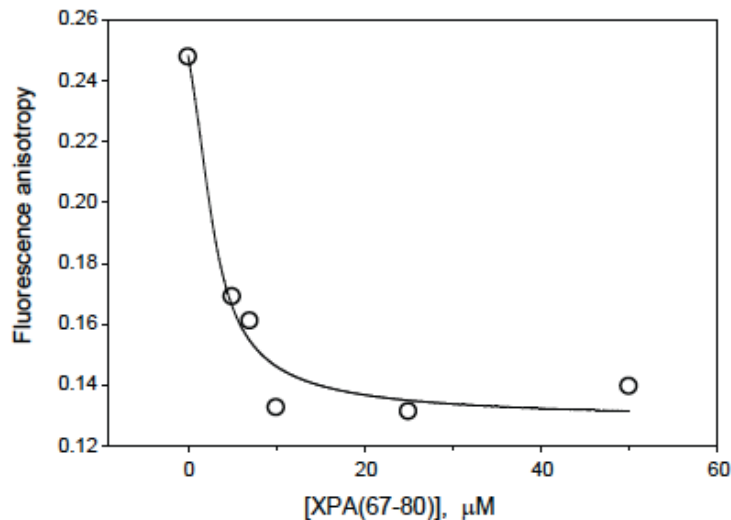
C) Sedimentation equilibrium analysis of ERCC1₉₂₋₂₁₄ (the central domain of ERCC1) alone and in complex with XPA₅₉₋₉₃. The natural logarithm of the absorbance at 280 nm is plotted *versus* the square of the relative radial position. The data for unbound ERCC1₉₂₋₂₁₄ (open circles) and its complex with XPA₅₉₋₉₃ (open triangles) are plotted in a similar matter. The curves represent the best fit of these data to Eq. 1 (Materials and methods), yielding molecular weights of 15 kDa for unbound ERCC1₉₂₋₂₁₄ and 19.4 kDa for ERCC1₉₂₋₂₁₄-XPA₅₉₋₉₃, in good agreement with the prediction for a 1:1 binding stoichiometry.

2.



Suppl Figure 2. **The XPA₆₇₋₈₀ peptide binds specifically to ERCC1₉₂₋₂₁₄.** The XPA₆₇₋₈₀ peptide labeled with 6FAM at the N-terminus (10 nM peptide) was mixed with ERCC1₉₂₋₂₁₄ at the concentrations shown. Peptide binding was recorded as an increase in the anisotropic fluorescence emission (calculated by the methods described in Material and methods). The binding isotherm of ERCC1 to the XPA₆₇₋₈₀ peptide was well fit by a simple hyperbolic 1:1 isotherm, yielding a K_D of $0.78 \pm 0.06 \mu\text{M}$.

3.



Suppl Figure 3. **The XPA₆₇₋₈₀ peptide is a competitive inhibitor of single-stranded DNA binding to ERCC1₉₂₋₂₁₄.** Binding of a 6FAM-labeled single-stranded DNA 40mer to the central domain of ERCC1 was monitored by fluorescence polarization of the labeled DNA. DNA binding activity is plotted as a function of added XPA₆₇₋₈₀ inhibitor. The theoretical curve given by Eq. 9 (solid line) corresponds to the best fit of the data to the dissociation equilibrium constant of 300 nM for the ERCC1-XPA complex.

Chapter 3:

The XPA-binding domain of ERCC1 is required for nucleotide excision repair but not other DNA repair pathways

Adapted from the manuscript by Barbara Orelli, T. Brooke McClendon, Oleg V. Tsodikov, Tom Ellenberger, Laura J. Niedernhofer and Orlando D. Schärer, published in "Journal of Biological Chemistry" in 2010, volume 285, pages 3705-3712.

Abstract

The endonuclease ERCC1-XPF incises the damaged strand of DNA 5' to a lesion during nucleotide excision repair (NER) and has additional, poorly characterized functions in interstrand crosslink (ICL) repair, double-strand break repair and homologous recombination. XPA, another key factor in NER, interacts with ERCC1 and recruits it to sites of damage. We identified ERCC1 residues that are critical for the interaction with XPA and assessed their importance for NER *in vitro* and *in vivo*. Mutation of two conserved residues (N110 and Y145) located in the XPA binding site of ERCC1 dramatically affected NER, but not nuclease activity on model DNA substrates. In ERCC1-deficient cells expressing ERCC1-N110A/Y145A, the nuclease was not recruited to sites of UV damage. The repair of UV-induced (6-4) photoproducts was severely impaired in these cells and they were hypersensitive to UV irradiation. Remarkably, the ERCC1-N110A/Y145A protein rescues the sensitivity of ERCC1-deficient cells to crosslinking agents. Our studies suggest that ERCC1-XPF engages in different repair pathways through specific protein-protein interactions and that these functions can be separated through the selective disruption of these interactions. We discuss the impact of these findings for understanding how ERCC1 contributes to resistance of tumor cells to therapeutic agents such as cisplatin.

Introduction

The preservation of the genetic information contained in DNA is essential for proper cell function and is ensured by multiple DNA repair pathways. Among these, nucleotide excision repair (NER) clears the genome of bulky, helix-distorting DNA lesions, such as those formed by UV-light, environmental mutagens and antitumor agents [126, 127]. Two subpathways of NER exist that differ in their method of damage recognition. In transcription-coupled repair (TC-NER), lesions in the transcribed strand of genes block the progression of RNA-polymerase II, triggering NER [26]. In global genome repair (GG-NER), helix-distorting lesions anywhere in the genome are recognized by the XPC-RAD23B heterodimer [128], in some cases with help of UV-DDB [129]. The subsequent steps of NER are believed to be similar for both subpathways and occur by the sequential assembly of the NER proteins at the site of the lesion [130-132]. Recruitment of TFIIH containing two helicase subunits XPB and XPD leads to the separation of the damaged and undamaged DNA strands [133, 134]. This enables subsequent NER factors to bind, including XPA, the single-stranded binding protein RPA and the endonuclease XPG [131]. The last factor to be recruited to this pre-incision complex is the endonuclease ERCC1-XPF [130, 135]. Once ERCC1-XPF is properly positioned on the DNA, via its interactions with XPA and RPA [136, 137], it incises the damage strand 5' to the lesion, followed by XPG making the 3' incision [138], allowing the replicative DNA polymerases and associated factors to fill the gap and restore the original DNA sequence [139-141].

Inherited defects in NER cause xeroderma pigmentosum (XP) characterized by extreme photosensitivity and risk of skin cancer [126]. Genetic defects in NER factors underlie additional disorders. Mutations in XPB, XPD, TTD-A and XPG (all associated with TFIIH) can cause Cockayne syndrome (CS), combined XP/CS or trichothiodystrophy (TTD), characterized by severe developmental defects and neurodegeneration, due to the additional role of these gene products in transcription [142]. Mutations in ERCC1 cause cerebro-oculo-

facio-skeletal syndrome, whereas mutations in XPF that severely affect protein expression cause accelerated aging (XFE, progeroid syndrome [143, 144]). Mice completely deficient in ERCC1-XPF also age rapidly and have a dramatically reduced life span [86, 145, 146]. The severe phenotype caused by deficiency of ERCC1-XPF, relative to XP, has been ascribed to the additional role of this NER factor in the repair of interstrand crosslinks (ICLs) [143].

The recruitment of ERCC1-XPF to various DNA repair pathways is predicted to be mediated through specific protein-protein interactions. The interaction between XPA and ERCC1 is essential for NER involving a region of XPA encompassing three consecutive glycines (residues 72-74) [147-149]. The structural basis for the interaction between XPA and ERCC1 was recently established [150, 151]. A short and unstructured peptide of XPA, XPA₆₇₋₈₀, including the three aforementioned glycine residues undergoes a disorder-to-order transition upon binding to the central domain of ERCC1 (**Figure 1**). This 14 amino acid stretch of XPA is necessary and sufficient to mediate its interaction with ERCC1 and the XPA₆₇₋₈₀ peptide can inhibit NER activity *in vitro* [150].

These findings prompted us to investigate how the XPA-binding region of ERCC1 contributes to NER activity and other DNA repair functions of ERCC1-XPF. Herein, we report mutations in the central domain of ERCC1 that severely impact NER activity *in vitro* and *in vivo*. Importantly, these mutations did not affect the ability of ERCC1-XPF to function in other DNA repair pathways. Our studies suggest that the roles of ERCC1-XPF can be separated by disrupting specific protein interactions that target the endonuclease to different DNA repair pathways.

Results

A short polypeptide from XPA (residues 67-80) binds in a groove on the central domain of ERCC1 spanning residues 105 to 160. Mutations that alter the strictly conserved XPA residues G72, G73, G74, or F75 abolish NER activity *in vitro* [150]. To study the functional role of the XPA-binding groove of ERCC1 in

NER and possibly ICL and DSB repair, we set out to design mutations in ERCC1 that would disrupt the interaction with XPA. Inspection of the XPA-binding site suggested that three absolutely conserved residues in ERCC1 might be important for this interaction (**Figure 1**): ERCC1 residue N110 packs against XPA residue F75, ERCC1 Y145 contacts XPA G74, and ERCC1 Y152 contacts XPA residues G73 and G72 (**Figure 2**). These ERCC1 residues are located on 3 different aspects of the pocket that accepts the XPA peptide, and their side chains contribute a substantial portion of the binding surface. ERCC1 residues N110, Y145 and Y152 were mutated to alanine using site-directed mutagenesis and we additionally generated the double mutants N110A/Y145A and Y145A/Y152A.

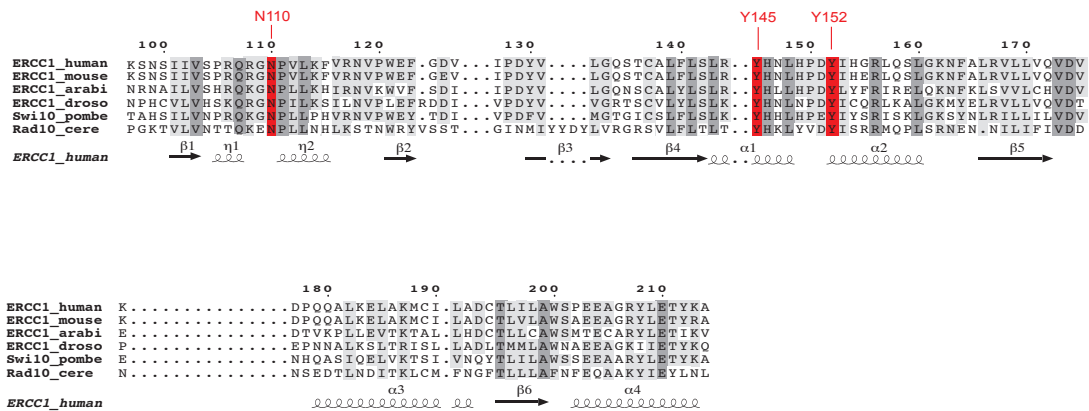


Figure 1. **Sequence alignment of the central domain of ERCC1** (residues 96-214). Absolutely conserved residues are highlighted in dark grey, highly conserved residues in light grey. The absolutely conserved N110, Y145 and Y152 that have been mutated in this study and that affect the interaction of ERCC1 with XPA are shown in red.

Mutations in the XPA-binding domain of ERCC1 affect NER, but not the nuclease activity of ERCC1-XPF

The mutant ERCC1 proteins were co-expressed with wild-type XPF in Sf9 insect cells, and the resulting heterodimers were purified in three

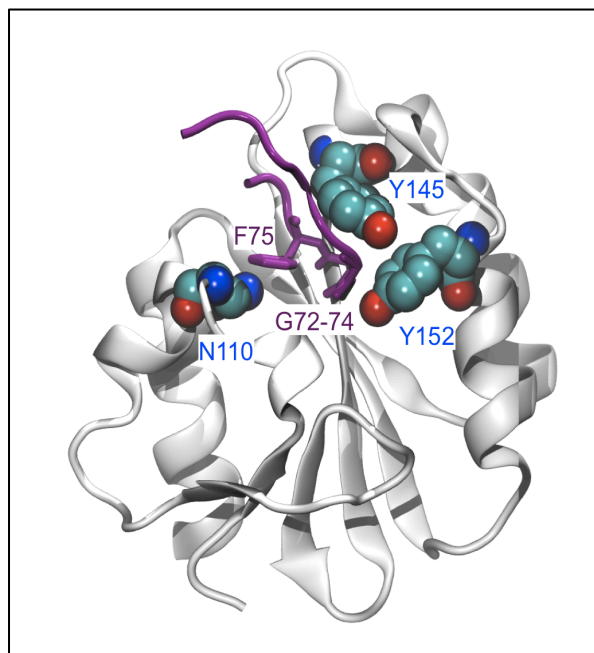


Figure 2. **Structure of an XPA peptide bound to the central domain of ERCC1.** ERCC1 is shown in gray, and the XPA peptide with the highly conserved residues 72-75 (GGGF) is shown in purple. Residues selected for site-directed mutagenesis in ERCC1 are high-lighted in atom color. The picture adapted from [3].

chromatographic steps using nickel-NTA, size exclusion and heparin columns [152]. All of the mutant ERCC1 proteins eluted from the size exclusion column as proper heterodimers (**Figure 3A**), indicating that mutations in the XPA-binding domain of ERCC1 did not disrupt the protein fold of ERCC1 or its interaction with XPF. All the proteins were judged to be >95% pure (**Figure 3B**).

We first tested the effects of the ERCC1 N110A, Y145A and Y152A mutations on the ability of ERCC1-XPF to incise DNA. The ERCC1 mutant protein complexes were incubated with a stem-loop DNA substrate in the presence of $MnCl_2$ [153] and the release of a 10-mer oligonucleotide product was detected by denaturing PAGE analysis (**Figure 4A**). ERCC1-XPF heterodimers containing mutant or wild-type ERCC1 subunits processed this model DNA substrate with similar efficiencies, cleaving at the ss/dsDNA junction of the stem loop. These results indicate that mutation of the N110, Y145 and Y152 residues in ERCC1 does not affect the DNA binding and nuclease activities of the ERCC1-XPF heterodimer.

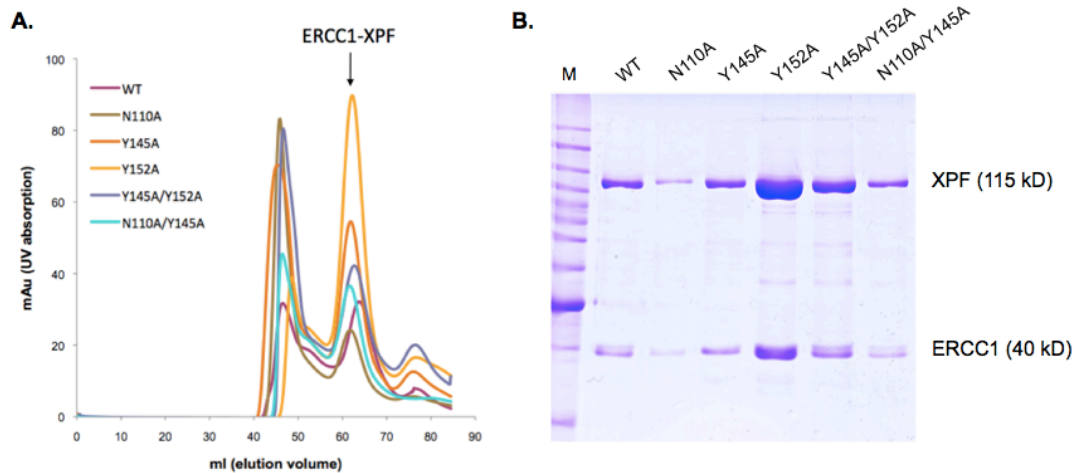


Figure 3. **Purification of wild-type and mutant ERCC1 proteins.** A) Overlay of chromatograms after size-exclusion purification of wild-type and mutant ERCC1 proteins in complex with wild-type XPF. The heterodimer ERCC1-XPF complexes (1:1) eluted around 65 mL elution volume (second peak, marked with an arrow). The first peak (around 42 mL elution volume) corresponds to protein in aggregated state and the third peak (~ 75 mL) to single ERCC1 molecules. B) 10% SDS-denaturing gel of the purified ERCC1-XPF complexes after 3 purification steps (Nickel-NTA agarose, gel filtration and heparin). Molecular weights of ERCC1 and XPF are indicated. M: BenchMark protein ladder.

We next tested the effects of these mutations on NER activity in cell free extracts. A plasmid containing a site-specific 1,3-intrastrand cisplatin DNA crosslink was incubated with a cell-free extract from XPF-deficient cells (XP-F cells are devoid of both XPF and ERCC1 proteins [154-156]) that was complemented with recombinant ERCC1-XPF proteins containing wild-type or mutant ERCC1 subunits [157]. The unsupplemented XP-F cell extract lacked detectable NER activity (**Figure 4B**, lane 1). The addition of ERCC1-XPF wild-type protein to the extract restored NER activity, generating the characteristic excision products of 24-32 nucleotides in length (**Figure 4B**, lane 2 and 3). All mutations in the XPA-binding site of ERCC1 led to a decrease in NER activity, with the strongest effects observed for the ERCC1-N110A single, ERCC1-Y145A/Y152A and ERCC1-N110A/Y145A double mutants (**Figure 4B**, lanes 4-13). The activity of ERCC1-N110A/Y145A was only slightly above the background level measured with the catalytically inactive mutant XPF-D720A

[138] (**Figure 4B**, lane 14-15). These results demonstrate that an intact XPA-binding pocket in ERCC1 is required for NER activity *in vitro*.

XPA-binding mutants of ERCC1 do not localize to sites of UV damage

Having established that the XPA-interaction mutants of ERCC1 are defective in NER *in vitro*, we assessed whether they prevent the recruitment of ERCC1-XPF to sites of UV damage in living cells. Based on the *in vitro* results (**Figure 4**), we chose the ERCC1-N110A, ERCC1-Y145A and ERCC1-N110A/Y145A mutants for the cellular studies. ERCC1-deficient UV20 CHO cells [158] were transduced with recombinant lentiviral vectors expressing mutant and wild-type ERCC1 cDNAs [138, 159]. Immunoblotting revealed that the transduced UV20 cells stably expressed human ERCC1 protein (**Figure 5A**). UV20 cells expressing wild-type and mutant ERCC1 were UV-irradiated through a polycarbonate filter with 5 μ m pores to generate a pattern of localized DNA damage that could be visualized by immunofluorescence microscopy [130]. One hour after UV irradiation, the cells were fixed and the presence of (6-4) photoproducts [(6-4)PPs] and of ERCC1 at sites of UV damage was monitored by immunofluorescence. As expected, UV20 cells expressing wild-type ERCC1 showed nearly complete (~90%) co-localization of the nuclease with sites of (6-4)PPs (**Figure 5B**). By contrast, the single mutants ERCC1-N110A or ERCC1-Y145A showed less efficient co-localization with UV lesions. ERCC1-N110A was detected at 23%, ERCC1-Y145A at only 9% of the sites of UV damage (**Figure 5C**). ERCC1-N110A/Y145A was observed at sites of UV damage in less than 3% of the cases (**Figures 5B and C**), even if this protein accumulates in the nucleus. These results further support the conclusion that the reduced NER activity of these ERCC1 mutants is due to their failure to interact with XPA.

UV lesions persist in cells expressing ERCC1-N110A/Y145A

To further test the conclusion that the recruitment of ERCC1-N110A/Y145A to NER complexes was impaired, we measured the rate of UV

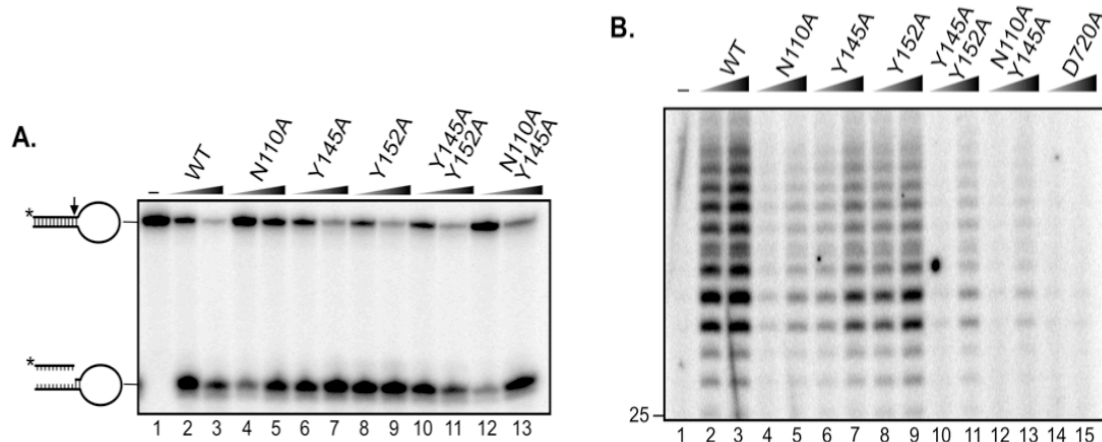


Figure 4. **Mutations in the XPA-binding domain of ERCC1 affect NER activity but not nuclease activity *in vitro*.** A) Incision of a stem loop substrate by wild-type and mutant ERCC1-XPF. A 5-³²P-labeled stem-loop DNA substrate (6.7 nM) was incubated with 6.7 nM (lanes 2, 4, 6, 8, 10, and 12) or 26.8 nM (lanes 3, 5, 7, 9, 11, and 13) ERCC1-XPF in the presence of 0.4 mM MnCl₂. B) NER activity of wild-type and mutant ERCC1-XPF. A plasmid containing a site-specific 1,3-intrastrand cisplatin DNA cross-link (50 ng) was incubated with a whole cell extract from ERCC1-XPF-deficient cells (XP2YO) complemented with recombinant ERCC1-XPF containing the indicated mutations in ERCC1 (N110A, Y145A, Y152A) or XPF (D720A). The excised DNA fragments of 24–32 nucleotides were detected by annealing a complementary oligonucleotide containing a non-complementary 4G overhang and filling in with [α -³²P]dCTP. Protein concentrations of ERCC1-XPF were 13.4 nM (lanes 2, 4, 6, 8, 10, 12 and 14) and 53.6 nM (lanes 3, 5, 7, 9, 11, 13, and 15). A labeled low molecular weight DNA ladder (New England Biolabs) was used as a marker. The position of a 25-mer is indicated.

lesion repair in ERCC1-deficient UV20 cells and UV20 cells expressing either wild-type ERCC1 or ERCC1-N110A/Y145A. Cells were UV-irradiated to generate sites of local DNA damage, fixed at various time points after irradiation and the amount of damage remaining was assessed by immunodetection of (6-4)PPs. Immediately after UV irradiation, 45-55% of the cells contained (6-4)PPs, indicating the fraction of cells where a filter pore overlapped with the nucleus (**Figure 6A**). At 24 hrs, 15% of the UV20 cells still stained positively for (6-4)PPs (**Figure 6B**). This defines the rate of removal of (6-4)PPs from the genome in the absence of NER. 6-4PPs are likely diluted out during cells division in 24hrs (UV20 cells have a doubling time of approximately 12 hrs) or are perhaps eventually removed by other pathways such as homologous recombination. Expression of wild-type ERCC1 in UV20 cells led to a dramatic increase in the rate of (6-4)PPs removal, with only 5% of nuclei containing foci 4 hrs post-

irradiation and 0% by 8 hrs post-irradiation. By contrast, the slope of the curve indicating removal of (6-4)PPs in cells expressing ERCC1-N110A/Y145A closely resembled that of untransduced UV20 cells, indicating that NER is severely affected if the XPA-ERCC1 interaction is disrupted.

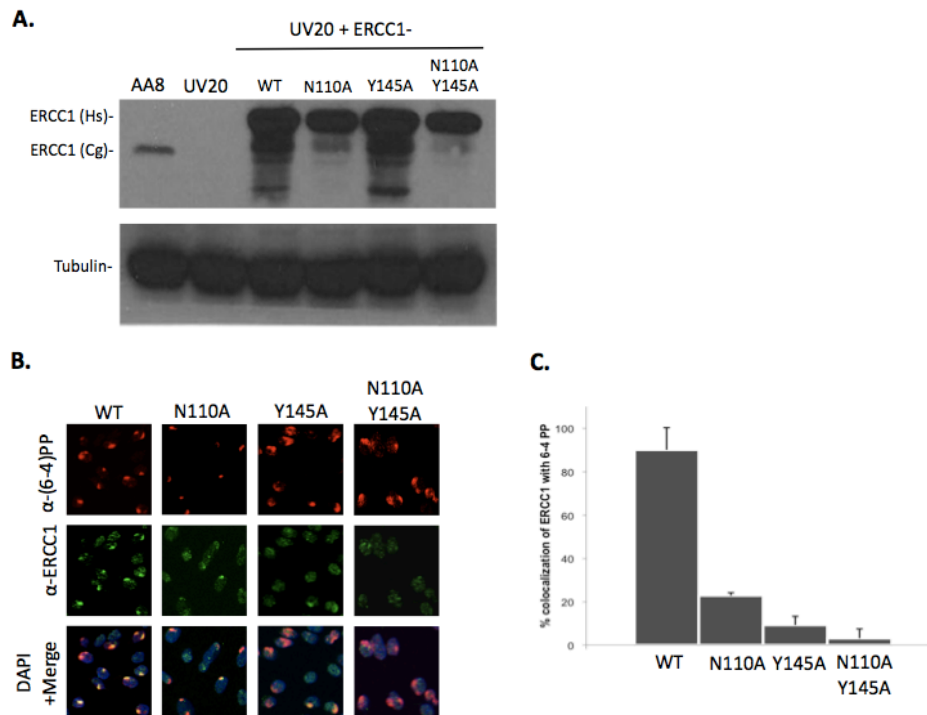


Figure 5. Mutations in the XPA-binding domain of ERCC1 affect its recruitment to sites of UV damage. A) Expression levels of ERCC1 in transduced UV20 cells. Transduced cells express human ERCC1 tagged with hemagglutinin. Note that human ERCC1 has a slower mobility than the CHO protein due to larger size (297 amino acids versus 293 amino acids) and the presence of the hemagglutinin tag. Tubulin was used as a loading control. B) ERCC1-deficient CHO cells were transduced with wild-type or mutant ERCC1 and irradiated with UV light (120 J/m^2) through a polycarbonate filter with $5 \mu\text{m}$ pores and then fixed and stained for ERCC1 (green) and (6-4)PPs (red). The nuclei were stained with DAPI (4'-6'-diamino-2-phenylindole) (blue). C) Graphical representation of the percentage of co-localization of ERCC1 with (6-4)PPs in UV20 cells expressing various mutants of ERCC1. Data represent the average of at least three independent experiments \pm S.D. (error bars). 100 cells were counted for each experiment.

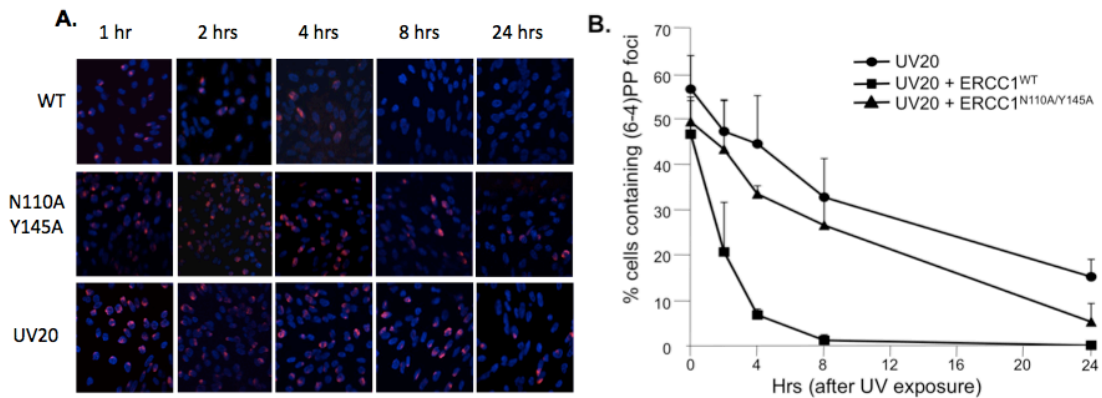


Figure 6. **UV damage persists in UV20 cells expressing ERCC1-N110A/Y145A but not wild-type ERCC1.** A) untransduced UV20 cells or cells expressing wild-type ERCC1 or ERCC1-N110A/Y145A were UV-irradiated as described in the legend for Fig. 5, cultured for 0, 1, 2, 4, 8, or 24 hrs following UV irradiation, and then fixed and stained for (6-4)PP. B) graphic representation of the percentage of cells with persistent (6-4)PPs at various time points. Data represent the average of at least three independent experiments \pm S.D. (error bars). 100 cells were counted for each experiment.

Mutations in the XPA-binding domain of ERCC1 inhibit NER, but not ICL or DSB repair

Having established the importance of the XPA-binding domain of ERCC1 for NER, we wished to determine if this domain is also important for other DNA repair activities of ERCC1-XPF. To test this, UV20 cells expressing wild-type ERCC1, ERCC1-N110A, ERCC1-Y145A or ERCC1-N110A/Y145A were tested for their sensitivity to UV irradiation, crosslinking agents (mitomycin C and cisplatin) and ionizing radiation by clonogenic survival assays (**Figure 7**). As expected, untransduced UV20 cells were hypersensitive to all of these genotoxins relative to parental wild-type AA8 cells. Furthermore, expression of wild-type ERCC1 corrected the sensitivity to all genotoxins. Cells expressing either ERCC1-N110A or ERCC1-Y145A showed slightly increased sensitivity to UV compared to wild-type cells and corrected UV20 cells. However, UV20 cells transduced with ERCC1-N110A/Y145A were significantly more sensitive to UV than either AA8 or corrected cell lines, although not as sensitive as UV20 cells, demonstrating that mutations in the XPA-interacting domain of ERCC1 affect

long-term survival following exposure to UV irradiation. Interestingly, all of the ERCC1 mutations studied here supported normal resistance to mitomycin C (**Figure 7B**), cisplatin (**Figure 7C**), and ionizing radiation (**Figure 7D**) at levels comparable to AA8 cells or UV20 cells expressing wild-type ERCC1. These observations provide direct experimental evidence that the ERCC1-XPA interaction is required only for NER and not for ICL and DSB repair activities. The data of the ERCC1-N110A/Y145A mutant demonstrate that the functions of ERCC1-XPF in NER can be separated from its functions in ICL and DSB repair by selectively blocking its interaction with XPA.

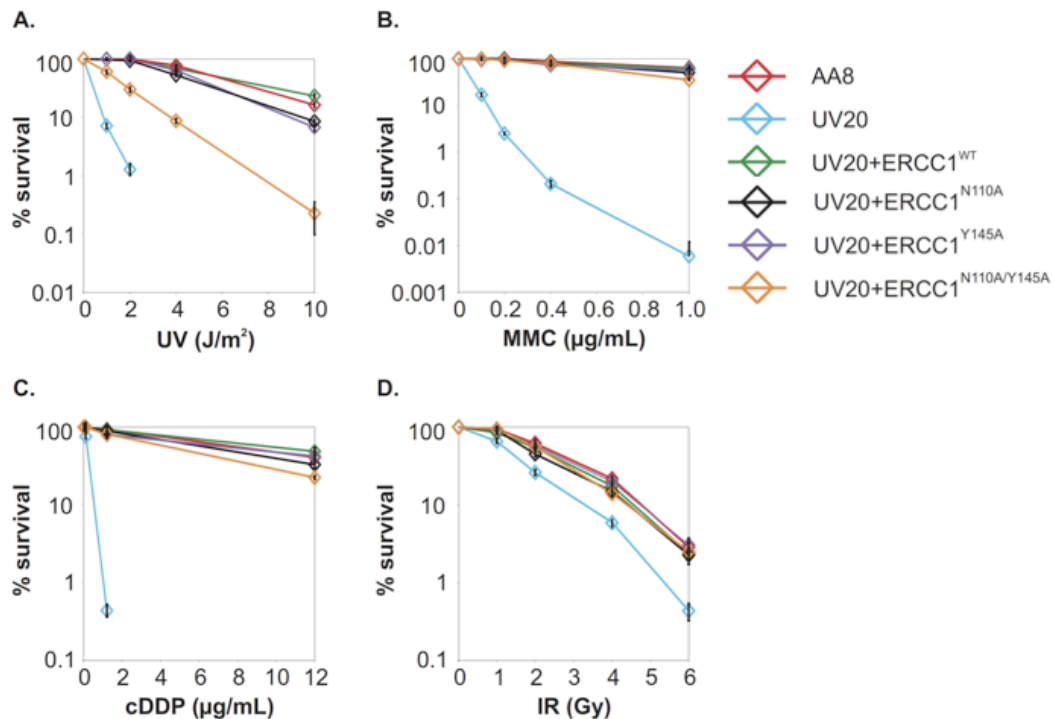


Figure 7. **Mutations in the XPA-binding domain of ERCC1 inhibit NER but not ICL or DSB repair.** A–D) clonogenic survival assays to measure the sensitivity of CHO cell lines AA8 (WT) (red diamonds), *Erc1*-deficient UV20 (blue diamonds), and UV20 expressing ERCC1-WT (green diamonds), ERCC1-N110A (black diamonds), ERCC1-Y145A (purple diamonds), or ERCC1-N110A/Y145A (yellow diamonds) to UV-C (A), mitomycin C (MMC) (B), cisplatin (C), or ionizing radiation (D). The data are plotted as the percentage of colonies that grew on the treated plates relative to untreated plates \pm S.E. (error bars). cDDP, cis-diamminedichloroplatinum(II). Experiments performed by T. Brooke McClendon.

Discussion

Known functional domains of ERCC1-XPF

ERCC1-XPF is a structure-specific endonuclease that cleaves at junctions between single-stranded and double-stranded DNA, incising 3' ssDNA overhangs. Genetic and biochemical data demonstrate the importance of ERCC1-XPF in multiple genome maintenance mechanisms including NER, ICL repair, double-strand break repair and telomere biology [160-163]. Several functional domains have been identified in the ERCC1-XPF heterodimer: the two proteins interact through two helix-hairpin-helix (HhH) domains at their C-termini [111] and these domains are also implicated in DNA binding [117, 151, 164, 165]. Adjacent to the (HhH)₂ domain, XPF contains the active site nuclease domain [152]. The N-terminal half of XPF is made up of an SF2 type helicase-like domain. This domain lacks conserved ATP-binding domains and is deficient in ATP binding and helicase activity with a possible role in ss/dsDNA junction binding [118, 166]. ERCC1, although evolutionarily related to XPF, is considerably smaller, lacking the helicase domain [76]. The N-terminal region of ERCC1 is of unknown structure and function that is expendable for NER [111]. Its central domain is structurally homologous to the nuclease domain of XPF, but lacks the essential acidic residues of the active site [76, 165]. Instead, the groove contains basic and aromatic residues and appears to have ssDNA binding activity [165, 167].

Our present knowledge of ERCC1-XPF therefore suggests a number of interaction sites with DNA, but less is known about how ERCC1-XPF is recruited to different DNA repair pathways through protein-protein interactions. The only protein whose interaction with ERCC1 is understood in some detail is XPA [147-149]. Structural studies of the XPA peptide bound to ERCC1 show that it contacts ERCC1 through a conserved GGGF motif and that it undergoes a disorder-to-order transition upon binding ERCC1 [150, 151].

Conserved residues in the XPA-binding domain of ERCC1 are required for NER, but not other DNA repair pathways

In the present study we demonstrated the importance of the XPA-binding pocket in the central domain of ERCC1 for NER activity, but not other DNA repair functions. Among the proteins with mutations in the XPA-binding pocket in ERCC1 investigated, ERCC1-N110A/Y145A showed the most severe effects and was almost completely devoid of NER activity *in vitro* and *in vivo* (**Figures 2B, 4**). This defect in NER is due to a weakened interaction with XPA, since the protein is not recruited to sites of UV damage in cells (**Figure 3**) while the nuclease activity of ERCC1-N110A/Y145A-XPF protein is unaffected (**Figure 2A**). UV20 cells that lack functional ERCC1 protein are sensitive to UV irradiation, the crosslinking agents cisplatin and mitomycin C and to ionizing radiation. Expression of ERCC1-N110A/Y145A, which is devoid of NER activity, corrects the defects in other repair processes (**Figure 5**) demonstrating a clear separation of function in ERCC1-XPF. We speculate that these point mutations in a transgenic animal would result in a mild phenotype like NER-deficient *Xpa*^{-/-} mice [168] rather than the severe phenotype of *Ercc1*^{-/-} or *Xpf*^{-/-} mice [86, 143, 145, 146].

How is ERCC1-XPF recruited to DNA repair pathways other than NER?

While these data and our previous work [150] defined the region in ERCC1 required for its function in NER through interaction with XPA, we know less about how ERCC1-XPF is recruited to sites of ICL and DSB repair. Several additional protein partners were reported for ERCC1 and XPF. ERCC1 interacts with the mismatch repair protein MSH2 and it has been suggested that MSH2 and ERCC1 work together in a replication-independent ICL repair pathway [169, 170]. However, the sensitivity of MSH2-deficient cells to crosslinking agents is much less pronounced than that of ERCC1-deficient cells [171], making it unlikely that the interaction with MSH2 is required for the major ICL repair pathways. XPF is also reported to interact with hRad52, an association that might

direct ERCC1-XPF to sites of homologous recombination or single-strand annealing [172].

The *Drosophila* homolog of XPF, MEI-9, interacts with ERCC1 as well as MUS312. MUS312 mutants and a MEI-9 mutant are hypersensitive to crosslinking agents but not UV irradiation, strongly suggesting a role in ICL repair [173]. Recent studies have identified SLX4 as a human homolog of MUS312 [174-177]. SLX4 interacts with a number of endonucleases, including ERCC1-XPF, MUS81-EME1 and SLX1. It is therefore likely that SLX4 serves as a platform to coordinate the activity of various endonucleases and has a key role in targeting ERCC1-XPF to sites of ICL repair.

Which function of ERCC1-XPF causes resistance to cisplatin in tumor cells?

In addition to its role in protecting cells against the deleterious effects of DNA damage, ERCC1 is a potential target for cancer chemotherapy. Numerous studies have correlated the levels of ERCC1 in tumors as well as polymorphisms in the ERCC1 gene with response to platinum-based chemotherapy and survival [178, 179]. A common perception is that this resistance to cisplatin is due to enhanced levels of NER [180]. By contrast, other studies have indicated that the treatment of cells with siRNA against ERCC1, but not against XPA, renders cells sensitive to crosslinking agents [181]. Our studies show directly that a defect in the interaction between ERCC1 and XPA that disrupts NER has no major effect on the cellular sensitivity to the chemotherapeutic agents cisplatin and MMC. It therefore appears that NER mediated by ERCC1 is not a key determinant of cellular sensitivity to cisplatin. Cisplatin, like other ICL-forming agents, forms a variety of adducts including 1,2 and 1,3-*intrastrand* crosslinks as well as 1,2-*interstrand* crosslinks [182]. Among these the 1,3-*intrastrand* crosslink is an excellent NER substrate, while the major, but less distorting 1,2-*intrastrand* cisplatin adduct is less well repaired by NER and may be shielded from NER by additional proteins [183-188]. The 1,2-*interstrand* cisplatin on the other hand does not appear to be recognized by the NER machinery at all [184]. The

sensitivity of ERCC1-deficient cells to cisplatin is therefore almost certainly due to the presence of the 1,2-*interstrand* crosslinks, where ERCC1-XPF plays a role in the unhooking and/or homologous recombination step [161, 189]. These observations again emphasize the importance of finding additional sites for protein-protein interactions in ERCC1-XPF and interacting proteins that target the heterodimer to sites of ICL and DSB repair.

Materials and methods

Protein expression and purification

Site-directed mutagenesis was used to introduce point mutations in pFastBac1-ERCC1 (QuickChange kit) as described in [152]. ERCC1 wild-type, ERCC1-N110A, ERCC1-Y145A, ERCC1-Y152A, ERCC1-N110A/Y145A and ERCC1-Y145A/Y152A were co-expressed with wild-type XPF in Sf9 insect cells. The heterodimers were purified over nickel affinity, size-exclusion and heparin chromatography as described [152]. Protein concentrations ranged from 0.1 to 0.3 mg/ml.

Nuclease assay

Nuclease assays of wild-type and mutant ERCC1-XPF on a stem-loop substrate were carried out as described [83, 152]. A substrate consisting of a 12 base-pair stem with a 22 nucleotide loop (5'-GCCAGCGCTCGGT22CCGAGCGCTGGC) was 5' end-labeled using T4 polynucleotide kinase and [α -³²P]-ATP. The DNA substrate (100 fmol) was suspended in nuclease buffer (15 μ l: 25 mM Tris-HCl pH 8.0, 40 mM NaCl, 10% glycerol, 0.5 mM β -mercaptoethanol, 0.1 mg/ml BSA) containing 0.4 mM MnCl₂, then incubated with ERCC1-XPF (100 or 400 fmol). The reactions were incubated at 30°C for 15 min then stopped by adding 10 μ l of loading dye (90% formamide, 10 mM EDTA) and heating at 95°C for 5 min. Samples were separated by 15% denaturing PAGE (0.5x TBE) and the reaction products were

visualized using a PhosphorImager (Typhoon 9400; Amersham Biosciences).

In vitro NER assay

XPF-deficient cell extracts and the plasmid containing a 1,3-intrastrand cisplatin adduct were prepared and NER assays carried out as described [157, 159]. 3 μ l of XP-F cell extract in 100 mM KCl was combined with 2 μ l of 5x repair buffer (200 mM Hepes-KOH, 25 mM MgCl₂, 110 mM phosphocreatine [di-Tris salt, Sigma], 10 mM ATP, 2.5 mM DTT and 2 mg/ml BSA, pH 7.8), 0.2 μ l 2.5 mg/ml creatine phosphokinase (rabbit muscle CPK, Sigma) and either purified ERCC1-XPF and/or NaCl (to a final NaCl concentration of 70 mM) and incubated at 30°C for 10 min. Then 1 μ l of closed circular plasmid DNA (50 ng) containing a 1,3-intrastrand cisplatin crosslink was added and the mixture incubated at 30°C for 45 min. After placing the samples on ice, 0.5 μ l of 1 μ M 35-mer oligonucleotide that anneals to the excision product (5'-GGGGGAAGAGTGCACAGAAGAAGACCTGGTTCGACCP-3') was added and the mixture heated to 95°C for 5 min. The samples were allowed to cool to room temperature for 15 min to allow annealing. 1 μ l of a Sequenase/[α -³²P]-dCTP mix (0.5 units of Sequenase and 2.5 μ Ci of [α -³²P]-dCTP per reaction) was added. After incubating at 37°C for 3 min, 1.2 μ l of dNTP mix (100 μ M of each dATP, dTTP, dGTP; 50 μ M dCTP) was added and the mixture incubated for another 12 min to extend the excised product with radiolabeled dCTP. The reactions were stopped by adding 8 μ l of loading dye (90% formamide, 10 mM EDTA) and heating at 95°C for 5 min. The samples were loaded on a 14% sequencing gel (0.5x TBE) and run at 45 W for 2 hrs. The reaction products were visualized using a PhosphorImager (Typhoon 9400, Amersham Biosciences).

Cell culture

Human fibroblast cells XP2YO (XPF-deficient, GM08437) were cultured at 37°C in a 5% CO₂ humidified incubator in Dulbecco's Modified Eagle's Medium (DMEM, Invitrogen) supplemented with 10% fetal bovine serum, 2 mM L-glutamine, 100 U/ml penicillin and 0.1 mg/ml streptomycin. Chinese hamster

ovary cells (CHO) AA8 (wild-type), UV20 (ERCC1-deficient) and UV20 transduced with a lentiviral vector expressing wild-type or mutant hERCC1 were cultured in DMEM supplemented with 10% fetal bovine serum (Atlanta Biologicals), 1% penicillin-streptomycin and 1% nonessential amino acids (Gibco).

Lentiviral cell transduction

The cDNA of wild-type ERCC1, ERCC1-Y145A, ERCC1-N110A, and ERCC1-N110A/Y145A were cloned into the lentiviral vector pWPXL by substituting the GFP cDNA. 293T cells were co-transfected with the lentiviral vector containing the different constructs, the packaging plasmid psPAX2 and the envelope plasmid pMD2G. Details of the vectors, the production of high-titer viruses and lentiviral transduction can be found through LentiWeb and in [190, 191]. UV20 CHO cells at 50% confluency were infected with the viral particles containing the different ERCC1 recombinant constructs with an MOI of 10 and cultured as described above. The transduction efficiency was assessed by immunofluorescence.

Local UV irradiation and immunofluorescence

Cells were seeded and cultured on glass coverslips and processed as described [130]. Briefly, cells were covered with a polycarbonate filter with 5 μm pores (Millipore) and irradiated with 120 J/m^2 using a UV-C Lamp (EL Series, UVP, Model UVLS-28). After a recovery period, the cells were washed with PBS, permeabilized with 0.2% Triton X-100 in PBS for 30 sec then fixed with 3% paraformaldehyde containing 0.2% Triton X-100 for 15 min at RT. Cells were washed with PBS containing 0.1% Triton five times. To detect (6-4)PPs, cells were treated with 0.07M NaOH in PBS for 5 min and washed. Cells were blocked with PBS+ (PBS containing 0.15% glycine and 0.5% BSA) for 30 min then incubated with the primary antibodies (mouse monoclonal antibody 64M-2 against (6-4)PP (kindly provided by Stuart Clarkson, Geneva, Switzerland), 1:400; rabbit polyclonal antibody FL-297 against ERCC1 (Santa Cruz

Biotechnology), 1:300, diluted in PBS+) for 2 hrs under dark and humid conditions. After washing out the antibodies with PBS containing 0.1% Triton, cells were quickly blocked with PBS+ and incubated with the secondary antibodies (Cy3-conjugated goat anti-mouse (Jackson ImmunoResearch), 1:1500; Alexa-488 conjugated goat anti-rabbit (Molecular Probes, Invitrogen), 1:800, diluted in PBS+) for 1 hr under dark and humid conditions. After a final wash with PBS containing 0.1% Triton the samples were embedded in Vectashield mounting medium (Vector) containing DAPI (4'-6'-diamino-2-phenylindole) at a concentration of 0.1 mg/ml. Cells were analyzed using a confocal microscope (Zeiss LSM 510). For quantification, at least 100 cells were analyzed and counted each in three independent experiments.

Clonogenic survival assays

Exponentially growing cells were plated in triplicate in 6 cm dishes at 250-5,000 cells per plate depending on the cell line and dose of genotoxin used. After allowing the cells to adhere overnight, they were exposed transiently to genotoxins. For UV, the media was removed; the cells were washed with PBS, irradiated with UV-C (254 nm), then the media replenished. For MMC or cDDP, the cells were treated with media containing the drug for 1 h at 37°C, then washed twice with PBS and incubated in drug-free media. To measure ionizing radiation sensitivity, cells were irradiated with a ¹³⁷Cs source. Four days after exposure, the cultures were fixed and stained with 50% methanol, 7% acetic acid and 0.1% Coomassie blue. Colonies (defined as ≥20 cells) were counted using a Nikon stereomicroscope with 10x eyepiece. The data were plotted as the number of colonies that grew on the treated plates relative to untreated plates ± SEM for a minimum of two independent experiments.

Immunoblotting

Cells were trypsinized, washed with PBS, and lysed with 100 µl NETT buffer (100 mM NaCl, 50 mM Tris base pH 7.5, 5 mM EDTA pH 8.0, 0.5% Triton X-100) containing Complete™ mini protease inhibitor cocktail (Roche Molecular

Biochemicals). 60 μ g of protein was resolved by SDS-PAGE (8%) and transferred to a nitrocellulose membrane. ERCC1 was detected with antibody D-10 (for both human and hamster, 1:100, Santa Cruz), or FL-297 (human only, 1:200, Santa Cruz). Tubulin (1:200, Abcam) was used as a loading control. Secondary antibodies used were: goat anti-rabbit IgG HRP (1:5000, Promega) and goat anti-mouse IgG HRP (1:5000, Promega).

Acknowledgments

I would like to thank Arthur J. Campbell for help with Figure 1.

Chapter 4:

Repair efficiency of ERCC1 and XPA mutants on different NER lesions

Introduction

NER recognizes and repairs a large number of structurally diverse lesions, such as those formed by UV-light and environmental mutagens [21]. The striking versatility of NER suggested that the NER machinery does not recognize lesions *per se* but rather conformational abnormalities in the DNA induced by them. It was shown that chemical modifications of bases were not the only determinant to trigger NER [192]. Helical distortion and thermodynamic destabilization that disturb normal base-pairing were shown to be parameters that induce repair by NER. Consequently, a “bipartite model of substrate discrimination” has been proposed positing that NER recognizes thermodynamic destabilization of the DNA helix in a first step and subsequently verifies the presence of a chemical alteration [192, 193]. It was further shown that the distortion and degree of thermodynamic destabilization of the DNA was responsible for the recruitment of NER factors and proportional to the repair efficiency [194-197]. It is so far believed that the binding affinity of the recognition factor XPC-RAD23B to the damaged DNA is the key determinant of the NER reaction [193, 198, 199]. By contrast the question to what extent the nature of the lesion affects subsequent steps in NER has received less attention.

The work of my thesis is concerned with one late step in NER, the XPA-mediated recruitment of the endonuclease ERCC1-XPF to NER complexes. Recruitment of ERCC1-XPF triggers incision of the damaged strand 5' to the lesion, the recruitment of the replication machinery and the second incision performed by the endonuclease XPG [57, 200, 201]. The interaction between XPA and ERCC1 is essential for NER [46, 106, 202] and based on the structural characterization of this interaction [3, 151] we identified residues in both ERCC1 and XPA that are critical for NER activity [3, 202]. The ERCC1-binding region of XPA contains a conserved motif that consists of three consecutive glycines (G72-74) and a highly conserved phenylalanine (F75) and mutations or deletions in this region in XPA abolish NER activity *in vitro* [3, 106]. In this chapter we investigated the effect of mutations of the ERCC1-XPA interaction *in vitro* and *in*

vivo. We thus provide the first evidence that the nature of the lesions affects specific interactions between NER proteins in late steps of the NER reaction.

Results

ERCC1-binding mutants of XPA are able to recruit ERCC1-XPF to sites of UV damage...

Mutating or deleting key residues of the conserved G-rich motif in the ERCC1-binding region of XPA resulted in severe defects in NER *in vitro* ([3], see Chapter 2). The inability of XPA mutant proteins (XPA-F75A, XPA- Δ G73 and XPA- Δ G73/ Δ G74) to restore the NER activity of an XPA-deficient cell extract was attributed to the weakened interaction between XPA and ERCC1. We therefore assessed whether mutations in XPA prevent recruitment of ERCC1-XPF to sites of UV lesions in living cells. XP-A cells were transduced with lentiviral particles containing wild-type and mutant XPA cDNAs. The expression and the stability of each XPA protein were evaluated by Western blot (**Figure 1**), indicating that all of the lentivirally transduced cells expressed XPA at similar levels. XP-A cells expressing either wild-type or mutated XPA protein were UV-irradiated through a polycarbonate filter containing 5 μ m pores to generate local UV lesions that can be detected by immunofluorescence microscopy [24]. One hour after UV irradiation, the cells were fixed, and the presence of 6-4 photoproducts (6-4PPs) and of ERCC1 at sites of UV damage was monitored by immunofluorescence. As expected, in cells expressing XPA-WT proteins ERCC1 was found to colocalize with UV photoproducts (**Figure 2A**). Surprisingly, in cells expressing XPA-F75A, ERCC1 also perfectly colocalized with sites of UV lesions (90% estimated colocalization) and cells expressing XPA- Δ G73 and XPA- Δ G73/ Δ G74 showed intermediate levels of ERCC1 recruitment to UV lesions (50-60% estimated colocalization) (**Figure 2A**). These results indicate that the single point mutation (F75A) or the deletion of one or two glycines in the highly conserved G-motif of XPA is not sufficient to disrupt the interaction between XPA and ERCC1 *in vivo*.

These observations suggest that interaction with another region of ERCC1 or interactions between ERCC1-XPF and other protein can compensate for the loss of contacts caused by the mutations or deletions in the GGGF-motif of XPA.

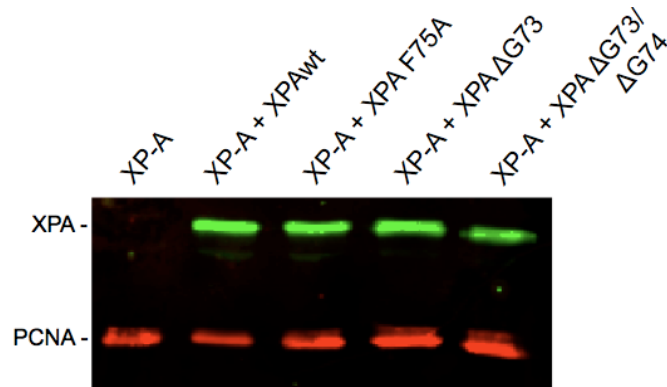


Figure 1. **Expression levels of XPA in transduced XP-A cells.** Transduced cells express XPA protein tagged with hemagglutinin (HA). 30 μ g protein were loaded on a 10% SDS-gel. XPA proteins were detected using a polyclonal rabbit antibody (1:800). PCNA was used as a loading control and detected using a monoclonal mouse antibody (Dako Cytomation, 1:1500).

...but they are deficient in repairing UV-lesions

Although XPA-F75A, XPA- Δ G73 and XPA- Δ G73/ Δ G74 were recruited to sites of UV damage in living cells, these proteins were unable to support NER *in vitro*. To determine whether these mutant XPA proteins support the repair of UV lesions *in vivo*, we analyzed the presence of UV lesions at 24 hours after UV irradiation. As expected, cells expressing wild-type XPA efficiently removed UV lesions and the ERCC1 protein was homogenously distributed throughout the nucleus (**Figure 2B**). By contrast, in cells expressing either XPA-F75A, XPA- Δ G73 or XPA- Δ G73/ Δ G74 the damage still persisted and ERCC1-XPF was found at sites of UV lesions at this time point (**Figure 2B**). These results show that despite the ability of the XPA mutants to recruit ERCC1-XPF to sites of UV damage, they are not able to repair UV lesions, confirming the defect in the NER activity of the XPA mutants established in *in vitro* experiments (see Chapter 2).

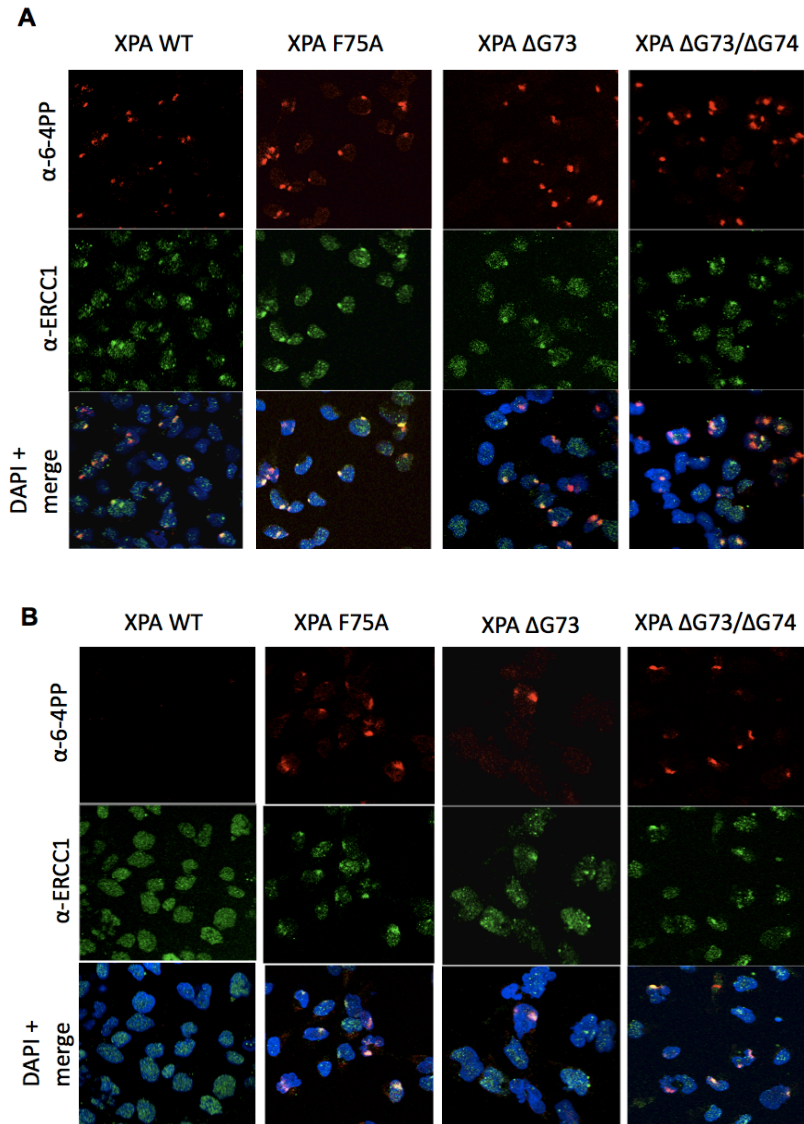


Figure 2. Mutations in the ERCC1-binding domain of XPA do not impair the recruitment of ERCC1 to sites of damage sites but affect the repair of UV lesions. A) XP-A cells expressing wild-type or mutant XPA were UV-irradiated at dose of 120 J/m² through a polycarbonate filter with 5 μm pores. One hour after UV exposure cells were fixed and stained for 6-4 photoproducts (red) and ERCC1 (green). The nuclei were stained with DAPI (blue). B) Same as in A except the cells were fixed and treated for immunofluorescence 24 hours after UV irradiation (120 J/m²).

The nature of the substrate affects late steps in NER

Having established that the ERCC1 and XPA mutants, containing mutations in the respective interacting domains, displayed impaired NER activity both *in vitro* and *in vivo*, we assessed whether the different NER lesions would influence the repair rates of the mutants. We have previously shown that the XPA₆₇₋₈₀ peptide acts as a specific inhibitor in the NER reaction of 1,3-intrastrand cisplatin lesions ([3], see Chapter 2). Similarly, XPA mutants, carrying mutations in the ERCC1-binding region, displayed only marginal *in vitro* NER activity on this substrate ([3], see Chapter 2). Like 1,3-intrastrand cisplatin crosslinks, acetylaminofluorene (AAF) adducts induce thermodynamic destabilization and a severe degree of distortion in the DNA helix and are therefore efficiently repaired by the NER machinery [203, 204]. We first compared the ability of the XPA₆₇₋₈₀ peptide to inhibit the NER activity of cisplatin or AAF adducts in HeLa cell-free extracts (**Figure 3A**). The XPA₆₇₋₈₀ peptide inhibited the excision of the platinated DNA substrate already in the low micromolar range (4.6 μ M), whereas a concentration of the peptide of 138 μ M (30-fold increase) was needed to obtain a similar degree of inhibition with the AAF substrate. To better understand whether this difference was specific to NER inhibition by this peptide or whether it was intrinsic to changes in the XPA-binding pocket of ERCC1, we compared the NER activity of the XPA-F75A mutant on cisplatin and AAF lesions. As expected, XPA-WT protein efficiently excised both lesions (**Figure 3B**, lanes 1-8), whereas neither lesion was repaired in the absence of XPA protein (data not shown). Interestingly, XPA-F75A, which we have previously shown to be completely deficient in processing cisplatin 1,3-intrastrand crosslinks (**Figure 3B**, lanes 9-12, [3]), showed reduced, but significant, repair activity on AAF substrates (**Figure 3B**, lanes 13-16). We also tested whether XPA- Δ G73 and XPA- Δ G73/ Δ G74 as well as ERCC1-N110A/Y145A, all of which had minimal or no NER activity on cisplatin adducts *in vitro* and 6-4PPs *in vivo*, were similarly able to repair AAF adducts. Intriguingly, all of these mutant XPA and ERCC1 proteins complemented the repair activity of AAF adducts in XPA- or ERCC1-deficient cell extracts to a significant degree (**Figure 3C**). These results demonstrate that

mutations in ERCC1 and XPA affect the repair of at least three different NER lesions in different ways. To best of our knowledge these data are the first demonstration that the nature of the substrate influences the rate of NER not only during the recognition and verification of the lesion, but also in subsequent steps in NER.

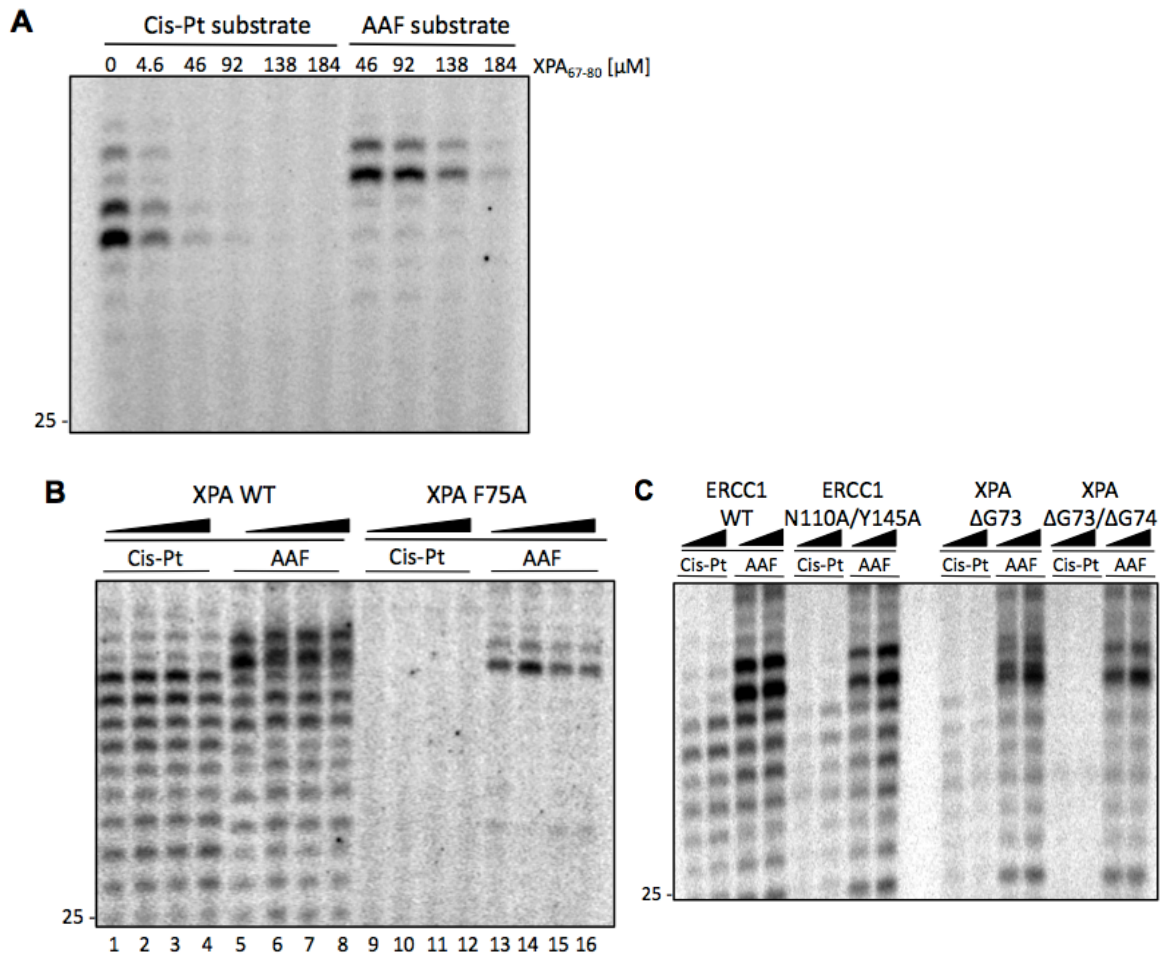


Figure 3. *In vitro* NER activity of ERCC1 and XPA mutants on cisplatin and AAF lesions. A) The *in vitro* NER inhibition of the XPA₆₇₋₈₀ peptide varies with different substrates. HeLa cell extract was incubated with increasing concentrations of the XPA₆₇₋₈₀ peptide in the presence of a plasmid containing either a 1,3-intrastrand crosslink or an AAF adduct. Products were visualized by a fill-in reaction following annealing to an oligonucleotide complementary to the excision product with a 4-nt overhang [4]. The marker DNA ladder is labeled Low Molecular Weight DNA ladder. B/C) XPA and ERCC1 mutants repair different lesions with different efficiency. In B, XP-A cell extract was complemented with either XPA WT or XPA F75A (lanes 1, 5, 9 and 13: 20 nM; lanes 2, 6, 10 and 14: 50 nM; lane 3, 7, 11 and 15: 80 nM; lanes 4, 8, 12 and 16: 110 nM) in the presence of a plasmid containing either a 1,3-intrastrand cisplatin crosslink or an AAF adduct. Products were visualized as in A). In C, XP-F cell extract was complemented with either ERCC1 WT or ERCC1 N110A/Y145A, XP-A cell extract was complemented with either XPA ΔG73 or XPA ΔG73/ΔG74 in the presence of a plasmid containing either a 1,3-intrastrand cisplatin crosslink or an AAF adduct. Protein concentrations were 20 and 80 nM. Products were visualized as in A).

Discussion

A second XPA-binding region in ERCC1?

In this chapter we have demonstrated that mutations in the highly conserved G-rich motif in XPA impair the repair of UV lesions. Although all the investigated XPA mutants were able to recruit ERCC1-XPF to sites of damage (**Figure 2A**), the lesions still persisted 24 hours after UV irradiation (**Figure 2B**). Preliminary clonogenic survival assays also showed high sensitivity of cells expressing the XPA mutants towards UV light (McClendon TB and Niedernhofer LJ, unpublished data), confirming the *in vivo* NER defect. The fact that ERCC1-XPF is still recruited to UV lesions if the XPA-ERCC1 interaction face is mutated and that these mutations still permit the repair of dG-AAF lesions at reduced levels suggests that additional interaction surfaces between ERCC1-XPF and other NER proteins facilitate the overall reactions. Such interaction partners may include the RPA protein [200] or the XPB subunit of TFIIH [27]. Based on the observations outlined below, we hypothesize that a second interaction surface between XPA and ERCC1 is required for full NER activity. In addition to the GGGF-motif, XPA contains a stretch of eight glutamic acid residues and mutations in those residues leads to partial sensitivity to UV irradiation [106]. We propose that these acidic residues might interact with basic ERCC1 residues located adjacent to the XPA-binding pocket, in particular K114 and R117 (**Figure 4**). We have generated cell lines expressing ERCC1-K114E/R117E and preliminary clonogenic survival assay indicated that cells expressing ERCC1-K114E/R117E are approximately as sensitive to UV irradiation as cells expressing ERCC1-N110A/Y145A (McClendon, TB and Niedernhofer LJ, unpublished data). We are currently purifying the recombinant mutant ERCC1 proteins, ERCC1-K114E/R117E and ERCC1-N110A/K114E/R117E, as heterodimers with XPF, to test for their NER activity on various substrates *in vitro*. We predict that at least the triple mutant will have lower activity on all NER substrates than ERCC1-N110A. In addition, we generated cell lines expressing

these mutants to study the recruitment of the mutant ERCC1 proteins to sites of UV lesions. Here too, we expect the triple mutant, ERCC1-N110A/K114E/R117E, to have a more severe defect in NER activity and localization to sites of UV damage than the double mutant because of the disruption of contacts in the two XPA binding regions.

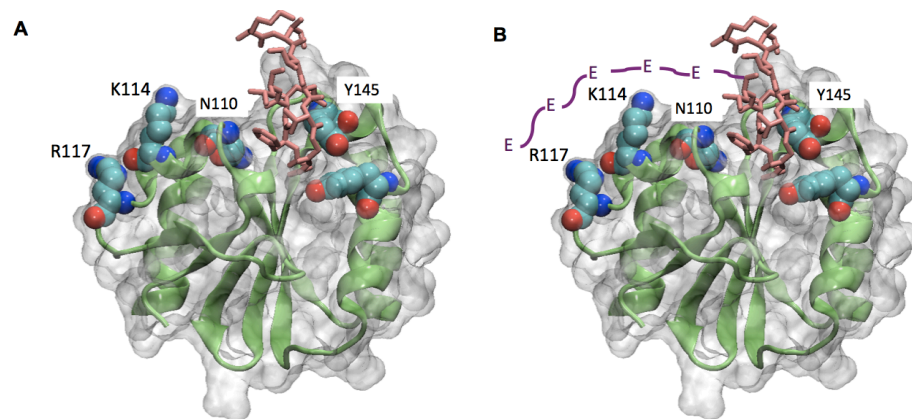


Figure 4. **A second putative XPA-binding region in ERCC1.** Structure of the central domain of ERCC1 (green) in complex with the XPA₆₇₋₈₀ peptide (pink) (figure adapted from [3]). A) ERCC1 residues (atom colors) N110 and Y145 are located in the groove that accommodates the XPA peptide. Residues K114 and R117 are located on the surface adjacent the XPA-binding groove. B) Predictive model on how the glutamic acid cluster of XPA (deep purple) folds over the central domain of ERCC1. ERCC1 residues K114 and R117 are proposed to be involved in the interacting with XPA.

Repair efficiency of ERCC1 and XPA mutants varies with different lesions

The broad specificity of NER to deal with different types of lesions relies on its multi-partite recognition model. It is not the chemical modification of the DNA bases that triggers the recruitment of the NER proteins, but rather abnormal thermodynamic and structural parameters of the DNA helix induced by lesions. The initial damage recognition factor XPC-RAD23B, involved in the detection of lesions throughout the genome, senses the distortion in the helix and its destabilization. The greater the destabilization induced by the lesion the better the lesion is repaired (for a review see [21]. These structural and dynamic variations affect only early steps in the NER reaction, such as the binding of XPC-RAD23B to the damaged DNA and the unwinding of the two strands by TFIIH around the lesion, without influencing the coordinated recruitment of subsequent NER factors. 6-4 photoproducts (6-4PPs) are one of the major lesions caused by UV-light together with cyclobutane pyrimidine dimers (CPDs). Unlike CPDs, 6-4PPs induce a pronounced distortion in the DNA [205] making them a much better substrate for NER than CPDs [193, 198, 206]. Reaction of cisplatin with DNA generates a variety of adducts which confer different constraints on the DNA. 1,3-intrastrand crosslinks induce a higher degree of unwinding and base pair distortion than 1,2-intrastrand crosslinks [207], accounting for their higher repair rate by NER [208-210]. A similar scenario is seen between the guanosine adducts aminofluorene (AF) and acetylaminofluorene (AAF). AF is pretty flexible and can intercalate in the major groove without disturbing any base pairing, whereas the acetyl group on AAF forces the compound to take a syn conformation around the glycosidic bond, making the formation of a regular Watson-Crick base-pair of dG-AAF impossible. Instead, the AAF moiety is placed inside the helix and the dG residue is dislodged to the major groove. This leads to a destabilization of the DNA helix and the more efficient repair of AAF versus AF adducts [203, 204].

In this chapter we have demonstrated that ERCC1 and XPA, harboring mutations that affect the binding between the two proteins, process 6-4PPs, cisplatin and AAF lesions with different efficiencies. This is the first indication that

the nature of the lesion influences specific interactions that occur only in steps subsequent to damage recognition and verification in NER. ERCC1 N110A/Y145A and the XPA deletion mutants (XPA Δ G73 and XPA Δ G73/ Δ G74) displayed a remarkable difference in processing a plasmid containing either a cisplatin 1,3-intrastrand crosslink or an AAF adduct. The different repair rates suggest that the nature of the lesion does not only influence the initial recognition of damage, but also the subsequent assembly of other NER factors, including XPA and ERCC1. Possibly, in the presence of an AAF adduct a greater opening of the double helix takes place, which allows a better positioning of late NER factors on the DNA and hence a more efficient incision of the DNA strand around the lesion. The introduced point mutations in ERCC1 and XPA weaken the interaction between the two proteins and that results in the formation of a less stable complex of the proteins with the DNA and other NER factors. A yet to be defined structural property of the dG-AAF/NER complex can apparently more efficiently compensate the weakening of the XPA-ERCC1 interaction. Comparing the composition of NER complexes in response to different lesions in one system, for example in living cells, would provide mechanistic insights into how NER processes different lesions. While local irradiation approaches are intrinsically limited to the generation of UV adducts, other approaches can be applied to the study of additional lesions in the same system. Fousteri *et al* have developed an NER-specific chromatin immunoprecipitation (ChIP) technique, based on an *in vivo* crosslink approach, to specifically study the composition of transcription-coupled repair (TCR) complexes in response to UV irradiation [211]. In their work they showed that TCR specific proteins, including CSA and CSB, are recruited to stalled RNA polymerase in response to UV irradiation. They further demonstrated that the presence of CSB in the TCR complexes is necessary for the recruitment of subsequent NER factors, such as TFIIH and XPG [211]. This technique could be expanded to study NER complexes in cells expressing ERCC1 or XPA mutant proteins in response to cisplatin, NA-AAF (*N*-acetoxy-2-acetylaminofluorene, the metabolic precursor of AAF) and UV treatment. Based on the *in vitro* experiments significant differences are expected

in the recruitment of ERCC1-XPF and other late factors depending on the lesion and on the mutations in ERCC1 or XPA.

Material and methods

Cell culture conditions and cell transduction

SV40-transformed human fibroblasts XP20S (XPA-deficient) were cultured in Dulbecco's Modified Eagle's Medium (DMEM, Invitrogen) supplemented with 10% fetal bovine serum and penicillin/streptomycin at 37 °C in the presence of 5% CO₂.

XPAWT, XPAF75A, XPA Δ G73 and XPA Δ G73/ Δ G74 cDNAs were cloned into the pWPXL lentiviral vector by substituting the GFP gene. Lentiviruses containing the different constructs were generated as described earlier [202] and LentiWeb (www.lentiweb.com). XP-A (XP20S) cells at 50% confluency were infected with the viral particles containing the different XPA recombinant constructs with a multiplicity of infection of 10 and cultured as described above. The transduction efficiency was assessed by immunofluorescence.

Immunoblotting

Cells were scraped in PBS from culture dish, washed twice with PBS and lysed with 300 μ l lysis buffer (50 mM potassium phosphate, 10% glycerole, 0.1% NP-40, 1 mM phenylmethanesulfonylfluoride, 5 mM β -mercaptoethanol, protease inhibitors cocktail tablet (Complete, Roche)). 30 μ g of protein was resolved by SDS-PAGE (10%) and transferred to a PVDF membrane (Hybond-LFP, GE Healthcare). XPA was detected with a polyclonal rabbit antibody (1:800, FL-273, Santa Cruz Biotechnology). PCNA (1:1500, monoclonal mouse Clone PC-10, DakoCytomation) was used as a loading control. Secondary antibodies were: AlexaFluor488 conjugated goat anti-rabbit IgG, Invitrogen, (1:800); Cy3-conjugated goat anti-mouse, JacksonImmunoResearch Laboratories (1:1500).

Local UV irradiation and immunofluorescence

Cells were seeded and cultured on glass coverslips and processed as described [130, 202]. Briefly, cells were covered with a polycarbonate filter containing 5 μm pores (Millipore) and irradiated with 120 J/m² UV light using a UV-C Lamp (EL Series, UVP, Model UVLS-28). The cells were incubated in culturing medium for different time points before being washed with PBS and permeabilized with PBS/0.2% Triton X-100 for 30 sec. Cells were fixed with paraformaldehyde containing 0.2% Triton X-100 for 15 min at room temperature and subsequently washed 5 times with PBS/0.1% Triton X-100. To detect the photoproducts, cells were treated with 0.07M NaOH in PBS for 5 min at room temperature and washed again with PBS/0.1% Triton X-100 as before. Cells were blocked with PBS+ (PBS containing 0.15% glycine and 0.5% BSA) for 30 min and then incubated with primary antibodies diluted in PBS+ for 1.5 hrs at room temperature under dark and humid conditions. Cells were washed again with PBS/0.1% Triton X-100, blocked quickly with PBS+ and then incubated with secondary antibodies diluted in PBS+ for 1 hr at room temperature under dark and humid conditions. After a final wash with PBS/0.1% Triton X-100, cells were briefly rinsed with PBS and mounted on microscope slides using Vectashield (Vector) mounting medium containing DAPI (4'-6'-diamino-2-phenylindole) at a concentration of 0.1 mg/ml. Cells were analyzed using a confocal microscope (Zeiss LSM 510).

The following antibodies were used for immunofluorescence detection. *Primary antibodies:* mouse monoclonal anti-(6-4) photoproducts (6-4PPs), Cosmo Bio Co. (1:400); rabbit polyclonal anti-ERCC1, SantaCruzBiotechnology (1:100). *Secondary antibodies:* AlexaFluor488 conjugated goat anti-rabbit IgG, Invitrogen, (1:800); Cy3-conjugated goat anti-mouse, JacksonImmunoResearch Laboratories (1:1500).

In vitro NER assay

This assay was performed using an established protocol (Shivji et al, 1999). Cell extracts and plasmid containing 1,3-intrastrand cisplatin adduct were

prepared as described previously [4]. The preparation of the plasmid containing the AAF-modified base was prepared as described previously [204]. HeLa (2 μ l), XP-A (3 μ l) or XP-F (3 μ l) cell extract, 2 μ l of 5x repair buffer (200 mM Hepes-KOH, 25 mM MgCl₂, 110 mM phosphocreatine (di-Tris salt, Sigma), 10 mM ATP, 2.5 mM DTT and 1.8 mg/ml BSA, adjusted to pH 7.8), 0.2 μ l 2.5 mg/ml creatine phosphokinase (rabbit muscle CPK, Sigma) and either purified XPA peptide, XPA or ERCC1-XPF protein (final NaCl concentration was 70 mM) in a total volume of 10 μ l were pre-incubated at 30°C for 10 min. One μ L of a covalently-closed circular DNA plasmid (50 ng) containing either the 1,3-interstrand cisplatin crosslink or the AAF adduct was added before incubating the mixture at 30 °C for 45 min. After placing the samples on ice, 0.5 μ l of 1 μ M of a complementary oligonucleotide (see below) was added and the mixtures heated at 95 °C for 5 min. The samples were allowed to cool down at room temperature for 15 min to allow the DNA to anneal. One μ L of a Sequenase/[α -³²P]-dCTP mix (0.5 units of Sequenase and 2.5 μ Ci of [α -³²P]-dCTP per reaction) was added before incubating at 37 °C for 3 min, 1.2 μ l of dNTP mix (100 μ M of each dATP, dTTP, dGTP; 50 μ M dCTP) was added and the mixture incubated for another 12 min. The reactions were stopped by adding 8 μ l of loading dye (90% formamide/10 mM EDTA) and heating at 95 °C for 5 min. The samples were run on a 20% sequencing gel (0.5x TBE) at 45 W for 2.5 hrs. A low molecular weight DNA marker (New England Biolabs) was used as a reference after end-labeling the DNA with [α -³²P]-dCTP and Klenow fragment polymerase. The reactions products were visualized using a PhosphorImager (Typhoon 9400, Amersham Biosciences).

Complementary oligonucleotides:

To detect DNA fragment containing 1,3-intrastrand cisplatin crosslink:

35-mer: 5'-GGGGGAAGAGTGCACAGAAGAAGACCTGGTTCGACCP-3'

To detect DNA fragment containing AAF adduct:

34-mer: 5'-GGGGCATGTGGCGCCGGTAATAGCTACGTAGCTCP-3'

Acknowledgement

I would like to thank Jung-Eun Yeo for providing the DNA substrate containing the AAF adduct and Arthur J. Campbell for figure 4.

Chapter 5:

**The N-terminal SF2 domain of XPF
targets ERCC1-XPF to sites of
interstrand crosslink repair**

Introduction

Structure-specific endonucleases are a group of proteins that cut specific DNA structures in a number of essential processes such as DNA repair, replication and recombination. The activity of these enzymes needs to be tightly regulated to avoid the inadvertent or excessive incision of DNA that could be deleterious for the cell. One prototypical endonuclease is ERCC1-XPF with roles in several DNA repair pathways, including nucleotide excision repair (NER), interstrand crosslink (ICL) repair, homologous recombination and telomere maintenance. These diverse roles of ERCC1-XPF are manifested in the complex and severe phenotype caused by mutations in these two genes in humans and mice that include early death, progeria and developmental abnormalities [71, 99]. An important question is therefore to understand which one of these functions contributes to the severe phenotype of ERCC1-XPF deficiency and how the endonuclease activity is targeted to various repair pathways.

Currently, we know most about the involvement of ERCC1-XPF in NER, where the protein performs the incision 5' to a lesion [21]. Following recognition of the damage by XPC-RAD23B and formation of a stable pre-incision complex involving TFIIH, XPA, RPA and XPG, ERCC1-XPF is recruited to NER complexes by interaction with the XPA protein. Early on it was shown that XPA cells in which the ERCC1-XPA interaction is abolished are highly UV-sensitive [106]. The structural basis for this interaction has recently been elucidated and has identified a well-defined groove in the central domain of ERCC1 as the XPA-binding pocket [3, 151]. Mutations in the binding pocket of ERCC1 or in the GGGF motif in XPA that is accommodated in it interfere with NER activity *in vitro* and *in vivo* [3, 202].

By contrast, we know less about how ERCC1-XPF is recruited to other DNA repair pathways. A tempting idea is that the well-defined groove in ERCC1 would serve as an interaction site for other proteins. However, we have shown that the XPA-binding site in ERCC1 is a specific NER element, since mutations in this region specifically impaired the NER function of the endonuclease without

affecting its role in other DNA repair pathways, such as interstrand crosslink (ICL) repair and double-strand break (DSB) repair via homologous recombination (Chapter 3 [202]).

A possible clue as to how ERCC1-XPF might be recruited to repair ICLs was provided by a number of recent papers characterizing the human SLX4 protein [65-67, 177]. Proteins of the SLX4 family interact with different structure-specific endonucleases, including SLX1, MUS81/EME1 and ERCC1-XPF, and might therefore have a key role in directing the activity of various endonucleases. Together with SLX1, SLX4 forms a structure-specific endonuclease with the ability to solve Holliday junctions as well as various types of flap structures [68, 212]. In an SLX1-independent way, SLX4 interacts with Rad1-Rad10, the yeast homolog of ERCC1-XPF, in the repair of double strand breaks during single strand annealing [213]. The *Drosophila* counterpart of SLX4, MUS312, interacts with the XPF homolog MEI9 in resolving meiotic DNA intermediates [173]. Although the true function(s) of human SLX4 remains to be determined, a striking observation is that cells depleted of SLX4, but not SLX1, are highly sensitive to crosslinking agents [65, 66]. It has therefore been suggested that SLX4 has a role in ICL repair that involves the coordination of the nuclease activities of ERCC1-XPF and MUS81-EME1, with whom SLX4 interacts through distinct domains in the N- and C-terminal halves, respectively [66]. Similarly, mutations in MUS312 renders cells sensitive to treatment with crosslinking agents [173]. Yildiz *et al* identified a point mutation in MEI9 that abolishes its interaction with MUS312 [173] and the equivalent substitution in human XPF (G325E) also leads to the disruption of the interaction of XPF with SLX4 [177].

Based on these observations, we set out to identify regions in ERCC1-XPF that are specifically required to target the endonuclease to sites of ICL repair. Our studies show that specific mutation in the N-terminal helicase-like domain of XPF renders cells specifically sensitive to crosslinking agents without affecting NER activity. Our studies demonstrate that NER and ICL repair functions of ERCC1-XPF can be separated by blocking specific protein-protein interactions and provide an opportunity to assess how various repair pathways

contribute to the complex and severe phenotype displayed by ERCC1- and XPF-deficient cells and patients.

Results

Following up on our demonstration that mutations in the XPA-binding pocket of ERCC1 affect NER, but not ICL repair activity (Chapter 3 [202]), we aimed to identify other regions in ERCC1-XPF that might selectively affect its function in ICL repair. We pursued the hypothesis that the N-terminal helicase-like region of XPF mediates the recruitment of ERCC1-XPF to sites of ICL repair based on two main findings. First, we targeted the interaction between XPF and the SLX4 protein since both proteins have been shown to play a role in processing ICLs [66]. SLX4 interacts with XPF via the N-terminal MUS312/MEI9 interaction-like region (MLR) [66, 173] and mutation of the conserved residue Gly325 to Glu abolishes the interaction between the two proteins in a yeast two hybrid system [177]. Second, we have serendipitously found that expression of an N-terminally GFP tagged in XPF protein in XP-F cells corrects the sensitivity of these cells to UV irradiation, but not towards ICL-forming agents (Niedernhofer, L. J., unpublished data), suggesting that the GFP tag selectively abolishes ICL repair, possibly by disturbing a protein-protein interaction mediated by the N-terminus of XPF.

To test our hypothesis that various parts of the N-terminal domain of XPF mediate protein-protein interactions for targeting the endonuclease to sites of ICL repair we set out to generate cell lines expressing XPF with various mutations in the N-terminal SF2-helicase like domain. We generated a putative SLX4-interaction mutant (G325E), tagged the N-terminus XPF with HA (HA-XPF, a smaller addition than the GFP protein) and deleted the first five amino acids (Δ 5N-XPF, to test whether the N-terminus itself is required for an interaction) (**Figure 1**). XPF-deficient cells (XP2YO) were transduced with recombinant lentiviral vectors expressing wild-type and mutant XPF cDNAs as described previously [201, 214]. These newly generated cell lines were used along with XP-

F cell lines complemented with wild-type and an active site mutant (D676A) XPF protein [79, 201] and ERCC1-deficient cells complemented with NER-deficient (N110A/Y145A) ERCC1 protein [202] to test how these modifications of ERCC1-XPF affect the various repair functions of the nuclease.

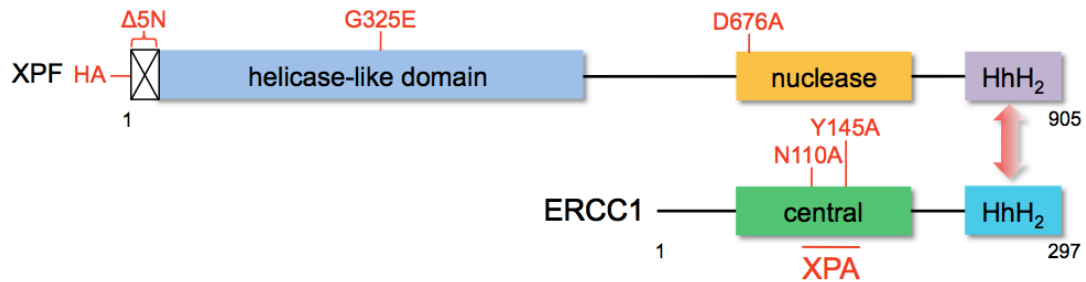


Figure 1. **Schematic representation of the ERCC1-XPF protein.** The mutations introduced into the protein to generate the different ERCC1-XPF mutant proteins are shown in red: the single amino acid substitution G325E, the addition of the HA tag and deletion of the first five amino acids. Additionally, XPF-D676A is an active site mutant and ERCC1-N110A/Y145A is a NER-specific deficient mutant. The functional domain of XPF are shown: the SF2 helicase-like domain (light blue), the nuclease domain (yellow) and the tandem helix-hairpin-helix (HhH)₂ domain (light purple).

XPF proteins with mutations in the N-terminus localize to sites of UV damage and efficiently repair UV lesions

We first tested the NER activity of the various cells expressing XPF and ERCC1 mutants by monitoring the recruitment of ERCC1-XPF to sites of UV lesions. Cells were UV-irradiated through a polycarbonate filter containing 5 μm pores to generate local UV damage in the cell nuclei [24] and one hour after UV exposure the cells were fixed. The presence of 6-4 photoproducts (6-4PPs), a major lesion caused by UV, and of ERCC1-XPF proteins at sites of damage were visualized by immunofluorescence microscopy. As expected, in cells expressing wild-type XPF the endonuclease co-localized completely with the photoproducts (**Figure 2A**). Cells expressing either XPF-G325E, HA-XPF or Δ5N-XPF showed a similar behavior (**Figure 2A**), indicating that mutations in the N-terminal region of XPF do not affect the recruitment of ERCC1-XPF to sites of UV damage. In

cells expressing the catalytically inactive mutant XPF-D676A the endonuclease was similarly found at sites of UV lesions (**Figure 2A**), confirming our previous results that the nuclease activity of XPF is not required for recruitment of ERCC1-XPF to NER complexes [201]. By contrast, as previously shown, mutations in the XPA-binding region of ERCC1 negatively affect the localization of the protein to sites of damage (Chapter 3 [202]) (**Figure 2A**).

The same experiment was used to assess that the overall NER activity of these cell lines by monitoring the presence of UV lesions and ERCC1-XPF 24 hours after UV exposure. In normal cells, the repair of 6-4PPs occurs within 4-8 hours [215], therefore any detection of 6-4PPs after that time would indicate a defect in NER activity. Accordingly, in cells expressing the catalytically inactive XPF-D676A mutant and the ERCC1-N110A/Y145A mutant unable to bind to XPA 6-4PPs were still present 24 hours after UV irradiation (**Figure 2B**). By contrast, in cells expressing XPF wild-type proteins no 6-4PPs were detected and ERCC1 was homogeneously distributed throughout the nucleus (**Figure 2B**). Similarly, in cells expressing XPF-G325E, HA-XPF or Δ 5N-XPF no spots containing UV lesions or ERCC1 were detected 24 hours after UV exposure (**Figure 2B**). These data demonstrate that none of our mutations in the N-terminal region of XPF interfere with the NER activity of ERCC1-XPF.

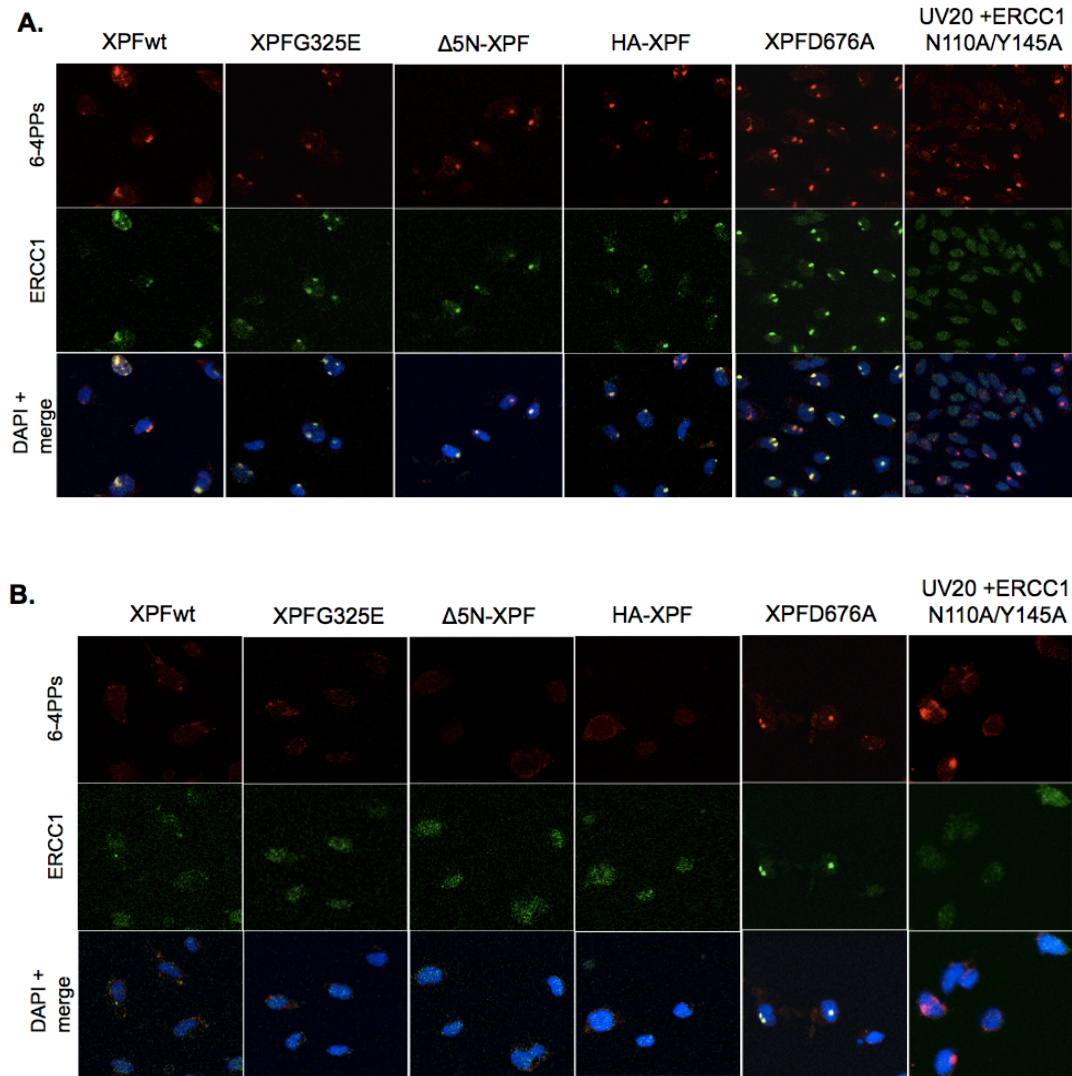


Figure 2. **Localization of ERCC1-XPF mutants to sites of UV damage.** A) XP-F cells expressing XPFwt, XPF-G325E, HA-XPF, Δ 5N-XPF or XPF-D676A and ERCC1-deficient UV20 cells expressing ERCC1-N110A/Y145A were UV-irradiated at dose of 120 J/m² through a polycarbonate filter with 5 μ m pores. One hour after UV exposure cells were fixed and stained for 6-4 photoproducts (red) and ERCC1 (green). The nuclei were stained with DAPI (blue). B) Same as in A except the cells were fixed and treated for immunofluorescence 24 hours after UV irradiation (120 J/m²).

XPF proteins with mutations in the N-terminus inhibit ICL repair but not NER

Having established that the mutations in the N-terminal half of the XPF protein do not interfere with the ability of ERCC1-XPF to be recruited to sites of UV lesions, we assessed whether this region is important for the activity of ERCC1-XPF in ICL repair. To test this, XP-F cells expressing XPF wild-type, XPF-G325E or XPF- Δ 5N were tested for their sensitivity to UV irradiation and the crosslink-forming agent mitomycin C (MMC) by clonogenic survival assays (**Figure 3**). As expected, XPF-deficient cells (XP2YO) were hypersensitive to both genotoxins, whereas expression of wild-type XPF corrected the sensitivity to both genotoxins. However, cells expressing either XPF-G325E or XPF- Δ 5N were significantly sensitive to MMC than the corrected cell line (**Figure 3A**), demonstrating that mutations in the N-terminal half of XPF affect survival ability after exposure to crosslink forming agents. By contrast, all the XPF mutations showed resistance to UV irradiation (**Figure 3B**). These results show that the activity of ERCC1-XPF in ICL repair is mediated by proteins binding to the N-terminal half of XPF. Furthermore, these observations provide further evidence that the activity of ERCC1-XPF in different repair pathways is regulated by specific protein-protein interactions involving specific regions of ERCC1-XPF.

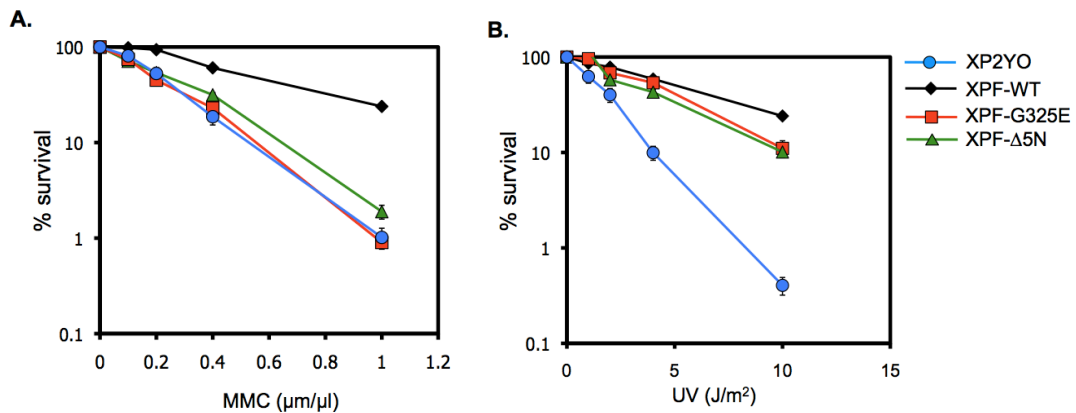


Figure 3. **Mutations in the N-terminal half of XPF inhibit ICL repair but not NER.** A-B. Clonogenic survival assays to measure the sensitivity of XP-F cells (XP2YO) (blue circles), and XP-F cells expressing XPF-WT (black diamonds), XPF-G325E (red squares) and XPF- Δ 5N (green triangles) to mytomycin C (MMC) (A) or UV-C (B). Experiments performed by Advaita Madireddy.

Discussion

Regulation of ERCC1-XPF in DNA repair

Structure-specific endonucleases are essential components of most DNA repair pathways, where they perform incisions of specific DNA intermediates necessary to remove lesions from the DNA and to resolve complex intermediate structures. Such DNA cutting enzymes could however prove to be a liability for cells since their activity, if not properly regulated, can lead to chromosome rearrangements and genome instability. Often such endonucleases can contribute to diverse pathways. One example of such a multifunctional structure-specific endonuclease is ERCC1-XPF, which participates in NER [28], interstrand crosslink (ICL) repair [89, 90] and homologous recombination (HR) [92]. Our previous work has shown that the activity of ERCC1-XPF is regulated through interaction with XPA in NER (**Figure 4**) (Chapter 2 and 3 [3, 202]) and that mutations in the XPA interaction domain of ERCC1 affect NER, but not other repair pathways (Chapter 3 [202]). Here we show that at least two regions in the N-terminal domain of XPF are involved in targeting the protein to ICL repair pathway(s). A point mutation (G325E) that abolishes the interaction with SLX4, a possible regulatory protein of various nuclease activities [173, 177] as well as mutations in the extreme N-terminus of XPF abolish the ICL repair activity of ERCC1-XPF. At present we do not know what the interaction partner of this latter region of XPF is.

The N-terminal half of XPF is made up of a helicase-like domain of the superfamily 2 helicases. In contrast to canonical SF2 proteins this XPF region lacks residues necessary for ATP hydrolysis [77] and contains a leucine rich insert between the two RecA-like domains that is made up of four parallel α -helices in the related archeal Hef protein [118]. Based on these structural features, it has been suggested that it contributes to specific ss/ds DNA junctions binding of ERCC1-XPF [81]. Interestingly, however, the truncated form of ERCC1-XPF missing the N-terminal half of XPF retained some low levels of nuclease activity on model substrates *in vitro*, suggesting that it might have roles

in addition to DNA binding [80]. Indeed, in the present study we show that the N-terminal region of XPF is specifically required for proper functioning of ERCC1-XPF in ICL repair likely by mediating protein-protein interactions relevant to ICL repair (**Figure 4**). Present work in our laboratory is aimed at defining these interactions and the domains in XPF that mediate them in detail.

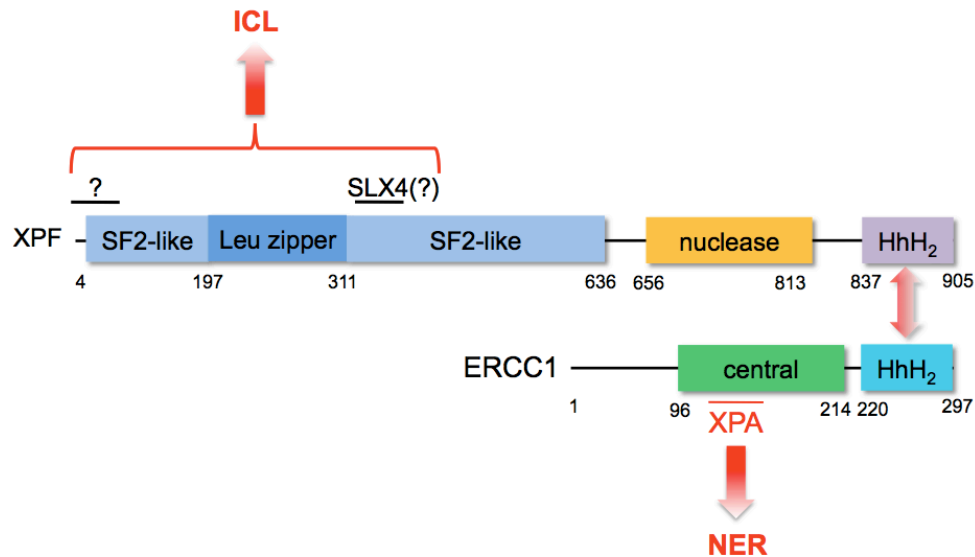


Figure 4. **Speculative model describing the regulation of ERCC1-XPF nuclease activity in different DNA repair pathways.** The functional domains of each protein are shown. The N-terminal half of XPF is required for targeting the endonuclease to sites of ICL repair, possibly mediated by the interaction of SLX4 with XPF. XPA recruits ERCC1-XPF to NER complexes by binding to the central domain of ERCC1.

In conclusion, our work demonstrates that the functions of ERCC1-XPF can be dissected by targeting specific protein-binding regions in the endonuclease. Applying these molecular findings into an animal model would allow us to confirm the hypothesis that the accelerated aging in ERCC1- and XPF-deficient patients and mice is due to a defect in ICL repair. Transgenic mice expressing XPF-G325E, a mutant specifically sensitive to crosslink forming agents, is expected to display the severe phenotype identical to ERCC1^{-/-} and XPF^{-/-} mice [99, 216]. The results from these experiments will yield critical new information about the types of DNA lesions that drive replicative senescence and

aging, which has important implications for understanding the biology of aging and how ERCC1-XPF mediates resistance of tumors to crosslinking agents such as cisplatin.

Materials and methods

Cell culture conditions and cell transduction

SV40-transformed human fibroblasts XP2YO (XPF-deficient, GM08437) were cultured in Dulbecco's Modified Eagle's Medium (DMEM, Invitrogen) supplemented with 10% fetal bovine serum and penicillin/streptomycin at 37 °C in the presence of 5% CO₂.

The lentivector XPFwt-pWPXL (containing a C-terminal HA-tag) was used as a PCR template to generate the following constructs: HA-XPFwt (HA-tag at the N-terminus), Δ 5N-XPFwt (deletion of first five amino acids) and XPF-G325E. The following primers were used for PCR (restriction sites are underlined and indicated, modified nucleotides are shown in italics, HA tag sequence is highlighted in green):

XPF-G325E: GGTCAGAATTCAGAGTGGCTGTTCTAGACTCCAGCACCTCG (*Xba*I)

HA-XPF: (*Mlu*I)

GCGTCACGCGTATG**TATCCCTACGACGTACCAGATTACGCC**GGAGGAGCGCCGCTGCTGG

Δ 5N-XPF: GCGTCACGCGTATGGAGTACGAGCGACAGCTGGTCCTGG (*Mlu*I)

The PCR products were purified using PCR Purification Kit (Qiagen) and the constructs HA-XPF and Δ 5N-XPF were subcloned into the XPFwt-pWPXL lentivector using the restriction enzymes *Eco*RI and *Mlu*I. Lentiviruses containing the different constructs were generated as described previously [202] and on the LentiWeb. XP-F cells at 50% confluency were infected with the viral particles containing the different XPF recombinant constructs with a multiplicity of infection of 10 and cultured as described above. The transduction efficiency was assessed by immunofluorescence.

Local UV irradiation and immunofluorescence

Cells were seeded and cultured on glass coverslips and processed as described [130]. Briefly, cells were covered with a polycarbonate filter containing 5 μm pores (Millipore) and irradiated with 120 J/m^2 UV light using a UV-C Lamp (EL Series, UVP, Model UVLS-28). The cells were incubated in culturing medium for different time points before washing with PBS and permeabilized with PBS/0.2% Triton X-100 for 30 sec. Cells were fixed with paraformaldehyde containing 0.2% Triton X-100 for 15 min at room temperature and subsequently washed 5 times with PBS/0.1% Triton X-100. To detect the photoproducts, cells were treated with 0.07M NaOH in PBS for 5 min at room temperature and washed again with PBS/0.1% Triton X-100 as before. Cells were blocked with PBS+ (PBS containing 0.15% glycine and 0.5% BSA) for 30 min and then incubated with primary antibodies diluted in PBS+ for 1.5 hrs at room temperature under dark and humid conditions. Cells were washed again with PBS/0.1% Triton X-100, blocked quickly with PBS+ and then incubated with secondary antibodies diluted in PBS+ for 1 hr at room temperature under dark and humid conditions. After a final wash with PBS/0.1% Triton X-100, cells were briefly rinsed with PBS and mounted on microscope slides using Vectashield (Vector) mounting medium containing DAPI (4'-6'-diamino-2-phenylindole) at a concentration of 0.1 mg/ml. Cells were analyzed using a confocal microscope (Zeiss LSM 510).

Antibodies

The following antibodies were used for immunofluorescence detection. *Primary antibodies:* mouse monoclonal anti-(6-4) photoproducts (6-4PPs), Cosmo Bio Co. (1:400); rabbit polyclonal anti-ERCC1, SantaCruzBiotechnology (1:100). *Secondary antibodies:* AlexaFluor488 conjugated goat anti-rabbit IgG, Invitrogen, (1:800); Cy3-conjugated goat anti-mouse, JacksonImmunoResearch Laboratories (1:1500).

Clonogenic survival assay

The survival ability of XP-F (XP2YO) cells expressing either wild-type or mutant proteins in response to UV light or MMC was determined as described previously (Chapter 3 [202]).

Acknowledgements

I would like to thank Advaita Madireddy in Dr. Niedernhofer's lab, for performing the clonogenic survival assays presented in this chapter.

References

1. Miyamoto, I., N. Miura, H. Niwa, J. Miyazaki, and K. Tanaka, *Mutational analysis of the structure and function of the xeroderma pigmentosum group A complementing protein. Identification of essential domains for nuclear localization and DNA excision repair.* J Biol Chem, 1992. **267**(17): p. 12182-7.
2. Park, C., D. Mu, J. Reardon, and A. Sancar, *The general transcription-repair factor TFIIH is recruited to the excision repair complex by the XPA protein independent of the TFIIIE transcription factor.* J Biol Chem, 1995. **270**(9): p. 4896-902.
3. Tsodikov, O.V., D. Ivanov, B. Orelli, L. Staresinic, I. Shoshani, R. Oberman, O.D. Schärer, G. Wagner, and T. Ellenberger, *Structural basis for the recruitment of ERCC1-XPF to nucleotide excision repair complexes by XPA.* EMBO J, 2007. **26**(22): p. 4768-76.
4. Shivji, M., J. Moggs, I. Kuraoka, and R. Wood, *Dual-incision assays for nucleotide excision repair using DNA with a lesion at a specific site.* Methods Mol Biol, 1999. **113**: p. 373-92.
5. Lindahl, T., *Instability and decay of the primary structure of DNA.* Nature, 1993. **362**(6422): p. 709-15.
6. Friedberg, E., G. Walker, W. Siede, R. Wood, R. Schultz, and T. Ellenberger, *DNA Repair and Mutagenesis.* 2005.
7. Lehmann, A., *DNA repair-deficient diseases, xeroderma pigmentosum, Cockayne syndrome and trichothiodystrophy.* Biochimie, 2003. **85**(11): p. 1101-11.
8. Kraemer, K.H., M.M. Lee, and J. Scotto, *Xeroderma pigmentosum. Cutaneous, ocular, and neurologic abnormalities in 830 published cases.* Arch Dermatol, 1987. **123**(2): p. 241-50.
9. Cleaver, J., *Defective repair replication of DNA in xeroderma pigmentosum.* Nature, 1968. **218**(142): p. 652-6.
10. Boyce, R. and P. Howard-Flanders, *Release of Ultraviolet Light-Induced Thymine Dimers from DNA in E. Coli K-12.* Proc Natl Acad Sci U S A, 1964. **51**: p. 293-300.
11. Setlow, R. and W. Carrier, *The Disappearance of Thymine Dimers from DNA: An Error-Correcting Mechanism.* Proc Natl Acad Sci U S A, 1964. **51**: p. 226-31.
12. Pettijohn, D. and P. Hanawalt, *Evidence for repair-replication of ultraviolet damaged DNA in bacteria.* J Mol Biol, 1964. **9**: p. 395-410.
13. Rasmussen, R.E. and R.B. Painter, *Evidence for repair of ultra-violet damaged deoxyribonucleic acid in cultured mammalian cells.* Nature, 1964. **203**: p. 1360-2.

14. De Weerd-Kastelein, E., W. Keijzer, and D. Bootsma, *Genetic heterogeneity of xeroderma pigmentosum demonstrated by somatic cell hybridization*. Nat New Biol, 1972. **238**(81): p. 80-3.
15. Lehmann, A., S. Kirk-Bell, C. Arlett, M. Paterson, P. Lohman, E. de Weerd-Kastelein, and D. Bootsma, *Xeroderma pigmentosum cells with normal levels of excision repair have a defect in DNA synthesis after UV-irradiation*. Proc Natl Acad Sci U S A, 1975. **72**(1): p. 219-23.
16. Masutani, C., R. Kusumoto, A. Yamada, N. Dohmae, M. Yokoi, M. Yuasa, M. Araki, S. Iwai, K. Takio, and F. Hanaoka, *The XPV (xeroderma pigmentosum variant) gene encodes human DNA polymerase eta*. Nature, 1999. **399**(6737): p. 700-4.
17. McCulloch, S., R. Kokoska, C. Masutani, S. Iwai, F. Hanaoka, and T. Kunkel, *Preferential cis-syn thymine dimer bypass by DNA polymerase eta occurs with biased fidelity*. Nature, 2004. **428**(6978): p. 97-100.
18. Svejstrup, J.Q., *Mechanisms of transcription-coupled DNA repair*. Nat Rev Mol Cell Biol, 2002. **3**(1): p. 21-9.
19. van Gool, A., E. Citterio, S. Rademakers, R. van Os, W. Vermeulen, A. Constantinou, J. Egly, D. Bootsma, and J. Hoeijmakers, *The Cockayne syndrome B protein, involved in transcription-coupled DNA repair, resides in an RNA polymerase II-containing complex*. EMBO J, 1997. **16**(19): p. 5955-65.
20. Bergmann, E. and J. Egly, *Trichothiodystrophy, a transcription syndrome*. Trends Genet, 2001. **17**(5): p. 279-86.
21. Gillet, L. and O. Scharer, *Molecular mechanisms of mammalian global genome nucleotide excision repair*. Chem Rev, 2006. **106**(2): p. 253-76.
22. de Laat, W., N. Jaspers, and J. Hoeijmakers, *Molecular mechanism of nucleotide excision repair*. Genes Dev, 1999. **13**(7): p. 768-85.
23. Sugasawa, K., J. Ng, C. Masutani, S. Iwai, P. van der Spek, A. Eker, F. Hanaoka, D. Bootsma, and J. Hoeijmakers, *Xeroderma pigmentosum group C protein complex is the initiator of global genome nucleotide excision repair*. Mol Cell, 1998. **2**(2): p. 223-32.
24. Volker, M., M. Mone, P. Karmakar, A. van Hoffen, W. Schul, W. Vermeulen, J. Hoeijmakers, R. van Driel, A. van Zeeland, and L. Mullenders, *Sequential assembly of the nucleotide excision repair factors in vivo*. Mol Cell, 2001. **8**(1): p. 213-24.
25. Riedl, T., F. Hanaoka, and J. Egly, *The comings and goings of nucleotide excision repair factors on damaged DNA*. EMBO J, 2003. **22**(19): p. 5293-303.
26. Hanawalt, P.C. and G. Spivak, *Transcription-coupled DNA repair: two decades of progress and surprises*. Nat Rev Mol Cell Biol, 2008. **9**(12): p. 958-70.

27. Evans, E., J. Moggs, J. Hwang, J. Egly, and R. Wood, *Mechanism of open complex and dual incision formation by human nucleotide excision repair factors*. EMBO J, 1997. **16**(21): p. 6559-73.
28. Sijbers, A., W. de Laat, R. Ariza, M. Biggerstaff, Y. Wei, J. Moggs, K. Carter, B. Shell, E. Evans, M. de Jong, S. Rademakers, J. de Rooij, N. Jaspers, J. Hoeijmakers, and R. Wood, *Xeroderma pigmentosum group F caused by a defect in a structure-specific DNA repair endonuclease*. Cell, 1996. **86**(5): p. 811-22.
29. O'Donovan, A., A. Davies, J. Moggs, S. West, and R. Wood, *XPG endonuclease makes the 3' incision in human DNA nucleotide excision repair*. Nature, 1994. **371**(6496): p. 432-5.
30. Shivji, M., V. Podust, U. Hubscher, and R. Wood, *Nucleotide excision repair DNA synthesis by DNA polymerase epsilon in the presence of PCNA, RFC, and RPA*. Biochemistry, 1995. **34**(15): p. 5011-7.
31. Moser, J., H. Kool, I. Giakzidis, K. Caldecott, L.H.F. Mullenders, and M.I. Fousteri, *Sealing of chromosomal DNA nicks during nucleotide excision repair requires XRCC1 and DNA ligase III alpha in a cell-cycle-specific manner*. Mol Cell, 2007. **27**(2): p. 311-23.
32. Ogi, T., S. Limsirichaikul, R.M. Overmeer, M. Volker, K. Takenaka, R. Cloney, Y. Nakazawa, A. Niimi, Y. Miki, N.G. Jaspers, L.H.F. Mullenders, S. Yamashita, M.I. Fousteri, and A.R. Lehmann, *Three DNA Polymerases, Recruited by Different Mechanisms, Carry Out NER Repair Synthesis in Human Cells*. Mol Cell, 2010. **37**(5): p. 714-727.
33. Gontijo, A.M.d.M.C., C.M. Green, and G. Almouzni, *Repairing DNA damage in chromatin*. Biochimie, 2003. **85**(11): p. 1133-47.
34. Solimando, L., M.S. Luijsterburg, L. Vecchio, W. Vermeulen, R. van Driel, and S. Fakan, *Spatial organization of nucleotide excision repair proteins after UV-induced DNA damage in the human cell nucleus*. Journal of Cell Science, 2009. **122**(Pt 1): p. 83-91.
35. Hwang, B.J., J.M. Ford, P.C. Hanawalt, and G. Chu, *Expression of the p48 xeroderma pigmentosum gene is p53-dependent and is involved in global genomic repair*. Proc Natl Acad Sci USA, 1999. **96**(2): p. 424-8.
36. Tang, J. and G. Chu, *Xeroderma pigmentosum complementation group E and UV-damaged DNA-binding protein*. DNA Repair (Amst), 2002. **1**(8): p. 601-16.
37. Wakasugi, M., A. Kawashima, H. Morioka, S. Linn, A. Sancar, T. Mori, O. Nikaido, and T. Matsunaga, *DDB accumulates at DNA damage sites immediately after UV irradiation and directly stimulates nucleotide excision repair*. J Biol Chem, 2002. **277**(3): p. 1637-40.
38. Fitch, M., S. Nakajima, A. Yasui, and J. Ford, *In vivo recruitment of XPC to UV-induced cyclobutane pyrimidine dimers by the DDB2 gene product*. J Biol Chem, 2003. **278**(47): p. 46906-10.

39. Nishi, R., S. Alekseev, C. Dinant, D. Hoogstraten, A. Houtsmuller, J. Hoeijmakers, W. Vermeulen, F. Hanaoka, and K. Sugawara, *UV-DDB-dependent regulation of nucleotide excision repair kinetics in living cells*. DNA Repair, 2009.
40. Gaillard, P., E. Martini, P. Kaufman, B. Stillman, E. Moustacchi, and G. Almouzni, *Chromatin assembly coupled to DNA repair: a new role for chromatin assembly factor I*. Cell, 1996. **86**(6): p. 887-96.
41. Green, C. and G. Almouzni, *Local action of the chromatin assembly factor CAF-1 at sites of nucleotide excision repair in vivo*. EMBO J, 2003. **22**(19): p. 5163-74.
42. Groth, A., W. Rocha, A. Verreault, and G. Almouzni, *Chromatin challenges during DNA replication and repair*. Cell, 2007. **128**(4): p. 721-33.
43. Matsuda, T., M. Saijo, I. Kuraoka, T. Kobayashi, Y. Nakatsu, A. Nagai, T. Enjoji, C. Masutani, K. Sugawara, F. Hanaoka, and al., et, *DNA repair protein XPA binds replication protein A (RPA)*. J Biol Chem, 1995. **270**(8): p. 4152-7.
44. You, J., M. Wang, and S. Lee, *Biochemical analysis of the damage recognition process in nucleotide excision repair*. J Biol Chem, 2003. **278**(9): p. 7476-85.
45. Li, R., P. Calsou, C. Jones, and B. Salles, *Interactions of the transcription/DNA repair factor TFIIH and XP repair proteins with DNA lesions in a cell-free repair assay*. J Mol Biol, 1998. **281**(2): p. 211-8.
46. Li, L., S. Elledge, C. Peterson, E. Bales, and R. Legerski, *Specific association between the human DNA repair proteins XPA and ERCC1*. Proc Natl Acad Sci U S A, 1994. **91**(11): p. 5012-6.
47. Morita, E.H., T. Ohkubo, I. Kuraoka, M. Shirakawa, K. Tanaka, and K. Morikawa, *Implications of the zinc-finger motif found in the DNA-binding domain of the human XPA protein*. Genes Cells, 1996. **1**(5): p. 437-42.
48. Asahina, H., I. Kuraoka, M. Shirakawa, E. Morita, N. Miura, I. Miyamoto, E. Ohtsuka, Y. Okada, and K. Tanaka, *The XPA protein is a zinc metalloprotein with an ability to recognize various kinds of DNA damage*. Mutat Res, 1994. **315**(3): p. 229-37.
49. Ikegami, T., I. Kuraoka, M. Saijo, N. Kodo, Y. Kyogoku, K. Morikawa, K. Tanaka, and M. Shirakawa, *Solution structure of the DNA- and RPA-binding domain of the human repair factor XPA*. Nat Struct Biol, 1998. **5**(8): p. 701-6.
50. Robins, P., C.J. Jones, M. Biggerstaff, T. Lindahl, and R.D. Wood, *Complementation of DNA repair in xeroderma pigmentosum group A cell extracts by a protein with affinity for damaged DNA*. The EMBO Journal, 1991. **10**(12): p. 3913-21.
51. Jones, C. and R. Wood, *Preferential binding of the xeroderma pigmentosum group A complementing protein to damaged DNA*. Biochemistry, 1993. **32**(45): p. 12096-104.

52. He, Z., L. Henricksen, M. Wold, and C. Ingles, *RPA involvement in the damage-recognition and incision steps of nucleotide excision repair*. *Nature*, 1995. **374**(6522): p. 566-9.
53. Wakasugi, M. and A. Sancar, *Order of assembly of human DNA repair excision nuclease*. *J Biol Chem*, 1999. **274**(26): p. 18759-68.
54. Buschta-Hedayat, N., T. Buterin, M. Hess, M. Missura, and H. Naegeli, *Recognition of nonhybridizing base pairs during nucleotide excision repair of DNA*. *Proc Natl Acad Sci U S A*, 1999. **96**(11): p. 6090-5.
55. Lee, J., C. Park, A. Arunkumar, W. Chazin, and B. Choi, *NMR study on the interaction between RPA and DNA decamer containing cis-syn cyclobutane pyrimidine dimer in the presence of XPA: implication for damage verification and strand-specific dual incision in nucleotide excision repair*. *Nucleic Acids Res*, 2003. **31**(16): p. 4747-54.
56. Missura, M., T. Buterin, R. Hindges, U. Hübscher, J. Kaspárková, V. Brabec, and H. Naegeli, *Double-check probing of DNA bending and unwinding by XPA-RPA: an architectural function in DNA repair*. *EMBO J*, 2001. **20**(13): p. 3554-64.
57. Camenisch, U., R. Dip, S. Schumacher, B. Schuler, and H. Naegeli, *Recognition of helical kinks by xeroderma pigmentosum group A protein triggers DNA excision repair*. *Nat Struct Mol Biol*, 2006. **13**(3): p. 278-84.
58. Liu, Y., H.-I. Kao, and R.A. Bambara, *Flap endonuclease 1: a central component of DNA metabolism*. *Annu Rev Biochem*, 2004. **73**: p. 589-615.
59. Lieber, M.R., *The FEN-1 family of structure-specific nucleases in eukaryotic DNA replication, recombination and repair*. *Bioessays*, 1997. **19**(3): p. 233-40.
60. Ip, S.C.Y., U. Rass, M.G. Blanco, H.R. Flynn, J.M. Skehel, and S.C. West, *Identification of Holliday junction resolvases from humans and yeast*. *Nature*, 2008. **456**(7220): p. 357-361.
61. West, Stephen C., *The search for a human Holliday junction resolvase*. *Biochem. Soc. Trans*, 2009. **37**(3): p. 519.
62. Ciccía, A., N. McDonald, and S.C. West, *Structural and functional relationships of the XPF/MUS81 family of proteins*. *Annu Rev Biochem*, 2008. **77**: p. 259-87.
63. Meetei, A.R., A.L. Medhurst, C. Ling, Y. Xue, T.R. Singh, P. Bier, J. Steltenpool, S. Stone, I. Dokal, C.G. Mathew, M. Hoatlin, H. Joenje, J.P. de Winter, and W. Wang, *A human ortholog of archaeal DNA repair protein Hef is defective in Fanconi anemia complementation group M*. *Nat Genet*, 2005. **37**(9): p. 958-63.
64. Ciccía, A., C. Ling, R. Coulthard, Z. Yan, Y. Xue, A.R. Meetei, E.H. Laghmani, H. Joenje, N. McDonald, J.P. de Winter, W. Wang, and S.C. West, *Identification of FAAP24, a Fanconi anemia core complex protein that interacts with FANCM*. *Mol Cell*, 2007. **25**(3): p. 331-43.

65. Munoz, I.M., K. Hain, A.-C. Declais, M. Gardiner, G.W. Toh, L. Sanchez-Pulido, J.M. Heuckmann, R. Toth, T. Macartney, B. Eppink, R. Kanaar, C.P. Ponting, D.M.J. Lilley, and J. Rouse, *Coordination of Structure-Specific Nucleases by Human SLX4/BTBD12 Is Required for DNA Repair*. Mol Cell, 2009. **35**(1): p. 116-127.
66. Fekairi, S., S. Scaglione, C. Chahwan, E.R. Taylor, A. Tissier, S. Coulon, M.-Q. Dong, C. Ruse, J.R.Y. Iii, P. Russell, R.P. Fuchs, C.H. McGowan, and P.-H.L. Gaillard, *Human SLX4 Is a Holliday Junction Resolvase Subunit that Binds Multiple DNA Repair/Recombination Endonucleases*. Cell, 2009. **138**(1): p. 78-89.
67. Svendsen, J.M., A. Smogorzewska, M.E. Sowa, B.C. O'Connell, S.P. Gygi, S.J. Elledge, and J.W. Harper, *Mammalian BTBD12/SLX4 Assembles A Holliday Junction Resolvase and Is Required for DNA Repair*. Cell, 2009. **138**(1): p. 63-77.
68. Fricke, W.M. and S.J. Brill, *Slx1-Slx4 is a second structure-specific endonuclease functionally redundant with Sgs1-Top3*. Genes & Development, 2003. **17**(14): p. 1768-78.
69. Busch, D., C. Greiner, K. Lewis, R. Ford, G. Adair, and L. Thompson, *Summary of complementation groups of UV-sensitive CHO cells mutants isolated by large scale screening*. Mutagenesis, 1989. **4**: p. 349-354.
70. Westerveld, A., J.H. Hoeijmakers, M. van Duin, J. de Wit, H. Odijk, A. Pastink, R.D. Wood, and D. Bootsma, *Molecular cloning of a human DNA repair gene*. Nature, 1984. **310**(5976): p. 425-9.
71. Jaspers, N., A. Raams, M. Silengo, N. Wijgers, L. Niedernhofer, A. Robinson, G. Giglia-Mari, D. Hoogstraten, W. Kleijer, J. Hoeijmakers, and W. Vermeulen, *First reported patient with human ERCC1 deficiency has cerebro-oculo-facio-skeletal syndrome with a mild defect in nucleotide excision repair and severe developmental failure*. Am J Hum Genet, 2007. **80**(3): p. 457-66.
72. Brookman, K.W., J.E. Lamerdin, M.P. Thelen, M. Hwang, J.T. Reardon, A. Sancar, Z.Q. Zhou, C.A. Walter, C.N. Parris, and L.H. Thompson, *ERCC4 (XPF) encodes a human nucleotide excision repair protein with eukaryotic recombination homologs*. Mol Cell Biol, 1996. **16**(11): p. 6553-62.
73. van Vuuren, A., E. Appeldoorn, H. Odijk, A. Yasui, N. Jaspers, D. Bootsma, and J. Hoeijmakers, *Evidence for a repair enzyme complex involving ERCC1 and complementing activities of ERCC4, ERCC11 and xeroderma pigmentosum group F*. EMBO J, 1993. **12**(9): p. 3693-701.
74. Biggerstaff, M., D. Szymkowski, and R. Wood, *Co-correction of the ERCC1, ERCC4 and xeroderma pigmentosum group F DNA repair defects in vitro*. EMBO J, 1993. **12**(9): p. 3685-92.
75. de Laat, W., A. Sijbers, H. Odijk, N. Jaspers, and J. Hoeijmakers, *Mapping of interaction domains between human repair proteins ERCC1 and XPF*. Nucleic Acids Res, 1998. **26**(18): p. 4146-52.

76. Gaillard, P.H. and R.D. Wood, *Activity of individual ERCC1 and XPF subunits in DNA nucleotide excision repair*. Nucleic Acids Res, 2001. **29**(4): p. 872-9.
77. Sgouros, J., P. Gaillard, and R. Wood, *A relationship between a DNA-repair/recombination nuclease family and archaeal helicases*. Trends Biochem Sci, 1999. **24**(3): p. 95-7.
78. Aravind, L., D. Walker, and E. Koonin, *Conserved domains in DNA repair proteins and evolution of repair systems*. Nucleic Acids Res, 1999. **27**(5): p. 1223-42.
79. Enzlin, J.H. and O.D. Schärer, *The active site of the DNA repair endonuclease XPF-ERCC1 forms a highly conserved nuclease motif*. EMBO J, 2002. **21**(8): p. 2045-53.
80. Tsodikov, O.V., J.H. Enzlin, O.D. Schärer, and T. Ellenberger, *Crystal structure and DNA binding functions of ERCC1, a subunit of the DNA structure-specific endonuclease XPF-ERCC1*. Proc Natl Acad Sci USA, 2005. **102**(32): p. 11236-41.
81. Newman, M., J. Murray-Rust, J. Lally, J. Rudolf, A. Fadden, P. Knowles, M. White, and N. McDonald, *Structure of an XPF endonuclease with and without DNA suggests a model for substrate recognition*. EMBO J, 2005. **24**(5): p. 895-905.
82. Tripsianes, K., G. Folkers, E. Ab, D. Das, H. Odijk, N. Jaspers, J. Hoeijmakers, R. Kaptein, and R. Boelens, *The structure of the human ERCC1/XPF interaction domains reveals a complementary role for the two proteins in nucleotide excision repair*. Structure, 2005. **13**(12): p. 1849-58.
83. de Laat, W., E. Appeldoorn, N. Jaspers, and J. Hoeijmakers, *DNA structural elements required for ERCC1-XPF endonuclease activity*. J Biol Chem, 1998. **273**(14): p. 7835-42.
84. Mu, D., C. Park, T. Matsunaga, D. Hsu, J. Reardon, and A. Sancar, *Reconstitution of human DNA repair excision nuclease in a highly defined system*. J Biol Chem, 1995. **270**(6): p. 2415-8.
85. Hoy, C., L. Thompson, C. Mooney, and E. Salazar, *Defective DNA cross-link removal in Chinese hamster cell mutants hypersensitive to bifunctional alkylating agents*. Cancer Res, 1985. **45**(4): p. 1737-43.
86. Weeda, G., I. Donker, J. de Wit, H. Morreau, R. Janssens, C.J. Vissers, A. Nigg, H. van Steeg, D. Bootsma, and J.H. Hoeijmakers, *Disruption of mouse ERCC1 results in a novel repair syndrome with growth failure, nuclear abnormalities and senescence*. Curr Biol, 1997. **7**(6): p. 427-39.
87. McWhir, J., J. Selfridge, D. Harrison, S. Squires, and D. Melton, *Mice with DNA repair gene (ERCC-1) deficiency have elevated levels of p53, liver nuclear abnormalities and die before weaning [see comments]*. Nat Genet, 1993. **5**(3): p. 217-24.
88. Muniandy, P.A., J. Liu, A. Majumdar, S.-t. Liu, and M.M. Seidman, *DNA interstrand crosslink repair in mammalian cells: step by step*. Critical Reviews in Biochemistry and Molecular Biology, 2010. **45**(1): p. 23-49.

89. De Silva, I.U., P.J. McHugh, P.H. Clingen, and J.A. Hartley, *Defining the roles of nucleotide excision repair and recombination in the repair of DNA interstrand cross-links in mammalian cells*. Mol Cell Biol, 2000. **20**(21): p. 7980-90.
90. Niedernhofer, L.J., H. Odijk, M. Budzowska, E. van Drunen, A. Maas, A.F. Theil, J. de Wit, N.G.J. Jaspers, H.B. Beverloo, J.H.J. Hoeijmakers, and R. Kanaar, *The structure-specific endonuclease Ercc1-Xpf is required to resolve DNA interstrand cross-link-induced double-strand breaks*. Mol Cell Biol, 2004. **24**(13): p. 5776-87.
91. Sargent, R.G., J.L. Meservy, B.D. Perkins, A.E. Kilburn, Z. Intody, G.M. Adair, R.S. Nairn, and J.H. Wilson, *Role of the nucleotide excision repair gene ERCC1 in formation of recombination-dependent rearrangements in mammalian cells*. Nucleic Acids Res, 2000. **28**(19): p. 3771-8.
92. Niedernhofer, L.J., J. Essers, G. Weeda, B. Beverloo, J. de Wit, M. Muijtjens, H. Odijk, J.H. Hoeijmakers, and R. Kanaar, *The structure-specific endonuclease Ercc1-Xpf is required for targeted gene replacement in embryonic stem cells*. EMBO J, 2001. **20**(22): p. 6540-9.
93. Zhu, X., L. Niedernhofer, B. Kuster, M. Mann, J. Hoeijmakers, and T. de Lange, *ERCC1/XPF removes the 3' overhang from uncapped telomeres and represses formation of telomeric DNA-containing double minute chromosomes*. Mol Cell, 2003. **12**(6): p. 1489-98.
94. Muñoz, P., R. Blanco, J.M. Flores, and M.A. Blasco, *XPF nuclease-dependent telomere loss and increased DNA damage in mice overexpressing TRF2 result in premature aging and cancer*. Nat Genet, 2005. **37**(10): p. 1063-71.
95. Wu, Y., N.J. Zacal, A.J. Rainbow, and X.-D. Zhu, *XPF with mutations in its conserved nuclease domain is defective in DNA repair but functions in TRF2-mediated telomere shortening*. DNA Repair (Amst), 2007. **6**(2): p. 157-66.
96. Hasty, P., J. Campisi, J. Hoeijmakers, H. van Steeg, and J. Vijg, *Aging and genome maintenance: lessons from the mouse?* Science, 2003. **299**(5611): p. 1355-9.
97. Schärer, O.D., *Hot topics in DNA repair: the molecular basis for different disease states caused by mutations in TFIIH and XPG*. DNA Repair, 2008. **7**(2): p. 339-44.
98. de Vries, A., C.T. van Oostrom, F.M. Hoffhuis, P.M. Dortant, R.J. Berg, F.R. de Gruijl, P.W. Wester, C.F. van Kreijl, P.J. Capel, and H. van Steeg, *Increased susceptibility to ultraviolet-B and carcinogens of mice lacking the DNA excision repair gene XPA*. Nature, 1995. **377**(6545): p. 169-73.
99. Niedernhofer, L., G. Garinis, A. Raams, A. Lalai, A. Robinson, E. Appeldoorn, H. Odijk, R. Oostendorp, A. Ahmad, W. van Leeuwen, A. Theil, W. Vermeulen, G. van der Horst, P. Meinecke, W. Kleijer, J. Vijg, N. Jaspers, and J. Hoeijmakers, *A new progeroid syndrome reveals that genotoxic stress suppresses the somatotroph axis*. Nature, 2006. **444**(7122): p. 1038-43.

100. Lombard, D.B., K.F. Chua, R. Mostoslavsky, S. Franco, M. Gostissa, and F.W. Alt, *DNA repair, genome stability, and aging*. Cell, 2005. **120**(4): p. 497-512.
101. Zhu, Y., J. Hu, Y. Hu, and W. Liu, *Targeting DNA repair pathways: a novel approach to reduce cancer therapeutic resistance*. Cancer Treat Rev, 2009. **35**(7): p. 590-6.
102. Helleday, T., E. Petermann, C. Lundin, B. Hodgson, and R.A. Sharma, *DNA repair pathways as targets for cancer therapy*. Nat Rev Cancer, 2008. **8**(3): p. 193-204.
103. Reed, E., *Platinum-DNA adduct, nucleotide excision repair and platinum based anti-cancer chemotherapy*. Cancer Treat Rev, 1998. **24**(5): p. 331-44.
104. Reed, E., *ERCC1 measurements in clinical oncology*. N Engl J Med, 2006. **355**(10): p. 1054-5.
105. Ahmad, A., J.H. Enzlin, N.R. Bhagwat, N. Wijgers, A. Raams, E. Appeldoorn, A.F. Theil, J.H. J Hoeijmakers, W. Vermeulen, N.G. J Jaspers, O.D. Schärer, and L.J. Niedernhofer, *Mislocalization of XPF-ERCC1 nuclease contributes to reduced DNA repair in XP-F patients*. PLoS Genet, 2010. **6**(3): p. e1000871.
106. Li, L., C. Peterson, X. Lu, and R. Legerski, *Mutations in XPA that prevent association with ERCC1 are defective in nucleotide excision repair*. Mol Cell Biol, 1995. **15**(4): p. 1993-8.
107. Park, C.H. and A. Sancar, *Formation of a ternary complex by human XPA, ERCC1, and ERCC4(XPF) excision repair proteins*. Proc Natl Acad Sci USA, 1994. **91**(11): p. 5017-21.
108. Saijo, M., I. Kuraoka, C. Masutani, F. Hanaoka, and K. Tanaka, *Sequential binding of DNA repair proteins RPA and ERCC1 to XPA in vitro*. Nucleic Acids Res, 1996. **24**(23): p. 4719-24.
109. McWhir, J., J. Selfridge, D.J. Harrison, S. Squires, and D.W. Melton, *Mice with DNA repair gene (ERCC-1) deficiency have elevated levels of p53, liver nuclear abnormalities and die before weaning*. Nat Genet, 1993. **5**(3): p. 217-24.
110. Rosenberg, E., M.M. Taher, N.B. Kuemmerle, J. Farnsworth, and K. Valerie, *A truncated human xeroderma pigmentosum complementation group A protein expressed from an adenovirus sensitizes human tumor cells to ultraviolet light and cisplatin*. Cancer Res, 2001. **61**(2): p. 764-70.
111. Sijbers, A.M., P.J. van der Spek, H. Odijk, J. van den Berg, M. van Duin, A. Westerveld, N.G. Jaspers, D. Bootsma, and J.H. Hoeijmakers, *Mutational analysis of the human nucleotide excision repair gene ERCC1*. Nucleic Acids Res, 1996. **24**(17): p. 3370-80.
112. Buchko, G., N. Isern, L. Spicer, and M. Kennedy, *Human nucleotide excision repair protein XPA: NMR spectroscopic studies of an XPA fragment containing the ERCC1-binding region and the minimal DNA-binding domain (M59-F219)*. Mutat Res, 2001. **486**(1): p. 1-10.

113. Buchko, G.W., S. Ni, B.D. Thrall, and M.A. Kennedy, *Structural features of the minimal DNA binding domain (M98-F219) of human nucleotide excision repair protein XPA*. Nucleic Acids Res, 1998. **26**(11): p. 2779-88.
114. Iakoucheva, L.M., A.L. Kimzey, C.D. Masselon, J.E. Bruce, E.C. Garner, C.J. Brown, A.K. Dunker, R.D. Smith, and E.J. Ackerman, *Identification of intrinsic order and disorder in the DNA repair protein XPA*. Protein Sci, 2001. **10**(3): p. 560-71.
115. Nishino, T., K. Komori, Y. Ishino, and K. Morikawa, *X-ray and biochemical anatomy of an archaeal XPF/Rad1/Mus81 family nuclease: similarity between its endonuclease domain and restriction enzymes*. Structure, 2003. **11**(4): p. 445-57.
116. Houtsmuller, A., S. Rademakers, A. Nigg, D. Hoogstraten, J. Hoeijmakers, and W. Vermeulen, *Action of DNA repair endonuclease ERCC1/XPF in living cells*. Science, 1999. **284**(5416): p. 958-61.
117. Nishino, T., K. Komori, Y. Ishino, and K. Morikawa, *Structural and functional analyses of an archaeal XPF/Rad1/Mus81 nuclease: asymmetric DNA binding and cleavage mechanisms*. Structure (Camb), 2005. **13**(8): p. 1183-92.
118. Nishino, T., K. Komori, D. Tsuchiya, Y. Ishino, and K. Morikawa, *Crystal structure and functional implications of Pyrococcus furiosus hef helicase domain involved in branched DNA processing*. Structure, 2005. **13**(1): p. 143-53.
119. Stauffer, M. and W. Chazin, *Structural mechanisms of DNA replication, repair, and recombination*. J Biol Chem, 2004. **279**(30): p. 30915-8.
120. Guzder, S., C. Sommers, L. Prakash, and S. Prakash, *Complex formation with damage recognition protein Rad14 is essential for Saccharomyces cerevisiae Rad1-Rad10 nuclease to perform its function in nucleotide excision repair in vivo*. Mol Cell Biol, 2006. **26**(3): p. 1135-41.
121. Walters, K.J., A.E. Ferentz, B.J. Hare, P. Hidalgo, A. Jasanoff, H. Matsuo, and G. Wagner, *Characterizing protein-protein complexes and oligomers by nuclear magnetic resonance spectroscopy*. Methods Enzymol, 2001. **339**: p. 238-58.
122. Walters, K.J., H. Matsuo, and G. Wagner, *A simple method to distinguish intermonomer nuclear overhauser effects in homodimeric proteins with C-2 symmetry*. Journal of American Chemical Society, 1997. **119**: p. 5958-5959.
123. Schwieters, C.D., J.J. Kuszewski, N. Tjandra, and G.M. Clore, *The Xplor-NIH NMR molecular structure determination package*. J Magn Reson, 2003. **160**(1): p. 65-73.
124. Tsodikov, O.V., M.T. Record, Jr., and Y.V. Sergeev, *Novel computer program for fast exact calculation of accessible and molecular surface areas and average surface curvature*. J Comput Chem, 2002. **23**(6): p. 600-9.

125. Hohl, M., F. Thorel, S. Clarkson, and O. Scharer, *Structural determinants for substrate binding and catalysis by the structure-specific endonuclease XPG*. J Biol Chem, 2003. **278**(21): p. 19500-8.
126. Friedberg, E.C., G.C. Walker, W. Siede, R.D. Wood, R.A. Schultz, and T. Ellenberger, *DNA Repair and Mutagenesis*. 2nd edition ed. 2005, Washington DC: ASM Press.
127. Gillet, L.C. and O.D. Scharer, *Molecular mechanisms of mammalian global genome nucleotide excision repair*. Chem Rev, 2006. **106**(2): p. 253-76.
128. Sugasawa, K., J.M. Ng, C. Masutani, S. Iwai, P.J. van der Spek, A.P. Eker, F. Hanaoka, D. Bootsma, and J.H. Hoeijmakers, *Xeroderma pigmentosum group C protein complex is the initiator of global genome nucleotide excision repair*. Mol Cell, 1998. **2**(2): p. 223-32.
129. Sugasawa, K., Y. Okuda, M. Saijo, R. Nishi, N. Matsuda, G. Chu, T. Mori, S. Iwai, K. Tanaka, K. Tanaka, and F. Hanaoka, *UV-induced ubiquitylation of XPC protein mediated by UV-DDB-ubiquitin ligase complex*. Cell, 2005. **121**(3): p. 387-400.
130. Volker, M., M.J. Mone, P. Karmakar, A. van Hoffen, W. Schul, W. Vermeulen, J.H. Hoeijmakers, R. van Driel, A.A. van Zeeland, and L.H. Mullenders, *Sequential assembly of the nucleotide excision repair factors in vivo*. Mol Cell, 2001. **8**(1): p. 213-24.
131. Riedl, T., F. Hanaoka, and J.M. Egly, *The comings and goings of nucleotide excision repair factors on damaged DNA*. Embo J, 2003. **22**(19): p. 5293-303.
132. Fousteri, M., W. Vermeulen, A.A. van Zeeland, and L.H. Mullenders, *Cockayne syndrome A and B proteins differentially regulate recruitment of chromatin remodeling and repair factors to stalled RNA polymerase II in vivo*. Mol Cell, 2006. **23**(4): p. 471-82.
133. Evans, E., J.G. Moggs, J.R. Hwang, J.M. Egly, and R.D. Wood, *Mechanism of open complex and dual incision formation by human nucleotide excision repair factors*. Embo J, 1997. **16**(21): p. 6559-73.
134. Tapias, A., J. Auriol, D. Forget, J.H. Enzlin, O.D. Scharer, F. Coin, B. Coulombe, and J.M. Egly, *Ordered conformational changes in damaged DNA induced by nucleotide excision repair factors*. J Biol Chem, 2004. **279**(18): p. 19074-83.
135. Wakasugi, M. and A. Sancar, *Assembly, subunit composition, and footprint of human DNA repair excision nuclease*. Proc Natl Acad Sci U S A, 1998. **95**(12): p. 6669-74.
136. de Laat, W.L., E. Appeldoorn, K. Sugasawa, E. Weterings, N.G. Jaspers, and J.H. Hoeijmakers, *DNA-binding polarity of human replication protein A positions nucleases in nucleotide excision repair*. Genes Dev, 1998. **12**(16): p. 2598-609.
137. Camenisch, U., R. Dip, S.B. Schumacher, B. Schuler, and H. Naegeli, *Recognition of helical kinks by xeroderma pigmentosum group A protein triggers DNA excision repair*. Nat Struct Mol Biol, 2006. **13**(3): p. 278-84.

138. Staresinic, L., A.F. Fagbemi, J.H. Enzlin, A.M. Gourdin, N. Wijgers, I. Dunand-Sauthier, G. Giglia-Mari, S.G. Clarkson, W. Vermeulen, and O.D. Scharer, *Coordination of dual incision and repair synthesis in human nucleotide excision repair*. EMBO J, 2009. **28**(8): p. 1111-20.
139. Mocquet, V., J.P. Laine, T. Riedl, Z. Yajin, M.Y. Lee, and J.M. Egly, *Sequential recruitment of the repair factors during NER: the role of XPG in initiating the resynthesis step*. EMBO J, 2008. **27**(1): p. 155-67.
140. Ogi, T. and A.R. Lehmann, *The Y-family DNA polymerase kappa (pol kappa) functions in mammalian nucleotide-excision repair*. Nat Cell Biol, 2006. **8**(6): p. 640-2.
141. Moser, J., H. Kool, I. Giakzidis, K. Caldecott, L.H. Mullenders, and M.I. Fousteri, *Sealing of chromosomal DNA nicks during nucleotide excision repair requires XRCC1 and DNA ligase III alpha in a cell-cycle-specific manner*. Mol Cell, 2007. **27**(2): p. 311-23.
142. Lehmann, A.R., *DNA repair-deficient diseases, xeroderma pigmentosum, Cockayne syndrome and trichothiodystrophy*. Biochimie, 2003. **85**(11): p. 1101-11.
143. Niedernhofer, L.J., G.A. Garinis, A. Raams, A.S. Lalai, A.R. Robinson, E. Appeldoorn, H. Odijk, R. Oostendorp, A. Ahmad, W. van Leeuwen, A.F. Theil, W. Vermeulen, G.T. van der Horst, P. Meinecke, W.J. Kleijer, J. Vijg, N.G. Jaspers, and J.H. Hoeijmakers, *A new progeroid syndrome reveals that genotoxic stress suppresses the somatotroph axis*. Nature, 2006. **444**(7122): p. 1038-43.
144. Jaspers, N.G., A. Raams, M.C. Silengo, N. Wijgers, L.J. Niedernhofer, A.R. Robinson, G. Giglia-Mari, D. Hoogstraten, W.J. Kleijer, J.H. Hoeijmakers, and W. Vermeulen, *First reported patient with human ERCC1 deficiency has cerebro-oculo-facio-skeletal syndrome with a mild defect in nucleotide excision repair and severe developmental failure*. Am J Hum Genet, 2007. **80**(3): p. 457-66.
145. McWhir, J., J. Selfridge, D.J. Harrison, S. Squires, and D.W. Melton, *Mice with DNA repair gene (ERCC-1) deficiency have elevated levels of p53, liver nuclear abnormalities and die before weaning [see comments]*. Nat Genet, 1993. **5**(3): p. 217-24.
146. Tian, M., R. Shinkura, N. Shinkura, and F.W. Alt, *Growth retardation, early death, and DNA repair defects in mice deficient for the nucleotide excision repair enzyme XPF*. Mol Cell Biol, 2004. **24**(3): p. 1200-5.
147. Park, C.H. and A. Sancar, *Formation of a ternary complex by human XPA, ERCC1, and ERCC4(XPF) excision repair proteins*. Proc Natl Acad Sci U S A, 1994. **91**(11): p. 5017-21.
148. Li, L., S.J. Elledge, C.A. Peterson, E.S. Bales, and R.J. Legerski, *Specific association between the human DNA repair proteins XPA and ERCC1*. Proc Natl Acad Sci U S A, 1994. **91**(11): p. 5012-6.
149. Li, L., C.A. Peterson, X. Lu, and R.J. Legerski, *Mutations in XPA that prevent association with ERCC1 are defective in nucleotide excision repair*. Mol Cell Biol, 1995. **15**(4): p. 1993-8.

150. Tsodikov, O.V., D. Ivanov, B. Orelli, L. Staresincic, I. Shoshani, R. Oberman, O.D. Scharer, G. Wagner, and T. Ellenberger, *Structural basis for the recruitment of ERCC1-XPF to nucleotide excision repair complexes by XPA*. *Embo J*, 2007. **26**(22): p. 4768-76.
151. Tripsianes, K., G.E. Folkers, C. Zheng, D. Das, J.S. Grinstead, R. Kaptein, and R. Boelens, *Analysis of the XPA and ssDNA-binding surfaces on the central domain of human ERCC1 reveals evidence for subfunctionalization*. *Nucleic Acids Res*, 2007. **35**(17): p. 5789-98.
152. Enzlin, J.H. and O.D. Scharer, *The active site of the DNA repair endonuclease XPF-ERCC1 forms a highly conserved nuclease motif*. *Embo J*, 2002. **21**(8): p. 2045-53.
153. de Laat, W.L., E. Appeldoorn, N.G. Jaspers, and J.H. Hoeijmakers, *DNA structural elements required for ERCC1-XPF endonuclease activity*. *J Biol Chem*, 1998. **273**(14): p. 7835-42.
154. Biggerstaff, M., D.E. Szymkowski, and R.D. Wood, *Co-correction of the ERCC1, ERCC4 and xeroderma pigmentosum group F DNA repair defects in vitro*. *Embo J*, 1993. **12**(9): p. 3685-92.
155. van Vuuren, A.J., E. Appeldoorn, H. Odijk, A. Yasui, N.G. Jaspers, D. Bootsma, and J.H. Hoeijmakers, *Evidence for a repair enzyme complex involving ERCC1 and complementing activities of ERCC4, ERCC11 and xeroderma pigmentosum group F*. *Embo J*, 1993. **12**(9): p. 3693-701.
156. Yagi, T., R.D. Wood, and H. Takebe, *A low content of ERCC1 and a 120 kDa protein is a frequent feature of group F xeroderma pigmentosum fibroblast cells*. *Mutagenesis*, 1997. **12**(1): p. 41-4.
157. Shivji, M.K., J.G. Moggs, I. Kuraoka, and R.D. Wood, *Dual-incision assays for nucleotide excision repair using DNA with a lesion at a specific site*. *Methods Mol Biol*, 1999. **113**: p. 373-92.
158. Rolig, R.L., M.P. Lowery, G.M. Adair, and R.S. Nairn, *Characterization and analysis of Chinese hamster ovary cell ERCC1 mutant alleles*. *Mutagenesis*, 1998. **13**(4): p. 357-65.
159. Dunand-Sauthier, I., M. Hohl, F. Thorel, P. Jaquier-Gubler, S.G. Clarkson, and O.D. Schärer, *The spacer region of XPG mediates recruitment to nucleotide excision repair complexes and determines substrate specificity*. *J Biol Chem*, 2005. **280**(8): p. 7030-7.
160. Sijbers, A.M., W.L. de Laat, R.R. Ariza, M. Biggerstaff, Y.F. Wei, J.G. Moggs, K.C. Carter, B.K. Shell, E. Evans, M.C. de Jong, S. Rademakers, J. de Rooij, N.G. Jaspers, J.H. Hoeijmakers, and R.D. Wood, *Xeroderma pigmentosum group F caused by a defect in a structure-specific DNA repair endonuclease*. *Cell*, 1996. **86**(5): p. 811-22.
161. Niedernhofer, L.J., H. Odijk, M. Budzowska, E. van Drunen, A. Maas, A.F. Theil, J. de Wit, N.G. Jaspers, H.B. Beverloo, J.H. Hoeijmakers, and R. Kanaar, *The structure-specific endonuclease Ercc1-Xpf is required to resolve DNA interstrand cross-link-induced double-strand breaks*. *Mol Cell Biol*, 2004. **24**(13): p. 5776-87.

162. Ahmad, A., A.R. Robinson, A. Duensing, E. van Drunen, H.B. Beverloo, D.B. Weisberg, P. Hasty, J.H. Hoeijmakers, and L.J. Niedernhofer, *ERCC1-XPF endonuclease facilitates DNA double-strand break repair*. Mol Cell Biol, 2008. **28**(16): p. 5082-92.
163. Zhu, X.D., L. Niedernhofer, B. Kuster, M. Mann, J.H. Hoeijmakers, and T. de Lange, *ERCC1/XPF removes the 3' overhang from uncapped telomeres and represses formation of telomeric DNA-containing double minute chromosomes*. Mol Cell, 2003. **12**(6): p. 1489-98.
164. Newman, M., J. Murray-Rust, J. Lally, J. Rudolf, A. Fadden, P.P. Knowles, M.F. White, and N.Q. McDonald, *Structure of an XPF endonuclease with and without DNA suggests a model for substrate recognition*. Embo J, 2005. **24**(5): p. 895-905.
165. Tsodikov, O.V., J.H. Enzlin, O.D. Scharer, and T. Ellenberger, *Crystal structure and DNA binding functions of ERCC1, a subunit of the DNA structure-specific endonuclease XPF-ERCC1*. Proc Natl Acad Sci U S A, 2005. **102**(32): p. 11236-41.
166. Sgouros, J., P.H. Gaillard, and R.D. Wood, *A relationship between a DNA-repair/recombination nuclease family and archaeal helicases*. Trends Biochem Sci, 1999. **24**(3): p. 95-7.
167. Tripsianes, K., G. Folkers, E. Ab, D. Das, H. Odijk, N.G. Jaspers, J.H. Hoeijmakers, R. Kaptein, and R. Boelens, *The structure of the human ERCC1/XPF interaction domains reveals a complementary role for the two proteins in nucleotide excision repair*. Structure, 2005. **13**(12): p. 1849-58.
168. de Vries, A., C.T. van Oostrom, F.M. Hoffhuis, P.M. Dortant, R.J. Berg, F.R. de Gruijl, P.W. Wester, C.F. van Kreijl, P.J. Capel, H. van Steeg, and et al., *Increased susceptibility to ultraviolet-B and carcinogens of mice lacking the DNA excision repair gene XPA*. Nature, 1995. **377**(6545): p. 169-73.
169. Lan, L., T. Hayashi, R.M. Rabeya, S. Nakajima, S. Kanno, M. Takao, T. Matsunaga, M. Yoshino, M. Ichikawa, H. Riele, S. Tsuchiya, K. Tanaka, and A. Yasui, *Functional and physical interactions between ERCC1 and MSH2 complexes for resistance to cis-diamminedichloroplatinum(II) in mammalian cells*. DNA Repair (Amst), 2004. **3**(2): p. 135-43.
170. Zhang, N., X. Lu, X. Zhang, C.A. Peterson, and R.J. Legerski, *hMutSbeta is required for the recognition and uncoupling of psoralen interstrand cross-links in vitro*. Mol Cell Biol, 2002. **22**(7): p. 2388-97.
171. Wu, Q., L.A. Christensen, R.J. Legerski, and K.M. Vasquez, *Mismatch repair participates in error-free processing of DNA interstrand crosslinks in human cells*. EMBO Rep, 2005. **6**(6): p. 551-7.
172. Motycka, T.A., T. Bessho, S.M. Post, P. Sung, and A.E. Tomkinson, *Physical and functional interaction between the XPF/ERCC1 endonuclease and hRad52*. J Biol Chem, 2004. **279**(14): p. 13634-9.

173. Yildiz, O., S. Majumder, B. Kramer, and J.J. Sekelsky, *Drosophila MUS312 interacts with the nucleotide excision repair endonuclease MEI-9 to generate meiotic crossovers*. Mol Cell, 2002. **10**(6): p. 1503-9.
174. Fekairi, S., S. Scaglione, C. Chahwan, E.R. Taylor, A. Tissier, S. Coulon, M.Q. Dong, C. Ruse, J.R. Yates, 3rd, P. Russell, R.P. Fuchs, C.H. McGowan, and P.H. Gaillard, *Human SLX4 is a Holliday junction resolvase subunit that binds multiple DNA repair/recombination endonucleases*. Cell, 2009. **138**(1): p. 78-89.
175. Svendsen, J.M., A. Smogorzewska, M.E. Sowa, B.C. O'Connell, S.P. Gygi, S.J. Elledge, and J.W. Harper, *Mammalian BTBD12/SLX4 assembles a Holliday junction resolvase and is required for DNA repair*. Cell, 2009. **138**(1): p. 63-77.
176. Munoz, I.M., K. Hain, A.C. Declais, M. Gardiner, G.W. Toh, L. Sanchez-Pulido, J.M. Heuckmann, R. Toth, T. Macartney, B. Eppink, R. Kanaar, C.P. Ponting, D.M. Lilley, and J. Rouse, *Coordination of structure-specific nucleases by human SLX4/BTBD12 is required for DNA repair*. Mol Cell, 2009. **35**(1): p. 116-27.
177. Andersen, S.L., D.T. Bergstralh, K.P. Kohl, J.R. LaRocque, C.B. Moore, and J. Sekelsky, *Drosophila MUS312 and the vertebrate ortholog BTBD12 interact with DNA structure-specific endonucleases in DNA repair and recombination*. Mol Cell, 2009. **35**(1): p. 128-35.
178. Gossage, L. and S. Madhusudan, *Current status of excision repair cross complementing-group 1 (ERCC1) in cancer*. Cancer Treat Rev, 2007. **33**(6): p. 565-77.
179. Martin, L.P., T.C. Hamilton, and R.J. Schilder, *Platinum resistance: the role of DNA repair pathways*. Clin Cancer Res, 2008. **14**(5): p. 1291-5.
180. Olausson, K.A., P. Fouret, and G. Kroemer, *ERCC1-specific immunostaining in non-small-cell lung cancer*. N Engl J Med, 2007. **357**(15): p. 1559-61.
181. Cummings, M., K. Higginbottom, C.J. McGurk, O.G. Wong, B. Koberle, R.T. Oliver, and J.R. Masters, *XPA versus ERCC1 as chemosensitising agents to cisplatin and mitomycin C in prostate cancer cells: role of ERCC1 in homologous recombination repair*. Biochem Pharmacol, 2006. **72**(2): p. 166-75.
182. Jamieson, E.R. and S.J. Lippard, *Structure, Recognition, and Processing of Cisplatin-DNA Adducts*. Chem Rev, 1999. **99**(9): p. 2467-98.
183. Huang, J.C., D.B. Zamble, J.T. Reardon, S.J. Lippard, and A. Sancar, *HMG-domain proteins specifically inhibit the repair of the major DNA adduct of the anticancer drug cisplatin by human excision nuclease*. Proc Natl Acad Sci U S A, 1994. **91**(22): p. 10394-8.
184. Zamble, D.B., D. Mu, J.T. Reardon, A. Sancar, and S.J. Lippard, *Repair of cisplatin-DNA adducts by the mammalian excision nuclease*. Biochemistry, 1996. **35**(31): p. 10004-13.

185. Moggs, J.G., K.J. Yarema, J.M. Essigmann, and R.D. Wood, *Analysis of incision sites produced by human cell extracts and purified proteins during nucleotide excision repair of a 1,3-intrastrand d(GpTpG)-cisplatin adduct*. J Biol Chem, 1996. **271**(12): p. 7177-86.
186. Moggs, J.G., D.E. Szymkowski, M. Yamada, P. Karran, and R.D. Wood, *Differential human nucleotide excision repair of paired and mispaired cisplatin-DNA adducts*. Nucleic Acids Res, 1997. **25**(3): p. 480-91.
187. Guggenheim, E.R., D. Xu, C.X. Zhang, P.V. Chang, and S.J. Lippard, *Photoaffinity isolation and identification of proteins in cancer cell extracts that bind to platinum-modified DNA*. Chembiochem, 2009. **10**(1): p. 141-57.
188. Zhu, G. and S.J. Lippard, *Photoaffinity labeling reveals nuclear proteins that uniquely recognize cisplatin-DNA interstrand cross-links*. Biochemistry, 2009. **48**(22): p. 4916-25.
189. De Silva, I.U., P.J. McHugh, P.H. Clingen, and J.A. Hartley, *Defects in interstrand cross-link uncoupling do not account for the extreme sensitivity of ERCC1 and XPF cells to cisplatin*. Nucleic Acids Res, 2002. **30**(17): p. 3848-56.
190. Salmon, P., V. Kindler, O. Ducrey, B. Chapuis, R.H. Zubler, and D. Trono, *High-level transgene expression in human hematopoietic progenitors and differentiated blood lineages after transduction with improved lentiviral vectors*. Blood, 2000. **96**(10): p. 3392-8.
191. Salmon, P. and D. Trono, *Production and titration of lentiviral vectors*. Curr Protoc Neurosci, 2006. **Chapter 4**: p. Unit 4 21.
192. Hess, M., U. Schwitter, M. Petretta, B. Giese, and H. Naegeli, *Bipartite substrate discrimination by human nucleotide excision repair*. Proc Natl Acad Sci U S A, 1997. **94**(13): p. 6664-9.
193. Sugawara, K., T. Okamoto, Y. Shimizu, C. Masutani, S. Iwai, and F. Hanaoka, *A multistep damage recognition mechanism for global genomic nucleotide excision repair*. Genes Dev, 2001. **15**(5): p. 507-21.
194. Gunz, D., M.T. Hess, and H. Naegeli, *Recognition of DNA adducts by human nucleotide excision repair. Evidence for a thermodynamic probing mechanism*. J Biol Chem, 1996. **271**(41): p. 25089-98.
195. Geacintov, N., S. Broyde, T. Buterin, H. Naegeli, M. Wu, S. Yan, and D. Patel, *Thermodynamic and structural factors in the removal of bulky DNA adducts by the nucleotide excision repair machinery*. Biopolymers, 2002. **65**(3): p. 202-10.
196. Isaacs, R. and H. Spielmann, *A model for initial DNA lesion recognition by NER and MMR based on local conformational flexibility*. DNA Repair (Amst), 2004. **3**(5): p. 455-64.
197. Hess, M.T., U. Schwitter, M. Petretta, B. Giese, and H. Naegeli, *Site-specific DNA substrates for human excision repair: comparison between deoxyribose and base adducts*. Chem Biol, 1996. **3**(2): p. 121-8.

198. Kusumoto, R., C. Masutani, K. Sugasawa, S. Iwai, M. Araki, A. Uchida, T. Mizukoshi, and F. Hanaoka, *Diversity of the damage recognition step in the global genomic nucleotide excision repair in vitro*. *Mutat Res*, 2001. **485**(3): p. 219-27.
199. Min, J. and N. Pavletich, *Recognition of DNA damage by the Rad4 nucleotide excision repair protein*. *Nature*, 2007. **449**(7162): p. 570-5.
200. de Laat, W., E. Appeldoorn, K. Sugasawa, E. Weterings, N. Jaspers, and J. Hoeijmakers, *DNA-binding polarity of human replication protein A positions nucleases in nucleotide excision repair*. *Genes Dev*, 1998. **12**(16): p. 2598-609.
201. Staresincic, L., A. Fagbemi, J. Enzlin, A. Gourdin, N. Wijgers, I. Dunand-Sauthier, G. Giglia-Mari, S. Clarkson, W. Vermeulen, and O. Scharer, *Coordination of dual incision and repair synthesis in human nucleotide excision repair*. *EMBO J*, 2009. **28**(8): p. 1111-20.
202. Orelli, B., T.B. McClendon, O.V. Tsodikov, T. Ellenberger, L.J. Niedernhofer, and O.D. Scharer, *The XPA-binding domain of ERCC1 is required for nucleotide excision repair but not other DNA repair pathways*. *J Biol Chem*, 2010. **285**(6): p. 3705-12.
203. Mu, D., E. Bertrand-Burggraf, J.C. Huang, R.P. Fuchs, A. Sancar, and B.P. Fuchs, *Human and E.coli excinucleases are affected differently by the sequence context of acetylaminofluorene-guanine adduct*. *Nucleic Acids Res*, 1994. **22**(23): p. 4869-71.
204. Gillet, L., J. Alzeer, and O. Scharer, *Site-specific incorporation of N-(deoxyguanosin-8-yl)-2-acetylaminofluorene (dG-AAF) into oligonucleotides using modified 'ultra-mild' DNA synthesis*. *Nucleic Acids Res*, 2005. **33**(6): p. 1961-9.
205. Kim, J.K. and B.S. Choi, *The solution structure of DNA duplex-decamer containing the (6-4) photoproduct of thymidyl(3'-->5')thymidine by NMR and relaxation matrix refinement*. *Eur J Biochem*, 1995. **228**(3): p. 849-54.
206. Szymkowski, D., C. Lawrence, and R. Wood, *Repair by human cell extracts of single (6-4) and cyclobutane thymine-thymine photoproducts in DNA*. *Proc Natl Acad Sci U S A*, 1993. **90**(21): p. 9823-7.
207. Jamieson, E. and S. Lippard, *Structure, Recognition, and Processing of Cisplatin-DNA Adducts*. *Chem Rev*, 1999. **99**(9): p. 2467-98.
208. Zamble, D., D. Mu, J. Reardon, A. Sancar, and S. Lippard, *Repair of cisplatin--DNA adducts by the mammalian excision nuclease*. *Biochemistry*, 1996. **35**(31): p. 10004-13.
209. Huang, J., D. Zamble, J. Reardon, S. Lippard, and A. Sancar, *HMG-domain proteins specifically inhibit the repair of the major DNA adduct of the anticancer drug cisplatin by human excision nuclease*. *Proc Natl Acad Sci U S A*, 1994. **91**(22): p. 10394-8.
210. Szymkowski, D., K. Yarema, J. Essigmann, S. Lippard, and R. Wood, *An intrastrand d(GpG) platinum crosslink in duplex M13 DNA is refractory to repair by human cell extracts*. *Proc Natl Acad Sci U S A*, 1992. **89**(22): p. 10772-6.

211. Fousteri, M., W. Vermeulen, A.A. van Zeeland, and L.H.F. Mullenders, *Cockayne syndrome A and B proteins differentially regulate recruitment of chromatin remodeling and repair factors to stalled RNA polymerase II in vivo*. Mol Cell, 2006. **23**(4): p. 471-82.
212. Mullen, J.R., V. Kaliraman, S.S. Ibrahim, and S.J. Brill, *Requirement for three novel protein complexes in the absence of the Sgs1 DNA helicase in Saccharomyces cerevisiae*. Genetics, 2001. **157**(1): p. 103-18.
213. Flott, S., C. Alabert, G.W. Toh, R. Toth, N. Sugawara, D.G. Campbell, J.E. Haber, P. Pasero, and J. Rouse, *Phosphorylation of Slx4 by Mec1 and Tel1 Regulates the Single-Strand Annealing Mode of DNA Repair in Budding Yeast*. Mol Cell Biol, 2007. **27**(18): p. 6433-6445.
214. Dunand-Sauthier, I., M. Hohl, F. Thorel, P. Jaquier-Gubler, S. Clarkson, and O. Schärer, *The spacer region of XPG mediates recruitment to nucleotide excision repair complexes and determines substrate specificity*. J Biol Chem, 2005. **280**(8): p. 7030-7.
215. Mitchell, D.L. and R.S. Nairn, *The biology of the (6-4) photoproduct*. Photochem Photobiol, 1989. **49**(6): p. 805-19.
216. Tian, M., R. Shinkura, N. Shinkura, and F.W. Alt, *Growth Retardation, Early Death, and DNA Repair Defects in Mice Deficient for the Nucleotide Excision Repair Enzyme XPF*. Mol Cell Biol, 2004. **24**(3): p. 1200-1205.